Development of Efficient Algorithms for *JPEG*2000 Image Coder

A thesis

Submitted in the fulfillment of the

requirements for the award of the degree of

Doctor of Philosophy

Submitted by

Singara Singh

(Registration No. 90611502)

Under the supervision of

Dr. R. K. Sharma — **Professor**

Dr. M. K. Sharma — **Associate Professor**

School of Mathematics and Computer Applications

Thapar University

Patiala

June 2013

CERTIFICATE

I hereby certify that the work which is being presented in this thesis, in fulfillment of the requirements for the award of degree of DOCTOR OF PHILOSOPHY submitted in the School of Mathematics and Computer Applications (*SMCA*), Thapar University, Patiala, is an authentic record of my own work carried out under the supervision of Dr. R. K. Sharma and Dr. M. K. Sharma, and refers other researcher works which are duly listed in the reference section.

The matter presented in this thesis has not been submitted for the award of any other degree of this or any other university.

(Singara Singh)

Registration No. 90611502

This is to certify that the above statement made by the candidate is correct and true to the best of my knowledge and belief.

10.6.2013

(Dr. R. K. Sharma)

Professor

SMCA

Thapar University

Patiala-147004 (INDIA)

Supervisor

(Dr. M. K. Sharma)

Associate Professor

SMCA

Thapar University

Patiala-147004 (INDIA)

Supervisor

ABSTRACT

Compression of digital images has been a topic of research for many years and a number of image compression standards have been developed for different applications. The role of compression is to reduce bandwidth requirements for transmission and memory requirements for storage of all forms of data. Although, developments on technology front provide high speed digital communication and large memories, image compression is still of major importance. The advances in technologies generally result into increased demand for image communication, as well as demand for higher quality image printing and display.

The work presented in this thesis revolves around the improvements in the *JPEG*2000 image compression standard. We have proposed an Edge Adaptive Wavelet Lifting Scheme that deals with the edges present in an image efficiently. In this approach, the lifting direction is not restricted to horizontal and/or vertical direction only, but other lifting directions are also used if the edges present in an image are neither in horizontal nor in vertical direction. This approach represents the decomposed image more efficiently because there are less number of wavelet coefficients having large magnitude in the high pass subbands. Due to this approach, the energy of high pass subbands decreases and these subbands are represented more efficiently. It has been observed that proposed scheme improves *PSNR* by more than 4 *d*B when compared with the *JPEG*2000 lifting scheme.

Tile boundary artifacts in *JPEG*2000 compressed images have also been discussed in this thesis. We have proposed a post-processing technique to reduce tile boundary artifacts in *JPEG*2000 compressed images in this work. This technique reduces tile boundary artifacts which occur in an image when it is compressed at low bit rate using *JPEG*2000 standard. We have analyzed the effect of quantization on the region of the tile boundaries of *JPEG*2000 compressed images. The

analysis confirms that tiling artifacts are reduced by updating the high pass reconstructed samples lying on the boundary of the image tiles where the artifacts occur. Post-processing is applied on the output of *JPEG*2000 coding system and thus it can easily be blended with *JPEG*2000 standard. It has been shown that when one uses proposed method, tile boundary artifacts are reduced in terms of increase in *PSNR* value. This increase in *PSNR* value varies from 0.1 *d*B to 1 *d*B for different images considered in this work. The reductions in boundary artifacts have also been observed in visual quality of decompressed images.

Bit rate allocation to the tiles of an image has also been analyzed in this work. In *JPEG*2000 encoder, equal bit rate is assigned to each tile of an image. This assignment is suitable for the images with information contents equally distributed throughout the image. However, tiles of an image may have different complexities. Some of the tiles may have larger texture area while others may have larger smooth area. The quality of a reconstructed image varies a lot if all tiles in the image do not have same complexity. As such, we should include the complexity of a tile while assigning a bit rate to it. This is a known fact that entropy of a complex tile is more than the entropy of a smooth tile. So, we have proposed a method to assign bit rate to a tile based on the weights derived using zero-order entropy of a tile. Using this method, tiles of an image have been assigned different compression bit rates. Visual quality of reconstructed image is improved by assigning these bit rates to the tiles of an image. The proposed methodology improves the *PSNR* values for all images and for all bit rates considered in this work. Maximum *PSNR* improvement by the proposed method is 2 *d*B. Due to this improvement, the proposed methodology provides better visual quality in *JPEG*2000 reconstructed images than the conventional approach of *JPEG*2000 standard. This improvement has also been shown taking place when compared with *JPEG*2000 encoder and also with other existing algorithm proposed.

Next, Post Compression Rate Distortion (*PCRD*) optimization scheme of *JPEG*2000 has been discussed in this thesis. It has been observed that a considerable amount of computation and memory usage in *PCRD* optimization scheme in *JPEG*2000 is redundant. Motivated by this observation, an efficient rate control approach for *JPEG*2000 encoder is proposed, in which optimal Rate Distortion (*RD*) slope threshold is selected using the minimum *RD* slope of lower level horizontally and vertically low pass subbands of the wavelet decomposed image. Also, the passes of the code blocks of other subbands, whose *RD* slopes are less than the optimal *RD* slope, are skipped. The proposed approach reduces memory requirements and encoding time when compared with existing rate control approaches for *JPEG*2000 standard and also provides the same image quality as that of *PCRD* approach used in the *JPEG*2000 standard. The encoding time and memory usage in the proposed approach is 50-60% less than *PCRD* approach and comparable with existing approaches.

The work presented in this thesis, when combined with *JPEG*2000 standard, shall result into the reduction of storage and transmission costs of digital images.

ACKNOWLEDGEMENTS

First of all, I am highly indebted to my supervisors, Dr. R. K. Sharma and Dr. M. K. Sharma, SMCA, Thapar University, Patiala, for their untiring support, encouragement, and able guidance at each and every step throughout this research endeavor. It is really fortunate that I got an opportunity to learn the ABC of research from them, which will definitely go a long way in my professional carrier. I will always be grateful to them for their enthusiastic guidance and support which made this dissertation possible. It has indeed been a privilege to carry out this work under their supervision.

I am grateful to Director, Thapar University, Patiala for providing me to carry out this research work. I express my gratitude to Doctoral Committee for monitoring the progress and providing suggestions for improvement of my Ph. D. research work. I am equally indebted to SMCA, Thapar University to encourage me to pursue research work. I am thankful to my colleagues of SMCA for their constant support and cooperation during my research work. I appreciate the cooperation and support received from all my friends during this doctoral research project.

Finally, I would like to dedicate this thesis to my family. My parents have always supported me and to them I owe everything. I acknowledge the constant cooperation, hard work and moral support of my wife, Geeta Kasana. She has always been available to me for all kinds of support during this doctoral research work. I acknowledge support of my father-in-law Wing Commander S. C. Singh, mother-in-law Smt. Kamlesh Singh, brother-in-law Pradeep Kumar, sister-in-law Preeti Singh, daughter Sonal and son Varun during this research work.

Singara

(Singara Singh)

Date: 10.6.2013

Place: Thapar University, Patiala

LIST OF FIGURES

LIST OF TABLES

ABBREVIATIONS

ADL	Adaptive Directional Lifting
ALS	Adaptive Lifting Scheme
CAC	Constant Area Coding
CUP	Cleanup Pass
DA-DWT	Direction Adaptive-*DWT*
DCS	Difference Correlation Structure
DCT	Discrete Cosine Transform
DFT	Discrete Fourier Transform
DPCM	Differential Pulse Code Modulation
DWT	Discrete Wavelet Transform
EZW	Embedded Zero Wavelets
FFT	Fast Fourier Transform
GGD	Generalized Gaussian Density
HH	High High Pass Subband
HL	High Low Pass Subband
HVS	Human Visual System
ICT	Irreversible Component Transform
ISO	International Standard Organization
JPEG	Joint Photographic Expert Group
*JPEG*2000	Joint Photographic Expert Group 2000
LL	Low Low Pass Subband
LH	Low High Pass Subband

LRA	Lagrangian Rate Allocation
MCTF	Motion Compensated Temporal Filtering
MRP	Magnitude Refinement Pass
MSE	Mean Square Error
OTLPF	Odd Tile Length Low Pass First
PCRD	Post Compression Rate Distortion
PSNR	Peak Signal to Noise Ratio
PSOT	Priority Scanning with Optimal Truncation
RLE	Run Length Encoding
RCT	Reversible Component Transform
RD	Rate Distortion
SBRA	Successive Bit Rate Allocation
SPP	Significant Propagation Pass
SPIHT	Set Partitioning in Hierarchical Trees
WAL	Weighted Adaptive Lifting

NOTATIONS AND SYMBOLS

Notation	Description
B_i	i^{th} code Block
$D_i^{n_i}$	Distortion at the truncation point n_i for the code block B_i
E	Entropy of the image
H	Low pass filters
G	High pass filters
K_e	Lifting weight for even index set
K_o	Lifting weight for odd index set
(M, N)	Size of the image
(m', n')	Size of the tile
N_T	Number of tiles of an image
$\{n_i\}$	Set of truncation points
P	Prediction lifting operator
Pr	Probability
$S_i^{n_i}$	Rate distortion slope at the truncation point n_i for the code block B_i
$q_b(u, v)$	Quantized wavelet coefficients in subband b
$y_b^{'}$	Wavelet coefficient of subband b
$y_b^{''}$	Reconstructed wavelet coefficient of subband b
U	Update Operator
w_i	Weight of the i^{th} tile of the image
X	Input Image
Z	Number of bits per pixel

Δ_b	Quantization step size for subband b
λ_{opt}	Optimal *RD* slope

CONTENTS

Chapter 1

Introduction

1.1 Introduction

This chapter covers a brief introduction of the fundamentals that are essential for the development of efficient algorithms for digital image compression. This also includes the problem formulation and outline of the work presented in this thesis. The thesis outline along with the contribution of work done in this thesis is summarized in last section of this chapter.

1.2 Image Compression

In the field of information technology, usefulness of digital images for communicating information in our day-to-day life is very well established. A large amount of data is required for storing the images when compared with text and thus cost of storing and transmitting images is high when compared with text. As such, image compression has emerged as a widely researched area in information technology. Putting images, audio, and video on websites without compressing them is not appreciated as these shall utilize a very large storage. For example, transmission of high-definition uncompressed digital video with 1024×768 resolution, 24 bits/pixel, 25 frames (transmitted in one second) shall involve transmission of 1.7 GB data in one

hour. For stored multimedia, image compression is usually done once at storage time at the source and decoded in real time while viewing.

Image compression is the process of reducing the number of bytes required to represent an image. Image compression reduces the bytes taken by an image significantly and this consequently helps in reducing the consumption of expensive resources, such as hard disk space and/or transmission bandwidth.

1.3 Types of Image Compression

On the basis of reconstruction of original image from the compressed image, image compression is classified into two types. First type of compression is lossless compression, in which the original image is completely recovered from the compressed image and there is no loss of information. Lossless compression is preferred for archival purposes and often used for medical imaging, technical drawings, clip art, and comics *etc*. The most common formats for lossless compression include *zip*, *stuffit* and *gzip* which run under Windows, Apple, and UNIX operating systems, respectively.

Second type of image compression is lossy compression, in which original image cannot be recovered completely from the compressed image and there is some loss of information. An advantage in lossy compression is that it provides much higher compression ratio than lossless compression. Generally, this type of compression makes two passes. In first pass, well known transforms like Discrete Fourier Transform (*DFT),* Discrete Cosine Transform (*DCT*), and Discrete Wavelet Transform (*DWT*) *etc*. are used to transform the data into frequency domain. Once the data has been transformed, it is quantized, due to which some loss occurs. Finally, the transformed data is compressed using conventional lossless compression techniques. Here, amount of data loss depends upon the compression rate. The data loss is high at high

compression rate and is less at low compression rate. Lossy compression is particularly suitable for natural images such as photographs where minor loss of faithfulness is acceptable in order to achieve a substantial reduction in bit rate.

1.4 Redundancy in Image Data

Quite often, an image contains some data which has no relevant information or the information is repeated. This leads to a redundancy in image data. Image compression and coding techniques exploit these redundancies. Image data redundancy is of three types: coding redundancy, interpixel redundancy, and psychovisual redundancy. These are explained below, in brief.

- **Coding redundancy:** This type of redundancy occurs when some patterns are more common than others. This redundancy can be minimized by assigning smaller codes to frequent patterns as compared to other patterns. This assignment results into data compression. This type of encoding is reversible and generally implemented using look-up tables. Huffman coding and arithmetic coding techniques are the most common techniques of image encoding that explore the coding redundancy.
- **Interpixel redundancy:** This type of redundancy exploits the fact that an image very often contains strongly correlated pixels. In other words, an image has large regions where pixel values are same or almost same. This redundancy can be explored in several ways, one of them is predicting a pixel value based on the values of its neighboring pixels. In order to do so, original 2-*D* array of pixels is usually mapped to a different format, *e.g.*, an array of differences between adjacent pixels. If original image pixels can be reconstructed from the transformed data set, the mapping is said to be reversible. The compression techniques that explore interpixel redundancy include: Constant Area

Coding (*CAC*), Run-Length Encoding (*RLE*), and other predictive coding algorithms such as Differential Pulse Code Modulation (*DPCM*) *etc*.

- **Psychovisual redundancy:** A number of experiments on psychophysical aspects of human vision have proved that human eye does not respond with equal sensitivity to all incoming visual information. This has been established that certain information has less importance than others. This information is said to be psychovisual redundancy. The end result of applying image and video compression techniques that aim at reducing psychovisual redundant data is a compressed image file, whose size and quality are less than the original information, but whose resulting quality is still acceptable for the application at hand. The loss of quality that comes as a byproduct of such techniques is called as quantization, as to indicate that a wider range of input values is normally mapped to a narrower range of output values thorough an irreversible process.

1.5 Compression Model

A general image compression model consists of a source encoder, the storage or transmission media (also called as channel), channel encoder, channel decoder, and a source decoder, as shown in Figure 1.1. The source encoder reduces or eliminates any redundancies present in the input image, which usually leads to the saving of bits. Figure 1.2 depicts the details of source encoder. Main components of a source encoder are:

- **Transform:** This component of encoder transforms input data into a format designed to reduce interpixel redundancies present in the input image. This operation is generally reversible and may or may not directly reduce the amount of data required to represent

the image. Different types of transforms are *DCT*, *DFT*, Fast Fourier Transform *(FFT)* and *DWT etc*. (Ramkumar and Anand, 1997; Saha and Vemuri, 2000).

- **Quantizer:** This component of the model reduces the accuracy of mapping's outcome in accordance with some pre-defined criterion. It reduces the psychovisual redundancy of input image. This operation is not reversible and must be omitted if lossless compression is desired. Many different quantization schemes, including uniform scalar quantizer (Sayood, 2000) have been proposed in literature.
- **Entropy Encoder:** This encoder creates a fixed- or variable-length code to represent quantizer's output and maps the output in accordance with the code. In most cases, a variable-length code is used. This operation is reversible.

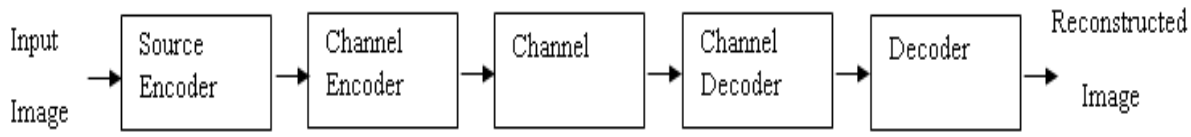

Figure 1.1: General Compression Model

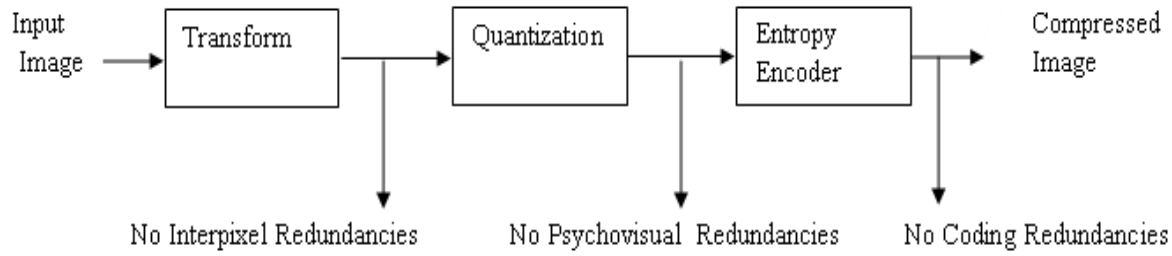

Figure 1.2: Encoder used in Compression Model

The steps performed on the decoder side are just a reverse of the steps performed on encoder side, as shown in Figure 1.3.

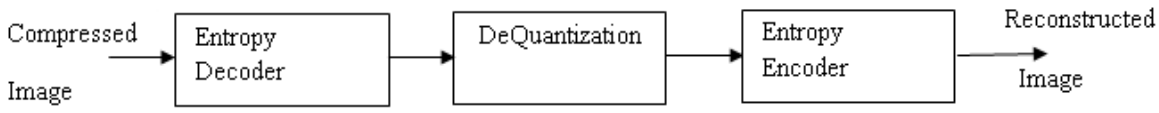

Figure 1.3: Decoder used in a Compression Model

Primarily, a channel encoder performs the following tasks.

- It adds controlled redundancy to the source encoded data to reduce the impact of errors that might have been produced by the channel.
- It increases noise immunity of source encoded data when the channel is noisy.

The steps performed by the channel decoder are just a reverse of steps performed on encoder side by channel encoder.

1.6 Image Quality Metric

In image compression, the reconstructed image is not always the same as the original image, and individual pixel values may be different from the values in the original image. To measure the quality of reconstructed image, it is required to introduce a quality metric. This metric should be such that it is correlated with visual appearance. Peak Signal to Noise Ratio (*PSNR*) between original and reconstructed image is the metric that has widely been used in literature for establishing image quality. *PSNR* is a function of Mean Square Error (*MSE*) and is defined as,

$$PSNR = 10\, log_{10} \frac{(2^z-1)^2}{MSE} \quad \ldots (1.1)$$

where z is the bit depth of the image and MSE is defined as,

$$MSE = \sum_{m=1}^{M} \sum_{n=1}^{N} \frac{(A_{mn} - B_{mn})^2}{M \times N} \quad \ldots (1.2)$$

where A_{mn} is the pixel of reconstructed image and B_{mn} is the corresponding pixel of original image, M and N are the height and width of the images, respectively.

Relative Percentage Improvement (RPI) in $PSNR$ is defined as

$$\frac{PSNR_{new}-PSNR_{old}}{PSNR_{old}} \times 100$$

where $PSNR_{new}$ is the $PSNR$ value when proposed algorithm is used with *JPEG*2000 encoder and $PSNR_{old}$ is the $PSNR$ when existing algorithm is used with *JPEG*2000 encoder.

1.7 *JPEG* and its Deficiency

The Joint Photographic Experts Group (*JPEG)* standard is a popular image compression scheme. This scheme is popular due to its low computational complexity. It was developed by the *JPEG* committee in 1992 and was designed for compressing color and grayscale images (Pannebaker and Mitchell, 1992). *JPEG* standard suffers from several deficiencies. The performance of *JPEG* coder is not relatively high anymore. Blocking artifacts cause a distortion which is very annoying and appear in images encoded with high compression. One potential reason behind these artifacts is the division of the image into eight by eight pixel blocks which are independently transformed by *DCT*, quantized and encoded. It is obvious that larger differences between two blocks on their common border will appear with a lower number of bits used for description of each block. Apparently, a transform, which can be used for much larger area, or even whole image, should be used. However, *DCT* does not provide good results for large areas. That is why the *JPEG* consortium chose *DWT* for transforming an image (Antonini *et al.*, 1992; Mittal, 2000; Taubman and Marcellin, 2002). Some of the wavelet based coders are: Embedded Zerotree Wavelets (*EZW*) proposed by Shapiro (1993) and Set Partitioning in Hierarchical Trees (*SPIHT*) proposed

by Said and Pearlman (1996). *SPIHT* is superior to *EZW* as it provides better visual quality at the same compression rate.

1.8 *JPEG*2000 Standard

In 2000, *JPEG* committee proposed new *JPEG*2000 standard which provides both lossless and lossy compression. It is based on *DWT* and arithmetic entropy coding, and it offers a number of novel features including the extraction of parts of the image for editing without decoding, concentrating on regions of interest with sharp visual quality and specified bit rate, and many more (Christopoulos *et al.*, 2000; Bhalod *et al.*, 2001; Skodras *et al.*, 2001; Boettcher and Fowler, 2007; Seo and Kang, 2010). *JPEG*2000 also supports different types of still images and motion images. It provides tools for a wide variety of applications, such as Internet, image library, and real-time transmission through wireless channels. Steps used in *JPEG*2000 encoder and decoder are shown in Figure 1.4.

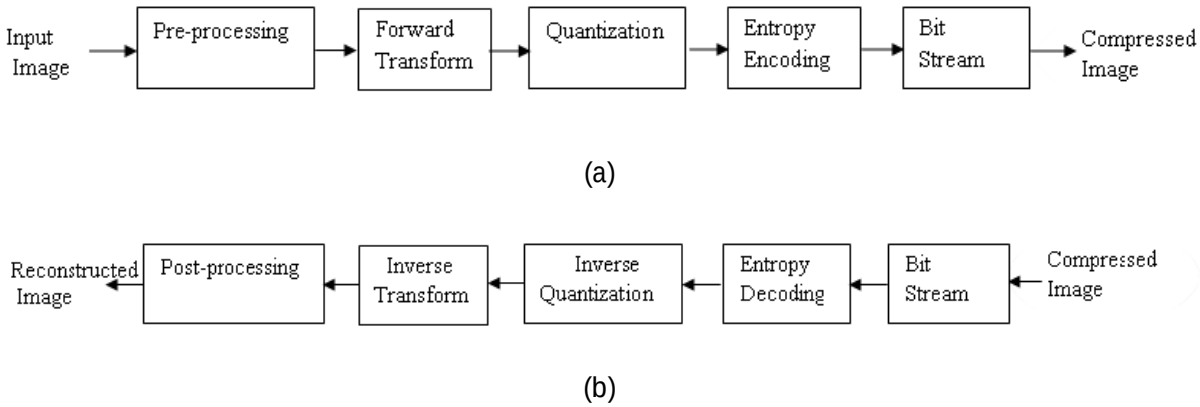

Figure 1.4: (a) Encoder steps (b) Decoder steps used in *JPEG*2000 standard

1.8.1 Pre-processing in *JPEG*2000

This process consists of the steps, namely, image tiling, nominal dynamic range and component transformation.

Image Tiling

*JPEG*2000 standard works on tiles of an image. The source image is partitioned into rectangular non-overlapping blocks called as tiles. This reduces memory requirements as tiles are compressed independently as if these were entirely independent images. All operations, including pre-processing, wavelet transform, quantization, and entropy coding, are performed independently on each tile of the input image. Tile dimensions are taken as powers of two, except for those tiles that are on the boundary of the image. Arbitrary tile sizes are allowed and the whole image can be considered as one tile. Tiling affects the image quality subjectively as well as objectively. Smaller tiles create more tiling artifacts as compared to larger tiles. As such, use of larger tiles shall result into better visual performance than the use of smaller tiles. Image degradation is high in case of low bit rate than high bit rate, when tiling is used.

Shifting of Nominal Dynamic Range

*JPEG*2000 encoder preprocesses the pixels of an image to have a nominal dynamic range of pixel values that is approximately centered about zero. Suppose that a component of an image has *z* bits/pixel. The pixels may either be signed or unsigned leading to a nominal dynamic range of $[-2^{z-1}, 2^{z-1}-1]$ or $[0, 2^{z}-1]$, respectively. If the pixel values are unsigned, the nominal range is not centered about zero. Thus, the nominal dynamic range of the pixels is adjusted by subtracting 2^{z-1} from each of the pixel values. For images, whose pixel values are represented by signed integers, such as computed tomography images, the nominal range is already centered about zero, and no processing is required. The post-processing stage of the decoder undoes the effects of pre-processing in the encoder. If the pixel values for a component of an image are unsigned, the original nominal dynamic range is restored.

Component Transformations

*JPEG*2000 supports multiple component images. Different components may not have the same bit depths. These components may either be signed or unsigned, as mentioned above. For reversible systems, the only requirement is that the bit depth of each output image component must be identical to the bit depth of the corresponding input image component. Component transformations improve compression and allow for visually relevant quantization. *JPEG*2000 standard supports two different component transforms, Irreversible Component Transform (*ICT*) and Reversible Component Transform (*RCT*) that can be used for lossy coding and lossless coding, respectively. Forward and inverse *ICT* transformations are achieved using (1.3) and (1.4), respectively, for *RGB* and *YCbCr* colour spaces.

$$\begin{pmatrix} Y \\ C_b \\ C_r \end{pmatrix} = \begin{pmatrix} 0.299 & 0.587 & 0.114 \\ -0.16875 & -0.33126 & 0.5 \\ 0.5 & -0.41869 & -0.08138 \end{pmatrix} \begin{pmatrix} R \\ G \\ B \end{pmatrix} \quad \ldots (1.3)$$

$$\begin{pmatrix} R \\ G \\ B \end{pmatrix} = \begin{pmatrix} 1.0 & 0 & 1.402 \\ 1.0 & -0.34413 & -0.71414 \\ 1.0 & 1.772 & 0 \end{pmatrix} \begin{pmatrix} Y \\ C_b \\ C_r \end{pmatrix} \quad \ldots (1.4)$$

1.8.2 *DWT* in *JPEG*2000

DWT is a subband transform which transforms images from spatial domain to frequency domain. It is implemented using the concept of filter banks. On the encoder side, analysis filters are used while on the decoder side, synthesis filters are used. These filters are further divided into two types: high pass filters and low pass filters. If image data is processed using:

(i) a high pass filter, high frequency information of the image is kept and low frequency information is lost.

(ii) a low pass filter, low frequency information of the image is kept and high frequency information is lost.

Two dimensional *DWT* is the combination of a one dimensional (1-*D*) horizontal and 1-*D* vertical *DWT*. The original image is decomposed in order to produce low pass and high pass filtered outputs of the image. These filtered outputs are then down-sampled by a factor of two in order to produce a set of subbands of the original image. Because of the down-sampling process, total number of wavelet coefficients is same as the number of original image samples. Output of 2-*D DWT* is the set of four subbands: *LL* (Low Low), *LH* (Low High), *HL* (High Low) and *HH* (High High), as shown in Figure 1.5. In this figure, *H* and *G* are low pass and high pass filters, respectively; *M* and *N* are the height and width of the image. *LL* subabnd is also called as approximation subband and other subbands are called as details subbands. Wavelet decomposition process can further be applied iteratively on the approximation subband to get a multiresolution decomposition of the original image.

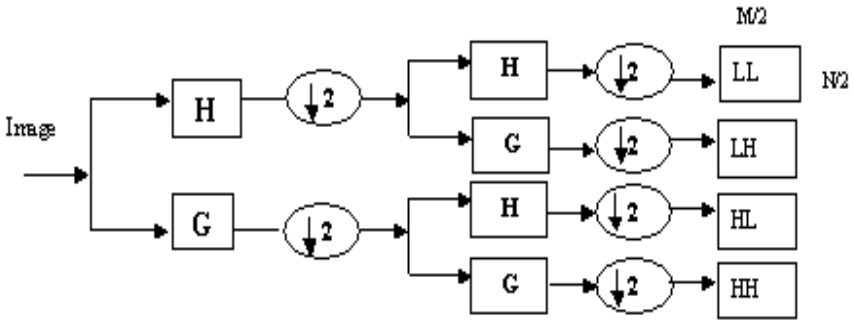

Figure 1.5: 2-*D* Wavelet Transform

An important property of wavelet transform is the conservation of energy of an image. The energy of an image is the sum of the squares of the pixel values, the energy in the wavelet transform of an image is the sum of the squares of its wavelet coefficients. During wavelet transform, energy of an image is divided between approximation and details subbands in such a way that total energy of the image does not change. However, during compression, energy of an image may reduce since thresholding changes the coefficient values and hence the compressed

image may contain less energy. The compaction of energy describes how much energy has been compacted into approximation subband and details subbands during wavelet transformation. Better compaction will occur when the magnitudes of the coefficients of details subbabds are significantly smaller than the magnitudes of the coefficients of approximation subband. Compaction is important when compressing images because the more energy that has been compacted into the approximation subband the less energy shall be lost during compression.

To achieve efficient lossy and lossless compression within a single standard, two wavelet transform filters are used in *JPEG*2000 standard. One is *CDF* 9/7 floating point filter which is used for lossy compression and the other is *LeGall* 5/3 filter which is simple to implement and has lossless capability. These two reversible integer-to-integer and irreversible real-to-real wavelet transforms are employed by *JPEG*2000 baseline encoder. The reversible integer-to-integer wavelet transform is *LeGall* 5/3 wavelet which is used for lossless compression and irreversible real-to-real wavelet transform is *CDF* 9/7 which is used for lossy compression (Antonini *et al.*, 1992; Said and Pearlman, 1996; Adams and Kossentini, 2000). Analysis filters coefficients and synthesis filter coefficients used by these wavelet transforms are given in Tables 1.1, 1.2, 1.3 and 1.4 (Taubman, 2000).

Table 1.1: *CDF* 9/7 analysis filter Coefficients

K	Low Pass Filter (H_k)	High Pass Filter (G_k)
0	0.6029490182363579	1.115087052456994
± 1	0.2668641184428723	-0.5912717631142470
± 2	-0.0782326652898785	-0.0575435262284995 7
± 3	-0.0168641184428749 5	0.0912717631142494 8
± 4	0.0267487574108097 6	

Table 1.2: *CDF* 9/7 synthesis filter coefficients

K	Low Pass Filter (H_k)	High Pass Filter (G_k)
0	1.115087052456994	0.6029490182363579
± 1	-0.5912717631142470	0.2668641184428723
± 2	-0.05754352622849957	-0.07822326652898785
± 3	0.09127176311424948	-0.01686411844287495
± 4		0.02674875741080976

Table 1.3: *LeGall* 5/3 analysis filter coefficients

K	Low Pass Filter (H_k)	High Pass Filter (G_k)
0	¾	1
± 1	¼	½
± 2	-¼	

Table 1.4: *LeGall* 5/3 synthesis filter coefficients

K	Low Pass Filter (H_k)	High Pass Filter (G_k)
0	1	¾
± 1	½	¼
± 2		-¼

Following the above procedure in reverse order, an image can be reconstructed from its subbands using inverse *DWT*. The synthesis filters, like in the case of one-dimensional processing, are identical to the analysis filters except for a time reversal.

1.8.3 Quantization in *JPEG*2000

In *JPEG*2000 encoder, after the *DWT* transform has been applied, the wavelet coefficients of each subband are quantized in lossy compression mode. Higher compression is achieved using quantization as quantization process decreases the precision required to represent the wavelet coefficients. Quantization of *DWT* subbands is one of the reasons for information loss in the encoder. Quantization is not performed in case of lossless compression. In Part 1 of the standard, quantization is performed by uniform scalar quantization with dead-zone about the origin. In dead-zone scalar quantization with step size Δ_b, the width of the dead-zone shall be $2\Delta_b$, as shown in Figure 1.6. Quantization step sizes are different for each subband, which is calculated based on the dynamic range of the wavelet coefficients of a subband. Uniform scalar quantization with dead-zone is calculated using the formula,

$$q_b(u,v) = sign\left(y'_b(u,v)\right)\left\lfloor\left|\frac{y'_b(u,v)}{\Delta_b}\right|\right\rfloor \quad \ldots (1.5)$$

where Δ_b is dynamic range of subband b, $y'_b(u,v)$ is wavelet coefficient and $q_b(u,v)$ is the quantized wavelet coefficient. The *sign* function is defined as,

$$sign(x) = \begin{cases} -1, & if\ x < 0 \\ 0, & if\ x = 0 \\ 1, & if\ x > 0 \end{cases}$$

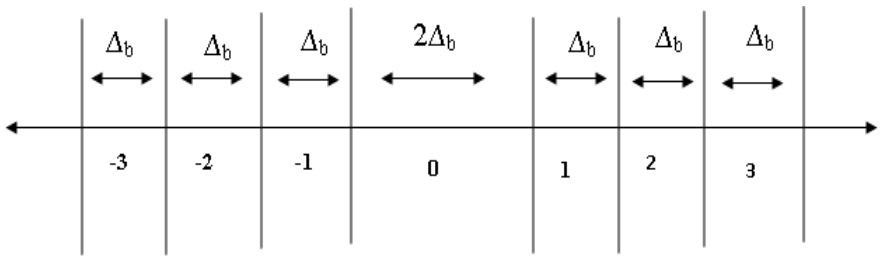

Figure 1.6: Quantizer steps in *JPEG*2000

All the resulting quantized *DWT* coefficients are signed integers. Here, computations up to the quantization step are carried out in two's complement form. After quantization, the quantized *DWT* coefficients are converted into sign-magnitude representation.

The quantizer step sizes for each subband used by the encoder are transmitted to the decoder using the code stream header. These step sizes specified in the header are relative and not the absolute quantities. That is, the quantizer step size for each subband is specified relative to the nominal dynamic range of the subband data.

At the decoder side, the dequantization stage tries to undo the effects of quantization. This process is not invertible and therefore results in information loss. The transform coefficients are obtained from the quantizer indices. Mathematically, the dequantization process is defined as,

$$y_b''(u,v) = sign\big(q_b(u,v)\big)\,(\,|\Delta_b . q_b(u,v)|) + \delta \qquad \ldots (1.6)$$

where δ is usually set to $\Delta_b/2$. y_b'' is the reconstructed wavelet coefficient of subband b.

1.8.4 Entropy Coding

The quantized wavelet coefficients of each subband are processed by the entropy coding process of *JPEG*2000 encoder. The entropy coding is divided into two steps, namely, *Tier*-1 and *Tier*-2 coding.

In *Tier*-1 coding, quantizer indices of wavelet coefficients for each subband are partitioned into code blocks and encoded independently. Size of the code block is a free parameter of the coding process, subject to the constraints: (i) the nominal width and height of a code block must be an integer power of two, (ii) the product of width and height cannot exceed 4096.

If the precision of the wavelet coefficients in the code blocks is *p*, then the code block is decomposed into *p* bit planes and these are sequentially encoded from the most significant bit plane to the least significantly bit plane. Each bit plane is first encoded by a fractional Bit Plane Coding (*BPC*) process to generate intermediate data in the form of a context and a binary decision value for each bit position. Embedded Block Coding with Optimized Truncation (*EBCOT*) has been adopted for *BPC* (Taubman, 2000; Taubman *et al.*, 2002). *EBCOT* encodes each bit plane in three coding passes, with a part of a bit plane being coded in each coding pass without any overlapping with the other two coding passes. Due to this reason, *BPC* is called fractional bit plane coding. The three coding passes in the order in which they are performed on each bit plane are Significant Propagation Pass (*SPP*), Magnitude Refinement Pass (*MRP*) and Cleanup Pass (*CUP*). In *SPP*, a bit is encoded if its location is not significant, but at least one of its eight-connected neighbors is significant. In *MRP*, all bits from locations that became significant in a previous bit plane are encoded. The *CUP* pass takes care of the bits of a bit plane which are not encoded in the first two passes.

In *JPEG*2000 encoder, *Tier*-1 is followed by *Tier*-2 encoding. The input to the *Tier*-2 encoding process is the set of bit plane coding passes of each code block generated during *Tier*-1 encoding. In *Tier*-2 encoding, the coding pass information is packaged into data units called packets, in a process referred to as packetization. Packets from all subbands are then collected in so-called layers. The way the packets are built up from the code block coding passes, and thus

which packets a layer will contain, is not defined by the *JPEG*2000 standard, but in general a codec tries to build layers in such a way that the image quality will increase monotonically with each layer, and the image distortion will shrink from layer to layer. Thus, layers define the progression by image quality within the code stream of a compressed image.

1.9 Deficiencies in *JPEG*2000

*JPEG*2000 standard has better performance as compared to *JPEG* and many new features are supported by this standard. However, there are some deficiencies in *JPEG*2000 standard. We have explored some of these deficiencies.

Owing to its advantages, such as multiresolution representation, good energy compaction, and decorrelation, *DWT* has become one of the important techniques for image and video compression in the last decade and has been adopted by *JPEG*2000 standard (Taubman, 2000; Mandal and Panchanathan, 2000; Mittal *et al.* 2008).

The wavelet based *JPEG*2000 not only presents superior coding performance over the *DCT* based *JPEG*, but also provides scalability in rate, quality and resolution. Conventionally, 2-*D DWT* is carried out as a separable transform by cascading two 1-*D* transforms in the horizontal and vertical direction. *DWT* can be efficiently implemented by the lifting scheme (Vetterli and Kovacevic, 1995; Brislawn, 1996; Daubechies and Sweldens, 1998; Calderbank *et al.*, 1998; Taubman, 1999; Jianfen and Zhengming, 2001; Jansen and Oonincx, 2005), where the wavelet filters are factored into several lifting steps, referred as split, predict, update, and normalize, respectively. Although very efficient in representing horizontal and vertical edges, this kind of lifting structure does not work well when the edges are neither horizontal nor vertical. As a matter of fact, natural images often contain significant direction information, which can be commonly approximated as linear edges on a local level. These edges may neither be horizontal

nor vertical. If not taken into account, such a fact will result in large magnitude in these high frequency coefficients. Owing to this, the compression ratio may be less in case of lossless image compression and *PSNR* may degrade in case of lossy image compression.

As explained above, *JPEG*2000 allows an image to be divided into rectangular blocks of same size called tiles, before compressing the image. In compression process of *JPEG*2000 encoder, equal bit rate is assigned to each tile of the image. This assignment is suitable for the images with information contents equally distributed throughout the image. However, tiles of an image may have different complexities. Some of the tiles may have larger texture area while others may have larger smooth area. The quality of a reconstructed image varies a lot if all the tiles in an image do not have same complexity. As stated earlier, tiling gives better memory utilization and better access under certain circumstances. It can significantly reduce the complexity on the encoder side. It is also useful in handling high resolution images. A difficulty that tiling introduces is the blocking artifacts that are significant when the images are compressed at low bit rate using *JPEG*2000 coding system.

In image and video coding, rate control is necessary to control the bit rate of an image/video such that it meets the channel bandwidth or end to end delay requirement. The main objective of implementing rate control is to allocate the target bit rate to an image/video so that overall distortion is minimized. *JPEG*2000 uses *EBCOT* to control the bit rate requirement. Optimized truncation is the rate control process that minimizes the rate distortion for a given bit rate. This process is applied after all the wavelet coefficients have been entropy coded and is referred to as Post Compression Rate Distortion (*PCRD)* optimization. *PCRD* optimization uses Lagrange optimization to control the rate precisely while maximizing the image quality. There are two possible directions for improving *PCRD* optimization scheme. Firstly, the computational power,

which is a function of contexts to be processed, is wasted since the source image must be lossless coded regardless of the target bit rate. Second, the memory requirement, which is measured by the amount required to buffer the bit streams until the truncations are determined, is large since all the bit streams, including those that are discarded finally, must be buffered until the transaction points are determined by the *PCRD* optimization. The solutions to these deficiencies in *JPEG*2000 standard have been proposed in the work presented in this thesis. We have addresses four potential deficiencies and have proposed algorithms to improve upon the existing algorithms implemented in *JPEG*2000 standard.

1.10 Outline of the Thesis

This thesis consists of seven chapters. Current chapter introduces the problem tackled in this thesis and also introduces the fundamentals related to the problem. In Chapter 2, literature survey related to *JPEG*2000 is carried out. This literature review has been carried out for edge adaptive lifting scheme, weighted bit rate allocations in *JPEG*2000, tile boundary artifacts reductions in *JPEG*2000, and rate distortion optimization in *JPEG*2000, separately. In Chapter 3, we have proposed an Edge Adaptive Wavelet Lifting scheme which can represent the edges present in an image efficiently. In this approach, the lifting direction is not restricted to horizontal and/or vertical directions only, but other lifting directions are also used if the edges present in an image are neither in horizontal nor in vertical direction. This approach represents the decomposed image more efficiently because there are less numbers of wavelet coefficients having large magnitude in the high pass subbands. Due to this approach, the energy of the high pass subbands decreases and these subbands are represented efficiently. So *PSNR* and visual quality of the reconstructed image increases.

In Chapter 4, a post-processing methodology has been proposed that can be applied along with *JPEG*2000 standard for reducing tile boundary artifacts of *JPEG*2000 compressed images. The methodology is motivated by the higher error in high pass reconstructed boundary samples than low pass reconstructed boundary samples. It has been shown that when one uses proposed method, tile boundary artifacts are reduced in terms of increase in *PSNR* value of the reconstructed images. The reductions in boundary artifacts have also been observed in visual quality of decompressed images.

In Chapter 5, an approach related to the rate allocation to the tiles of an image has been proposed. In *JPEG*2000, all tiles are assigned equal rate irrespective of their content. But in real time applications, all tiles do not have equal complexity. Some of the tiles have more smooth area while other tiles have more complex region. So there is a need to consider the complexity of a tile while assigning the bit rate to a tile of an image. We have proposed a weighted approach to assign the bit rate to a tile. The weights are calculated using the zero-order entropy of a tile. Using this approach, upto 2 *d*B improvement in *PSNR* has been achieved.

In Chapter 6, an efficient rate control approach for *JPEG*2000 encoder is proposed. In this approach, optimal *RD* slope threshold is selected using the minimum *RD* slope of lower level horizontally and vertically low pass (LL_0) subband of the wavelet decomposed image. Also, the passes of the code blocks of other subbands, whose *RD* slopes are less than the optimal *RD* slope, are skipped. The proposed approach reduces memory requirements and encoding time when compared with the existing rate control approaches for *JPEG*2000 standard and also provides the same image quality as that of *PCRD* approach used in the *JPEG*2000 standard.

Chapter 7 concludes the work done in this thesis. This also includes the main results from previous chapters. Contribution of the thesis in the area of image compression and future scope of work in this direction has also been included in this chapter.

Chapter 2

Literature Survey

2.1 Introduction

In this chapter, we shall review the literature related to the improvements in the processes of *JPEG*2000 standard. We have surveyed these processes and that lead us to the formulation of problems we have solved in this thesis. The comparative results given in this chapter are the results reported in the research papers reviewed in this work. Sections 2.2-2.5 of this chapter contain the review of work done. Section 2.2 contains the literature review related to the edge adaptive lifting schemes proposed in the literature. Section 2.3 deals with the literature review related to the artifacts reduction in *JPEG*2000 compressed images. Section 2.4 deals with the literature review related to the weighted bit rate allocation in *JPEG*2000 standard and section 2.5 presents the literature review related to the rate distortion optimization in *JPEG*2000 standard.

2.2 Edge Adaptive Lifting Scheme in *JPEG*2000

2-*D DWT* used in *JPEG*2000 coder is applied as a separable transform by cascading two 1-*D* transforms, which are applied along the vertical and the horizontal directions. An important shortcoming of this approach is that it fails to provide an efficient representation for the images that have sharp edges and textures which are not aligned along the vertical and horizontal

directions. It results into a large amount of signal energy in high-pass subbands. As a result, the ringing effects around edges can be observed clearly at low bit rates, when the images are decompressed.

Taubman and Zakhor (1994) proposed an adaptive wavelet transform based approach that adapts transform directions to the image content and utilizes orientation of local image features to avoid the highly objectionable Gibbs-like phenomena observed in reconstructed image at low bit rates. In this approach, the image is partitioned into blocks and each block is then sheared through a reversible resampling filter such that the edges in the sheared block are oriented either vertically or horizontally. Then conventional 2-*D DWT* is applied to the sheared block. The subjective image quality obtained by their approach is considerably enhanced over the conventional separable subband coding scheme, as well as other approaches including the scheme used in *JPEG* compression standard.

Wavelet based image coding algorithms, both lossy and lossless, use a fixed perfect reconstruction filter bank for coding and decoding all kinds of images. This generic approach of filter selection and usage may not always give the best compression from the viewpoint of a specific application. However, no systematic study has been done to see if using different wavelet filters for different image types improves the coding performance or not. To explore this problem, Saha and Vemuri (1999) used a variety of wavelets to compress different images at different compression ratios. They reported that the performance in lossy coders is image dependent and while some wavelet filters perform better than others depending on the image being coded, no specific wavelet filter performs uniformly better than others on all test images. This observation leads to the hypothesis that both for lossy and lossless compression, the most appropriate wavelets should be chosen adaptively depending on the statistical nature of image

being coded in order to achieve better compression. Saha and Vemuri (1999) also proposed some image features like spatial features, transform features, edge features to select the adaptive filter to compress the multimedia images.

Gouze *et al.* (1999) proposed a method to construct the quincunx wavelet transform which is the bidimensional extension of factorization of a wavelet transform into a lifting scheme for finite and symmetrical low pass filters. The objective of their method is to process quincunx images with appropriate transforms while using advantages offered by the lifting scheme.

Saha *et al.* (2000) proposed a lossy image coding to choose wavelet filters adaptively to match the image being encoded. Log energy entropy, variance and range of the wavelet coefficients of the combined subbands are important features proposed by them for determining appropriate wavelet filter to be used in compressing an image so that the best *PSNR* can be obtained.

Pennec and Mallat (2000) proposed a sparse image representation to take advantage of the geometrical regularity of edges present in images. A new class of one-dimensional wavelet orthonormal bases, called foveal wavelets, are introduced to detect and reconstruct singularities. Foveal wavelets are extended in two dimensions in order to follow the geometry of arbitrary curves. The resulting two dimensional bandelets define orthonormal families that can restore close approximations of regular edges with few non-zero coefficients. Edges are coded with quantized bandelet coefficients, and a smooth residual image is coded in a standard two-dimensional wavelet basis.

In most of filter banks, it is desired to obtain subsampled signals corresponding to different spectral regions of the original data. Gerek and Cetin (2000) proposed an adaptive filter bank with perfect reconstruction property. They proposed that there is no need to select a predetermined filter in different regions of the image because the proposed adaptive subband

decomposition scheme inherently updates the filter banks and finds ideal filters for each signal sample while preserving the reconstruction property. The proposed method produces visually better results by eliminating ringing artifacts. Specifically, for the images that contain sharp variations such as text, subtitles and graphics, their method outperforms existing methods in experimental studies.

Florido *et al.* (2001) proposed a new method for artifact reduction of upsampled multidimensional data. Their method is based on first upsampling the image data with conventional optimal Sinc interpolation and then applying a local filter that reduces the high frequencies associated to the ringing artifacts along the edges while leaving unchanged the directions orthogonal to them. The method is suitable when dealing with medical images that contain small structures, such as thin bones in an image**.**

Cohen and Matei (2001) presented a nonlinear and nontensor product approach which is adapted to the geometric fitting of the edges. The artifacts can be eliminated with this approach due to the tensor product and improve the visual quality of the *N* terms approximation. The associated transforms are inherently nonlinear and nontensor product, in contrast to classical wavelet basis decompositions over which they exhibit visual improvement in terms of compression. This approach can be viewed as a bridge between edge detection and the nonlinear multiresolution representations.

Guangjun *et al.* (2001) proposed new symmetric biorthogonal 9/7-tap wavelet based on a lifting scheme and the construction theorem of biorthogonal wavelets. Compared to *CDF* 9/7 wavelet adopted by *JPEG*2000, when the new wavelet is applied to image coding, the compression performance is exactly the same as that of the *CDF* 9/7 wavelet, while computational complexity

is reduced remarkably. The simulation shows that the new biorthogonal 9/7-tap wavelet is a very ideal alternative to *CDF* 9/7 wavelet.

Boulgouris *et al.* (2001) obtained optimal predictors of a lifting scheme. To enhance the efficiency of linear predictions, the scheme is applied for the lossless compression of still images using quincunx sampling and simple row–column sampling. Directional post-processing is used in the quincunx case, and adaptive-length post-processing in the row–column case. They further investigated context modeling and adaptive arithmetic coding of wavelet coefficients in a lossless compression framework, particularly to the modelling contexts and the adaptation of the arithmetic coder to the actual data. Experimental evaluation shows that the proposed lifting scheme performs better than the existing lifting schemes for lossless image coding.

Piella *et al.* (2002) proposed a class of adaptive update lifting schemes that do not require bookkeeping for perfect reconstruction. The choice of the update lifting filter is triggered by a binary threshold criteria based on a generalized gradient that is chosen in such a way that it only smooths homogeneous regions. The criteria can be chosen so that it ignores portions of a signal that are polynomial up to a given order. The update lifting filter modifies the signal in these polynomial regions but leaves other portions unaffected.

Piella and Heijmans (2002) proposed a framework for constructing adaptive wavelet decompositions using lifting scheme. It is assumed that the update filter utilizes local gradient information to adapt itself to the signal in the sense that smaller gradients evoke stronger update filters. As a result, sharp transitions in a signal will not be smoothed to the same extent as regions that are more homogeneous. In this framework, no bookkeeping is required in order to have perfect reconstruction.

Vargic (2002) proposed a new type of directional wavelet transform based on lifting scheme and quincunx sampling. Based on known separable wavelet predictors, they built a novel type 2-*D* wavelet transform with strong directional properties from 1-*D* prototype using lifting scheme. The resulting wavelet transform is applied on motion blurred images.

In a large number of applications of image and video, it would be useful to have a wavelet decomposition that take into account the characteristics of the image data. Considering this, Heijmans *et al.* (2002) proposed a method for the construction of nonlinear 2-*D* wavelet decompositions using an adaptive update lifting scheme. This method does not require any bookkeeping but it allows perfect reconstruction.

A new two-dimensional approach is proposed by Velisavljevic *et al.* (2002) which allows more directionalities than the horizontal and vertical. The proposed approach can be applied in many areas like denoising, nonlinear approximation and compression. The results on nonlinear approximation and denoising show interesting gains compared to the standard two-dimensional analysis.

Motion-compensated temporal wavelet decomposition is a framework which is used for fully scalable video compression schemes. The ghosting artifacts in low-pass temporal subbands may appear when a video is compressed using wavelet transform. Mehrseresht and Taubman (2003) proposed an approach to reduce these artifacts. In this scheme, the update steps are adaptively weighted according to the energy in the high-pass temporal sub-bands at the corresponding location. Experimental results show that the proposed algorithm can substantially remove ghosting from low-pass temporal frames. Importantly, at full frame-rate, the proposed algorithm has similar performance to the original motion-compensated temporal decomposition, with superior performance where the motion model fails significantly. While entirely skipping the

update steps accomplishes a similar objective, we show that the proposed method for adaptively weighting the update steps has better performance, especially in the presence of additive noise. Since the compressed bit-stream is scalable, the decoder does not generally have exactly the same information which the encoder used to determine weights for the update steps. Nevertheless, the proposed method exhibits good robustness to quantization error.

Claypoole *et al.* (2003) proposed a non linear wavelet transform for image coding using lifting scheme and also described how earlier families of nonlinear filter bank can be extended through the use of prediction functions operating on a casual neighbourhood of pixels. In this scheme, the update first scheme is used to maintain control over the multi-resolution properties of the wavelet transform despite the presence of these nonlinearities. In this scheme, they introduced an algorithm that switches between various linear predictors to avoid predicting across edges. This algorithm efficiently represents edges and compacts energy into coefficients of lower subbands of the wavelet transform. In addition, they employed a 2-*D* nonseparable window to make better predictor choices. This scheme provides some improvements while maintaining synchronization between the encoder and decoder. The adaptive lifting transform used in this scheme appears promising for lossy compression. It reduces edge artifacts and ringing, and improves *PSNR* performance on certain test images.

Christophe *et al.* (2004) proposed a lifting scheme in which predict operator uses two motion vector fields to bidirectionally predict frames from their neighbouring ones. They also proposed an optimal algorithm to estimate jointly these two motion vector fields subject to an optimization criterion directly related to the coding of the detail subbands and this algorithm provides substantial gains in terms of *PSNR*, with the same complexity as a separate estimation of the two motion vector fields.

A framework for adaptive generalized lifting filters has been proposed by Gouze *et al.* (2004). To design lifting filters to compute a multidimensional nonseparable wavelet transform, the approach enables the design of less expensive filters adapted to the data statistics to enhance the compression efficiency in a more general case. It is based on a two steps lifting scheme and joins the lifting theory with Wiener's optimization. The prediction step is designed in order to minimize the variance of the signal, and the update step is designed in order to minimize the reconstruction error.

Feng *et al.* (2004) introduced the energy distributed update steps for the temporal transform in lifting based motion compensated video coding. Their idea is to update where prediction is made by distributing high-pass signals to the low-pass frame. The scheme avoids complex and inaccurate inversion of the motion information that used in the traditional update steps, thus it reduces computations in temporal transform. Experimental results show that the coding performances can be improved up to 0.77 *d*B.

A generalized lifting scheme is introduced by Sole and Salembier (2004), in which the sums included in classical lifting scheme are generalized to include possibly nonlinear and/or adaptive operations. Experiments with a generalized prediction step are reported by them.

A novel lifting based joint compression/classification coder has been proposed by Fahmy and Panchanathan (2004). The proposed coder is based on bi-orthogonal filters and can operate in a scalable compression framework. A Lagrangian multiplier has been employed to achieve the best trade-off between compression and classification performance. The coder achieves a superior compression performance at a fixed classification rate or the best possible classification for a fixed compression rate. Simulations have been performed to demonstrate the compression and/or classification performance of the system in the context of the recent image compression standard,

namely *JPEG*2000. Simulation results show that the lifting based kernels generated from the proposed system are capable of achieving superior compression performance compared to the default kernels adopted in the *JPEG*2000 standard (at a classification rate of 70%). The generated kernels can also achieve a comparable compression quality with the *JPEG*2000 kernels whilst providing a 99% classification performance. In other words, the proposed lifting based system achieves the best trade off between compression and classification performance at the compressed bit-stream level in the wavelet domain.

Ding *et al.* (2004) proposed a Directionally Spatial Prediction (*DSP*) into the conventional lifting-based wavelet transforms and proposes a novel, efficient and flexible lifting structure. Each lifting stage can be performed at the direction, where pixels have a strong correlation, rather than always at the horizontal or vertical direction. The proposed *DSP* enables the predicting and updating process at the fractional pixel without any constraint on the interpolation, which fully exploit the spatial correlation among pixels. Furthermore in the 2-*D* transform, the direction of the first 1-*D* transform is no longer requested to be vertical to that of the second so that the second 1-*D* transform can utilize the spatial correlation better. The proposed *DSP* lifting guarantees the perfect reconstruction. We also investigate the techniques to efficiently estimate and code the directional data, thus increasing the precision of spatial prediction and reducing the overhead bits. Experimental results have shown that the proposed *DSP* lifting scheme can significantly outperform *JPEG*2000 in terms of *PSNR* (up to 2*d*B) and visual quality.

Tillier *et al.* (2005) have shown that it is possible to apply any transformation to the set of coefficients connected with a single pixel in the reference frame while preserving the perfect reconstruction of the scheme. In this study they considered different methods for efficient

processing of multiple connected pixels and proved that rather than choosing a single pixel for performing the update, averaging all the connected pixel leads to decrease the reconstructed error globally and also individually on most of the pixels involved in the spatiotemporal filtering. The theoretical results have been confirmed by simulation both on two band and three band motion compensated temporal filtering coders,

The issue of dynamic calculation of the optimal predictors in the sense of minimizing the prediction error variance is addressed by Li *et al.* (2005). They proposed a novel lifting integer wavelet transform based on Difference Correlation Structure (*DCS*) for finding the optimal lifting coefficient. First, a relationship between the performance of a linear predictor and the difference correlations of an image is established. Then, based on the lifting scheme, the effective prediction and update coefficients are derived in terms of correlation function. *DCS* lifting transform puts heavy emphasis on image inherent dependence. A distinct feature of this method is the use of the variance-normalized autocorrelation function of the difference image to construct a linear predictor and adapt the predictor to varying image sources. The proposed scheme also allows respective calculations of the lifting filters for the horizontal and vertical orientations. Experimental evaluation shows that the proposed method produces better results than the other well-known integer transforms for the lossless image compression

Chang *et al.* (2005) proposed a novel adaptive wavelet transform that exploits local image properties for image compression. It combines wavelet filters adaptive to edge orientations with quincunx subsampling to form a 2-*D* nonseparable transform through lifting. Significant improvement on both subjective and objective quality over the conventional separable transform is observed when this technique is used.

The conventional 2-*D* wavelet transform used in existing image coders is usually performed through 1-*D* filtering in the vertical and horizontal directions, which cannot efficiently represent edges and lines in images. Wang *et al.* (2005) proposed a curved wavelet transform in which transform is carried out by applying 1-*D* filters along curves present in image, rather than being restricted to vertical and horizontal directions. These curves are determined based on image content and are usually parallel to edges and lines in the image to be coded. The pixels along these curves can be well represented by a small number of wavelet coefficients. The results show significant improvement for images that contain a fair amount of sharp edges and lines. A new image coder has also been proposed by Wang *et al.* (2006) using curved wavelet transform. The code-stream syntax of the new coder is the same as that of *JPEG*2000, except that a new marker segment is added to the tile headers. Results of image coding and subjective quality assessment show that the new image coder performs better than *JPEG*2000. It is particularly efficient for images that contain sharp edges and can provide a *PSNR* gain of up to 1.67 *d*B for natural images when compared with *JPEG*2000.

Chang and Girod (2006) proposed an adaptive lifted discrete wavelet transform to locally adapt the filtering direction to the geometric flow in the image. Additionally, a bandeletization procedure is combined with directional lifting in a unified framework to further remove the correlation in the wavelet coefficients. Up to 2.8 *d*B improvement in *PSNR* over the conventional 2-*D CDF* 9/7 wavelet transform for natural images is reported by them.

Wu and Li (2006) proposed a system that provides an efficient scheme to code images and video by exploiting spatial correlations within an image by employing hybrid directional prediction and lifting wavelet techniques. In each lifting stage, the predicting and updating signals do not always come from horizontal or vertical samples as they do in other lifting schemes. The

predicting and updating signals can be selected along image linear edges so as to reduce the magnitude of high pass coefficients.

2-*D* edge adaptive lifting scheme, which is similar to Daubechies 5/3 wavelet, is proposed by Gerek and Cetin (2006). The 2-*D* prediction filter used in this lifting scheme predicts the value of the next polyphase component according to an edge orientation estimator of the image. Consequently, the prediction domain is allowed to rotate ±45˚ in regions with diagonal gradient. The gradient estimator is computationally inexpensive with additional costs of only six subtractions per lifting instruction, and no multiplications are required.

To efficiently capture geometrical structures characterized by directions other than horizontal and vertical directions, Velisavljevic *et al.* (2006) presented a transform based on partitioning of the discrete space using integer lattices, where 1-*D* filtering is performed along lines across the lattice. Their transform retains the separable filtering and subsampling and the simplicity of computations and filter design from the standard two-dimensional wavelet transform, unlike in the case of some other directional transform constructions (*e.g.*, curvelets, contourlets, or edgelets). The corresponding anisotropic basis functions are called directionlets. They showed that proposed transform has good approximation properties and is superior to the performance of the standard separable 2-*D* wavelet transform having the same complexity.

An embedded wavelet-based coder is proposed by Fowler *et al.* (2007) to exploit the directional selectivity of a 2-*D* complex dual-tree discrete wavelet transform. Although the dual-tree transform is redundant, a noise-shaping process increases the sparsity of the transform coefficients, resulting in a high degree of spatially coherent regions of insignificant coefficients. The transform coefficients are coded with binary set-partitioning using *k* dimensional trees, and

experimental results reveal rate-distortion results superior to the state-of-the-art *JPEG*2000 standard at low bitrates, particularly for images with strong directional features.

A 3-*D* subband coding via Motion Compensated Temporal Filtering (*MCTF*) using biorthogonal filters for video coding is proposed by Golwelkar and Woods (2007). In this coding, the forward motion field is used for *MCTF* with quarter pixel accuracy for both predict and update step of lifting scheme. They estimate and transmit a forward motion field between every consecutive frame and infer the backward motion field from this forward motion field. The objective is to trace motion vectors in the given group of pictures and do the temporal filtering along this subpixel motion trajectory. The proposed coding scheme reduces the motion vector bit rate by 10%-20% for Haar and 15%-30% for 5/3 *MCTF*.

Direction Adaptive *DWT* (*DA-DWT*) based on directional lifting is proposed by Chang and Girod(2007) which differs from other lifting based approaches in such a way that the directional filters in *DA-DWT* provide a more efficient representation for sharp features in the image. In addition, it requires less computation and the compression performance is less sensitive to image transposition. A mathematical analysis based on an anisotropic statistical image model is also presented to quantify the theoretical gain achieved by adapting the filtering directions. The analysis indicates that proposed *DA-DWT* is more effective than other lifting-based approaches. Experimental results report a gain of up to 2.5 *d*B in *PSNR* over the conventional *DWT* for typical test images. Subjectively, the reconstruction from the *DA-DWT* better represents the structure in the image and is visually more pleasing.

The generalized lifting framework allows the definition of nonlinear filter banks with perfect reconstruction. Rolon and Salembier (2007) investigated the use of generalized lifting to increase the sparseness of wavelet decompositions with application to image representation and coding.

As in the bandelet approach, the strategy proposed by them first applies separable wavelet decomposition and then process the details subbands to further decorrelate the signal representation. For second step, generalized lifting is used which allows nonlinear processing of the details subbands. In their work, the generalized lifting design is based on the probability density function of the details coefficients after the separable wavelet decomposition and its goal is to minimize the coefficients energy. This generalized lifting is shown to reduce the energy and the entropy of the subbands significantly. Furthermore, a simple quantification and entropy coding strategy has been proposed by them to compare the rate-distortion characteristics of wavelet.

Xu *et al.* (2007) proposed a lifting based 2-*D DCT* that can be implemented by separable 1-*D* transform in horizontal and vertical directions by taking image orientation features in a local window into account. The transform matrix of *DCT* is dependent on directional angle and interpolation used there. A *JPEG* image coding scheme is also proposed by them in order to evaluate the performance of proposed directional *DCT* like transform. In their scheme, first 1-*D* transform is performed according to image orientation features, and the second 1-*D* transform is still performed in the horizontal or vertical direction. Their experimentation shows that the performance of proposed directional *DCT* like transform can dramatically outperform the conventional *DCT* up to 2 *d*B even without modifying entropy coding. This approach is, however, not applicable for *JPEG*2000.

Ding *et al.* (2007) proposed an Adaptive Directional Lifting (*ADL*) based wavelet transform scheme which locally adapts the filtering directions according to the local properties of the image. In their scheme, instead of using the conventional interpolation filter for the directional prediction with fractional pixels accuracy, a new two-dimensional nonseparable adaptive

interpolation filter is proposed. The adaptive filter is calculated for every fractional-pel direction so as to minimize the energy of the prediction error. The tradeoff between reducing the prediction error and the overhead to code the interpolation filter has also been discussed by them. This enables coding gains of up to 0.98 *d*B, compared to *ADL* coder, and up to 2.4 *d*B, compared to the *JPEG*2000 for test images.

Zhang *et al.* (2008) proposed a multi-description coding scheme for images. Two side descriptions of the input image are generated by quincunx subsampling. The image decoding from a side description is performed by an interpolation process that exploits pixels' correlation. They have concluded that one side description is not amenable to existing image coding techniques. They overcome this difficulty with the help of *ADL* scheme as it is particularly suitable for decorrelating image pixels on the quincunx lattice.

Chang and Girod (2008) proposed a direction-adaptive block transform that exploits the directionality in images to improve the compression performance. This transform is the generalization of variable block-size transforms with the inclusion of non-rectangular partitions and directional transforms. As a block transform, it is directly combined with block-wise intra and inter prediction in video coding standards. Their experimental results show that the proposed transform outperforms the variable block-size 2-*D DCT* by up to 3 *d*B.

The problem of evaluating the reconstruction distortion in the wavelet domain is studied by Parrilli *et al.* (2008) when Adaptive Lifting Schemes (*ALS*) are used for the direct and inverse transform. The distortion evaluation is necessary in order to perform efficient resource allocation over the transform coefficients. *ALS* is a non-linear transformation that prevents using common techniques for distortion evaluation. Authors generalized the distortion computation technique to

it. Their experiments show that proposed method allows a reliable estimation of the distortion in the transform domain. This also resulted in improved coding performance.

In order to improve *ADL* scheme, Hui and Siu (2008) proposed a new directional angle coding scheme which uses the context-based adaptive binary arithmetic coding algorithm to code the prediction error by taking the direction information into account. Experiments performed by them reveal that performance of the *ADL* is improved up to 0.13 dB.

As, *ADL* based wavelet transform locally adapts the filtering directions to the local properties of the image. Instead of using the conventional interpolation filter for the directional prediction with fractional-pel accuracy, a new two-dimensional nonseparable adaptive interpolation filter is proposed by Dong *et al.* (2008). The adaptive filter is calculated for every fractional-pel direction so as to minimize the energy of the prediction error. This enables coding gains of up to 0.98 *d*B, compared to *ADL* coder, and up to 2.4 *d*B, compared to the *JPEG*2000 for test images.

Liu and Ngan (2008) proposed a new Weighted Adaptive Lifting (*WAL*) based wavelet transform which is designed to address the solutions to the problems in the *ADL* approach, such as mismatch between the predict and update steps, interpolation favouring only horizontal or vertical direction, and invariant interpolation filter coefficients for all images. The contribution of their approach is 2-fold: one is the improved weighted lifting, which maintains the consistency between the predict and update steps as far as possible and preserves the perfect reconstruction at the same time; another is the directional adaptive interpolation, which improves the orientation property of the interpolated image and adapts to statistical property of each image. Experimental results given by them show that the proposed *WAL* based wavelet transform for image coding outperforms the conventional lifting-based wavelet transform up to 3.06 *d*B in *PSNR* and

significant improvement in subjective quality is also observed. When compared with the *ADL* based wavelet transform, up to 1.22 *d*B improvement in *PSNR* is also reported by them.

Quan and Ho (2009, 2011) proposed a lifting scheme in which appropriate filter coefficients are selected and a median filter is employed to regard image edges. Experimental results given by them show that *PSNR* value of their scheme is improved by 0.75 *d*B as compared to the conventional lifting scheme of *JPEG*2000.

Hung and Hang (2009) proposed an adaptive wavelet coding scheme in which a decision method is used to identify whether the *LH*, *HL*, and *HH* wavelet subbands are suitable for directional decomposition. The basic concept behind this decision method is to detect the large impulses in the frequency domain. The transformed data are coded by the bit-plane arithmetic code to achieve scalability. Experimental results given by them show that this adaptive scheme has better results wavelet based contourlet scheme that applies the directional transform to all the *LH*, *HL* and *HH* subbands.

Peng *et al.* (2009) proposed the directional filtering transform to better exploit intra-frame correlation in *H*.264 intra-frame coding. It consists of a directional filtering and an optional *DCT* transform. In their directional filtering, there are two different approaches. One is the Uni-Directional Filtering (*UDF*) that is similar to *H*.264 directional intra prediction. In this approach, only samples from neighboring blocks can be used in prediction. Another is Bi-Directional Filtering (*BDF*) that exploits the correlations among samples from not only neighboring blocks but also the current block. The prediction structure in their approach is hierarchical multi-layer.

Pixel-wise direction estimation is used by Murakami *et al.* (2010) to decompose an image hierarchically into direction-adaptive subbands. The input image is divided into two parts: a base image subsampled from the input image and subband components. The subband components

consist of residuals of estimating the pixels skipped through the subsampling, which ensures the invertibility of the decomposition. The estimation is performed in a direction-adaptive way, whose optimal direction is determined by a L_1 norm criterion for each pixel, aiming to achieve good energy compaction that is suitable for image coding. Furthermore, since the L_1 norms are obtained from the base image alone, there is no need to retain the directional information explicitly, which is another advantage of our model. Their experiment shows that the proposed model can achieve lower entropy than conventional Haar or Duabechies 5/3 discrete wavelet transform in case of lossless coding.

Using the anisotropic model, Peng *et al.* (2010) analyzed the effect of transform orders in terms of theoretical coding gains. On the basis of this analysis, they proposed a directional filtering transform to better exploit correlations among samples in *H.*264 intraframe coding. This transform provides an evenly distributed set of prediction modes with an adaptive transform order. Both interblock and intrablock correlations are exploited in this scheme.

Satyabama and Annadurai (2010) proposed an adaptive lifting scheme in which prediction techniques based on the local properties of the image are used. This adaptive lifting scheme appears promising for image compression. It reduces edge artifacts and gives improved *PSNR* for edge dominated images.

Quan *et al.* (2011) proposed a lifting scheme in which the filter coefficients are selected and then median operator is used to regard the edges present in the images. They have reported an average *PSNR* gain of 0.75 *d*B over the conventional lifting scheme used in *JPEG*2000 standard.

A new adaptive wavelet transform using lifting scheme has been presented by Han *et al.* (2011). The proposed transform uses interpolating method to construct predict and update type lifting scheme based on the optimal criteria. Their scheme adaptively matches the property of local data

of the image at each scale. The novel framework introduced by them chooses the most suitable predictor and updater respectively, which differs from other adaptive methods making only one step adaptive. Experiments performed by them reveal that the proposed transform is efficient and demonstrate the potential utility of the new adaptive wavelet transform.

Kaaniche *et al.* (2011) proposed a 2-*D* non-separable lifting scheme that still enables progressive reconstruction and exact decoding of images. The prediction operator is designed by them by minimizing the variance of the detail coefficients.

With the objective of promising sparsity in a transform domain, Kaaniche *et al.* (2012) investigated techniques for optimizing sparsity criteria, which can be used for the design of all the filters defined in a non separable lifting structure. It should be noted that sparsest wavelet coefficients could be obtained by minimizing an ℓ_0 criterion. However, such a problem is inherently nonconvex and NP-hard. Unlike previous studies where prediction has been separately optimized by minimizing an ℓ_2 criterion, they used ℓ_1 criterion. Since the output of a prediction filter may be used as an input for the other prediction filters, such a filter is optimized by minimizing a weighted ℓ_1 criterion related to the global rate-distortion performance. More specifically, it will be shown that the optimization of the diagonal prediction filter depends on the optimization of the other prediction filters and vice-versa. Related to this fact, it is proposed to jointly optimize the prediction filters by using an algorithm that alternates between the optimization of the filters and the computation of the weights. Experimental results show the benefits which can be drawn from the proposed optimization of the lifting operators. But the proposed technique is nonseparable.

2.3 Artifacts Reduction in *JPEG*2000 Compressed Images

A good number of researchers have worked on reducing the tile boundary artifacts of *JPEG*2000 compressed images. Berkner and Schwartz (2002) proposed a detiling solution for wavelet based compressed images with an objective of modifying an image at the tile boundaries such that the image quality near those boundaries matches the quality inside of a tile. Their approach takes into account the four components that influence tile boundary artifacts: wavelet filters, maximal decomposition level, quantization and location of tile boundaries. Their solution eliminates the blocking artifacts by computing approximations that match the smoothness of the compressed image inside of a tile and is applicable to any wavelet filter specifically targets use in decoding of *JPEG*2000 compressed images. They have noted that it is very difficult to apply pre-processing while implementing the encoder, in order to reduce tiling artifacts.

A robust subband decomposition, which can deal with the problem of discontinuities between the tile boundaries without computational overheads and excessive memory requirements, is developed by Kharitonenko *et al*. (2002). They have proposed low complexity wavelet transform method which uses a point symmetric extension method in place of symmetric extension method of *JPEG*2000 standard, for improving the image quality. The lifting-based implementation of the filters used by them provides a very simple way of changing filter parameters at the boundaries that suits both hardware and software platforms. They have shown that visual quality of the decompressed images by using the point-symmetric extension as boundary extension in *JPEG*2000 is significantly better, but the obtained *PSNR* values is same as that of *JPEG*2000 standard.

A close examination of the wavelet transform has also been carried out by Wei *et al.* (2005) and it is shown that tile boundary artifacts are an inescapable consequence of the usual methods used

to choose tile size and the type of symmetric extension of the image data for decomposition. They proposed a novel method for reducing these tile-boundary artifacts. Their method employs odd tile sizes rather than the conventional even tile sizes. It has been shown by them that for the same bit rate, an image compressed using an Odd Tile Length Low Pass First (*OTLPF*) convention has significantly less boundary artifacts than an image compressed using even tile sizes. The *OTLPF* convention can also be incorporated into the *JPEG*2000 standard using extensions defined in Part 2 of this standard and not for the basic model.

A few other methods have also been proposed in literature in order to reduce tiling artifacts in wavelet based compression and have been put in two categorized. Methods in first category methods apply post-processing at the decoder side. A common problem with these methods is that they unavoidably introduce blurring, ringing and degrading. The problem of tiling artifacts is addressed by both encoder and decoder by the methods in second category. These methods generally give better performance than pure post- processing methods. Keeping this in view Liang *et al.* (2003) generalized the pre-processing and post-processing philosophy given by Tran *et al.* (2003) to the wavelet based image compression framework. A pre-processing operator is applied at tile boundaries before wavelet decomposition of each tile. Accordingly a post-processing is performed at the tile boundaries after inverse wavelet transform. The property of this method is that pre-processing and post-processing can be performed totally outside of existing *JPEG*2000 framework. It has been shown by them that at low bit rates the proposed post-processing itself is able to reduce the tiling artifacts significantly. The experimental results given by them show that low complexity approach leads to significantly *PSNR* improvement at tile boundaries and the visual quality is also enhanced.

Qin *et al.* (2004) proposed a post-processing approach to reduce tiling artifacts with the help of max-lift wavelet subband decomposition. Their approach is based on similar philosophy as given by Hyuk and Kin (2000) to use wavelet based subband decomposition to remove tiling artifacts in *JPEG*2000 images. However, they used non linear wavelet, namely, morphological max-lift wavelet. The computational complexity is significantly reduced because tile boundary area of an image needs to be processed and this wavelet is based on lifting scheme. Also, their experiments revealed that at low bit rate, image quality is enhanced after post-processing.

Symmetric extension is generally considered to be the main factor in causing tile artifacts; however, Hashimoto *et al.* (2005) showed that the differences in quantization accuracy between tiles are more significant reasons for tiling artifacts at middle or low bit rates. They proposed an effective *JPEG*2000 encoding method for reducing tiling artifacts. An algorithm is also developed by them to predict whether tiling artifacts will occur at a tile boundary in the rate control process and that locally improves quantization accuracy by the post quantization control. Another serious problem of reducing processing time in *JPEG*2000 is also addressed by them and they proposed a method in which the truncation points are predicted using the entropy of wavelet transform coefficients prior to the arithmetic coding. The results given by them confirmed that tiling artifacts are greatly reduced and that the coding process is considerably accelerated.

All these approaches are effective in reducing tiling artifacts of *JPEG*2000 compressed images but there is still a need to reduce these tile boundary artifacts to even lower levels.

2.4 Weighted Bit Rate Allocation in *JPEG*2000

In compression process of *JPEG*2000 encoder, equal bit rate is assigned to each tile of the image. This assignment is suitable for the images with information contents equally distributed

throughout the image. However, tiles of an image may have different complexities. Some of the tiles may have larger texture area while others may have larger smooth area. The quality of a reconstructed image varies a lot if all the tiles in an image do not have same complexity. It is a well known fact that tiling gives better memory utilization and better access under certain circumstances. It can significantly reduce the complexity on the encoder side. It is also useful in handling high resolution images. A difficulty that tiling introduces is the blocking artifacts that are significant when the images are compressed at low bit rate using *JPEG*2000 coding system. This section reviews the literature on this aspect of *JPEG*2000.

Daly *et al.* (2000) have developed two Human Visual System (*HVS*) based approaches for *JPEG*2000 encoded images. These approaches work together to take advantage from the masking properties of the visual system. Using these properties, the degradation of image fidelity could be managed as a function of increasing signal energy and an adaptive quantization scheme could be designed in order to allocate more levels to low amplitude coefficients.

A content dependent approach has been proposed by Battiato *et al*. (2002) that optimizes the visual quality of *JPEG*2000 compressed images using an adaptive approach to assign more bits to regions in which errors are more visible, maintaining the global bit rate unchanged. The approach proposed by them codes the most visually meaningful regions of the image using more bits then those used to code homogeneous zones, leaving the global bit rate unchanged. This approach does not modify the encoder, so the output bit stream is compliant to the *JPEG*2000 standard. The improvement in this approach is more clearly visible at low bit rate only, however no visual quality improvement is observed by them at high bit rate.

Ardizzone *et al.* (2003) proposed an approach for allocating a given bit rate to different image tiles in *JPEG*2000 encoding system, which aims to produce an image of superior quality if the

original image has an Informative Content (*IC*) not equally distributed across the image. The approach proposed by them is based on two observations. First, the information content of a tile is directly proportional to number of encoded bytes resulting from the code blocks coding of that tile. The second is that a number of encoded bytes approximately equal to the half of the number of bytes of the raw tile is obtained encoding the code blocks of one tile with a medium informative content. The results presented by them show that visual quality of decompressed images is better than the one produced with the traditional approach when the information content is not equally distributed across the image, and comparable to the traditional approach, when the information distribution is quite uniform.

Liu and Zhang (2006) proposed an efficient bit rate allocation algorithm for video sequences transmission in Motion *JPEG*2000. The algorithm proposed by them improved the visual quality of a video frame. However, their algorithm is applicable to the Motion *JPEG*2000 video sequences only.

2.5 Rate Distortion Optimization in *JPEG*2000

In image and video coding, rate control is necessary to control the bit rate of an image/video such that it meets the channel bandwidth or end to end delay requirements. The main objective of implementing rate control is to allocate the target bit rate to an image/video so that overall distortion is minimized. In *JPEG* image coding, the rate is controlled by using quantization step sizes or quality factors. However, *JPEG*2000 uses *EBCOT* to control the bit rate requirement. *EBCOT* is the rate control process that minimizes the rate distortion for a given bit rate for the image which is to be compressed. This process is applied after all the wavelet coefficients have been entropy coded and is referred to as *PCRD* optimization. *PCRD* optimization uses Lagrange optimization to control the rate precisely while maximizing the image quality. However, there

are two drawbacks of the *PCRD* optimization scheme. Firstly, the computational power, which is a function of contexts to be processed, is wasted since the source image must be lossless coded regardless of the target compression bit rate. Second, the memory requirement, which is measured by the amount required to buffer the bit streams until the truncation points are determined, is large since all the bit streams, including those that are discarded finally, must be buffered until the transaction points are determined by the *PCRD* optimization (Chen *et al.*, 2001).

A number of rate control approaches for video coding/transmission are investigated by many researcher and these approaches attain fairly good image quality To overcome the above problems, some previous works focus on the computational power and the memory requirement reduction for the *PCRD* optimization.

A technique for the *JPEG*2000 optimal rate allocation problem is by coefficients modeling. Kasner *et al.* (1999) assumed that the wavelet coefficients could be modeled by memoryless generalized-Gaussian density (*GGD*). By estimating the *GGD* parameter, the rate-distortion function can be approximated as required for the optimal rate allocation. This approach is included in Part-2 of *JPEG*2000 and is called Lagrangian Rate Allocation (*LRA*). In this approach, both the rate and distortion are estimated before the wavelet coefficients are actually encoded. A quantization stepsize of each subband is selected based on the estimation and the quantized wavelet coefficients are encoded without any truncation. However, the rate control accuracy depends heavily on the correctness of the *GGD* model assumption and the resulting bit rate can be different from the target value. *LRA* is thus an iterative technique which takes typically many iterations to achieve the target bit rate. In each iteration, the quantization stepsizes are required to be re-estimated and the wavelet coefficients are thus re-quantized and

entropy re-encoded again. The multiple quantization and entropy encoding processes heavily increase the complexity of this approach. In practice, the complexity of *LRA* is comparable to the *PCRD* approach.

Masuzaki *et al.* (2002) proposed an adaptive rate control technique for *JPEG*2000 image coding in embedded systems. Their technique predicts the number of coding passes and updates it adaptively in *Tier*-1 process. The working memory size is reduced by 13% for *JPEG*2000 encoding when their approach is used.

Chang *et al.* (2002) proposed a computation reduction technique for *JPEG*2000 lossy image compression. They used the *Tier*-2 feedback approach to reduce the redundant computation of *Tier*-1 of *EBCOT* process. The authors observed two properties for *RD* slopes. One is the monotonically decreasing property for the values of *RD* slopes in a code block. Second is that all values of the slopes of the included passes in final bit stream are higher than the threshold value after the set of truncation points is obtained. Based upon these observations, the authors proposed the *RD* optimization technique, which reduces the computation time of *Tier*-1 by 20% at high compression rate.

Yeung and Au (2005) proposed three rate control techniques for *JPEG*2000 image coding that efficiently reduce or remove the computation and memory usage redundancy over the conventional post-compression rate distortion method. The first method, called Successive Bit-plane Rate Allocation (*SBRA*), allocates the bit rate by using the currently available rate-distortion information only. The second method, called Priority Scanning Rate Allocation (*PSRA*), is based on the observation that it is possible to achieve optimal rate allocation without knowing the actual value of the *RD* slope. In this technique, the code block's priorities are defined and the code blocks are compressed according to prioritized ordering until the target bit

rate is achieved. This technique encodes a significantly smaller amount of data than *PCRD* but the rate-distortion performance is less than optimal. The third technique uses *PSRA* to achieve optimal truncation as *PCRD* without encoding of all the image details and is called Priority Scanning with Optimal Truncation (*PSOT*). In this, minimum *RD* slope is computed from the encoded data of *PSRA* technique, when the accumulated bit rate is larger than the target bit rate. Then all the feasible truncation points with *RD* slopes greater than or equal to minimum *RD* slope are encoded. Simulation results given by them suggest that the three proposed methods provide different tradeoff among visual quality, computational complexity, and working memory size. *SBRA* is memoryless and causal and requires the least computational complexity, lowest coding delay and achieves good visual quality. *PSRA* achieves higher *PSNR* than *SBRA* at the expense of larger working memory size and longer coding delay. *PSOT* gives the best *PSNR* but requires even more computation, delay and memory.

A fast and efficient rate control technique for computational reduction of *EBCOT* is proposed by Du *et al.* (2004). They observed that a higher bit plane has a higher *RD* slope than the lower bit plane, and the earlier coding pass has a higher *RD* slope than the later coding pass in the same bit plane. The *RD* slope values using look up table have been obtained and the optimal truncation points have been estimated. Each of the code blocks is assigned a priority on the basis of magnitude bit. This priority defines the encoding order of the code blocks. The coding of the code block continues till the target bit rate is not achieved. A large portion of the coding process of all the code blocks are skipped at low bit rate. Thus, computation of *EBCOT* is significantly reduced.

Chang *et al.* (2006) proposed a precompression quality control algorithm for *JPEG*2000 image coding which minimizes bit rate at a given image quality. In their algorithm, the truncation

points are selected before actual coding by the entropy encoder. To predict the truncation points, they used the propagation and randomness property of the embedded block coding.

Chapter 3

Edge Adaptive Lifting Scheme

3.1 Introduction

2-*D DWT* is performed by applying 1-*D DWT* first in the horizontal and then in vertical directions. Lifting Scheme is a method for designing wavelets and it provides efficient implementation of *DWT* as compared to the convolution based *DWT*. Lifting scheme based *DWT* is the second generation wavelet transform which forms the basis of new *JPEG*2000 image compression standard. *DWT* considers horizontal and vertical directions only in image compression, and cannot effectively represent the edges present in the image which are neither horizontal nor vertical. Natural images often contain significant direction information, which may commonly be approximated as linear edges on a local level. These edges may neither be horizontal nor vertical. If these edges are not taken into consideration, it will result in large magnitude in high frequency wavelet coefficients. In this chapter, we have analyzed existing adaptive and directional lifting schemes proposed by different researchers. On the basis of this analysis, we have proposed a new lifting scheme to decompose the images having edges and textures which are neither horizontal nor vertical.

3.2 Lifting Scheme

Lifting scheme, also known as second generation wavelet, is proposed by Sweldens (1996). It is a very general and highly flexible tool for building new wavelet decompositions and does not depend on the Fourier transform. Lifting scheme is efficient, because it takes less computation time and less memory than the convolution based wavelet transform. It is also easily to implement the inverse of transform. In this section, a brief overview of lifting scheme is presented.

Let $x(m,n)$ be a 2-D image data, where m and n are the pixel positions in the image. This data is first decomposed by a 1-D wavelet transform in horizontal direction and then in the vertical direction. Each 1-D wavelet transform can be factored into one or multiple lifting stages depending upon the number of coefficients of wavelet filter. A lifting stage is comprised of four steps – split, predict, update and normalize as shown in Figure 3.1 and illustrated below, in brief.

a. Split: $x(m,n)$ is split into the even subset $x_e(m,n)$ and the odd subset $x_o(m,n)$, where $x_e(m,n) = x(2m,\ n)$ and $x_o(m,n) = x(2m+1,\ n)$.
b. Predict: After splitting the data, the odd subset $x_o(m,n)$ is predicted from the neighboring even subset $x_e(m,n)$ using the predictor operator $P(\cdot)$, which is a linear combination of the neighboring even subset. The difference between the prediction value of $p_e(m,n)$ and the actual value of $x_o(m,n)$ is defined as the detail signal $h(m,n)$, which is the high pass frequency component of the wavelet subband.
c. Update: In this step, the even subset is updated using detail signal $h(m,n)$ and the update operator $U(\cdot)$ to produce the approximate signal $l(m,n)$ using the expression $l(m,n) = x_e(m,n) - U(d(m,n))$. This approximation signal is called as low pass frequency component.

d. Normalize: The outputs of the lifting are weighted by K_e and K_o. Even subset is normalized using K_e and odd subset is normalized using K_o. The values of these weights are different for different wavelets. These weights serve to normalize the energy of the underlying scaling and wavelet functions respectively.

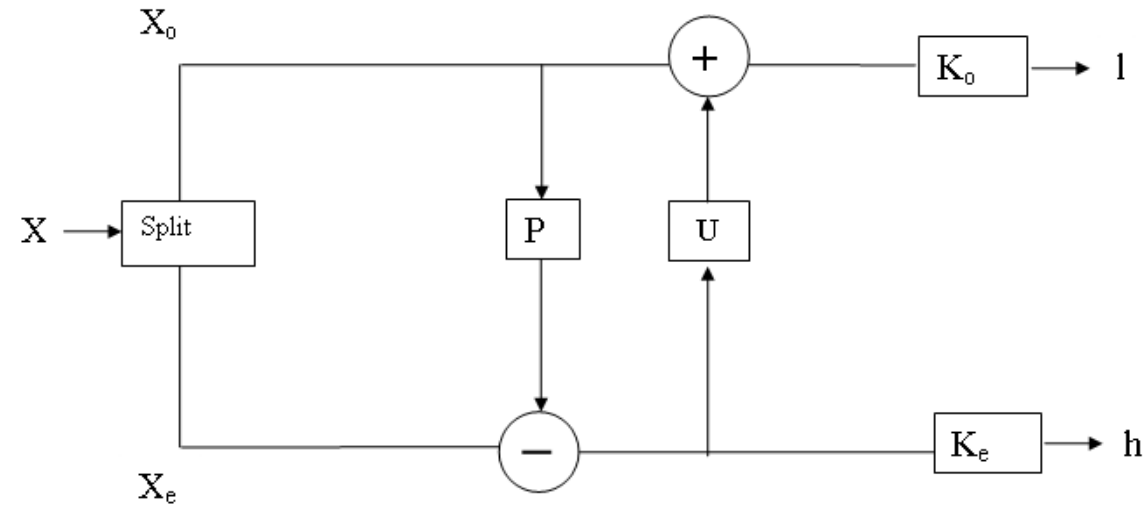

(a)

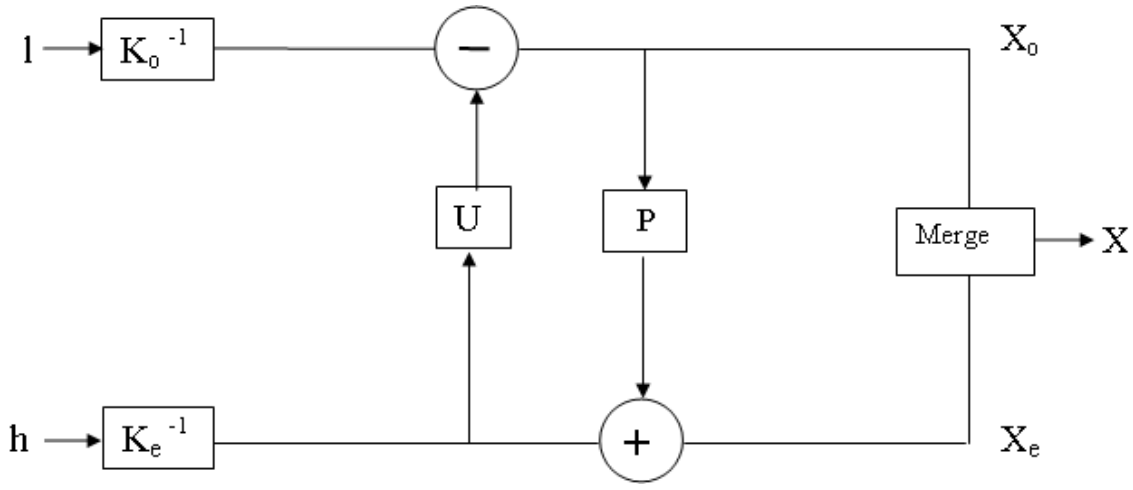

(b)

Figure 3.1: Lifting Scheme (a) Analysis Side (b) Synthesis Side

The inverse *DWT* using lifting scheme can be derived by traversing the above steps in the reverse direction. The low pass and high pass frequency components are scaled by K_e^{-1} and K_o^{-1}, respectively. Then update and predict lifting steps are applied after reversing the signs of the filter coefficients and finally merge (inverse of split) them into a single reconstructed image as shown in Figure 3.1(b).

3.3 Adaptive Directional Lifting Scheme

Lifting scheme is very effective in dealing with horizontal and vertical edges, but it does not work that well when the edges present in the image are neither horizontal nor vertical. Natural images often contain significant information about edge directions and the edges can be generally approximated as linear edges. These edges may neither be horizontal nor vertical. If not taken into consideration, these edges will result in large wavelet coefficients in high frequency subbands. This problem has been recognized by various researchers working in the area of image compression, feature extraction, image enhancement, image denoising and classification.

Based on the lifting structure, several approaches have been proposed to locally adapt the filtering direction of the linear edges in the images. Ding *et al.* (2007) incorporated directional prediction into the conventional lifting scheme to propose *ADL* scheme. *ADL* scheme involves two separable transforms, separable horizontal/vertical lifting based transform similar to conventional lifting scheme. The difference between the two schemes is in the prediction process. Instead of alternately applying horizontal and vertical lifting, *ADL* performs lifting-based prediction in local windows in the direction of high pixel correlation. Hence, it adapts far better to the image orientation features in local windows. The *ADL* transform is achieved by

existing 1-*D* wavelets and is seamlessly integrated into the global wavelet transform. The predicting and updating signals of *ADL* can be derived even at the fractional pixel precision level to achieve high directional resolution, while still maintaining perfect reconstruction. *ADL* chooses a direction of prediction in which the prediction error is minimal.

Prediction of each $x_o(m,n)$ is a linear combination of neighboring even coefficients having strong correlation. As shown in Figure 3.2, assume that the pixels have a strong correlation in the angle θ_v, where the integer pixels are marked by "O," the half pixels by "+" and the quarter pixels by "×" The prediction of $x(m, 2n+1)$ is taken as the linear combination of even polyphase samples identified by the arrows in Figure 3.2, specifically,

$$p_e(m,n) = \sum_i \alpha_i \, x_e(m + sign(i-1)\tan\theta_v, n+i) \quad \ldots (3.1)$$

where $sign$ function is defined as

$$sign(x) = \begin{cases} -1, & if\ x < 0 \\ 0, & if\ x = 0 \\ 1, & if\ x > 0 \end{cases}$$

The weights α_i are given by the lifting filter's taps. This is worth noting that $x_e(m + sign(i-1)\,tan\,\theta_v, n+i)$ is not necessarily sampled at an integer position.

In order to perform directional prediction in an arbitrary angle θ_v, *ADL* scheme needs to know the intensity values at $tan\,\theta_v$ fractional pixel locations. In other words, $\tan\theta_v$ used in (3.1) is generally not an integer. Hence, the interpolation of subpixels is required. For perfect reconstruction, the integer pixels used to interpolate the fractional pixel at angle θ_v have to be even polyphase samples $x_e(m,n)$. No odd polyphase samples $x_o(m,n)$ can participate in the prediction in this case. The interpolation used by *ADL* is given by

$$x_e(m + sign(i-1)\tan\theta_v, n+i) = \sum_k a_k \, x_e(m+k, n+i) \quad \ldots (3.2)$$

The subscript k indexes the integers around $sign(i-1)\ \tan\theta_v$, and a_k are the interpolation filtering parameters. In this approach, Sinc interpolation technique is adopted. Sinc interpolation is a popular technique used in image processing operations which has been proposed by Yaroslavsky (2002).

Theoretically, the prediction angle can be a continuous variable. However, in *ADL* nine uniformly quantized discrete angles $\theta_{i,}\ i = 0, \pm1, \pm2, \pm3, \pm4,$ are used which are sufficient to reap all the coding gains of *ADL*. Equivalently, the interpolation is done at the spatial resolution of quarter pixel.

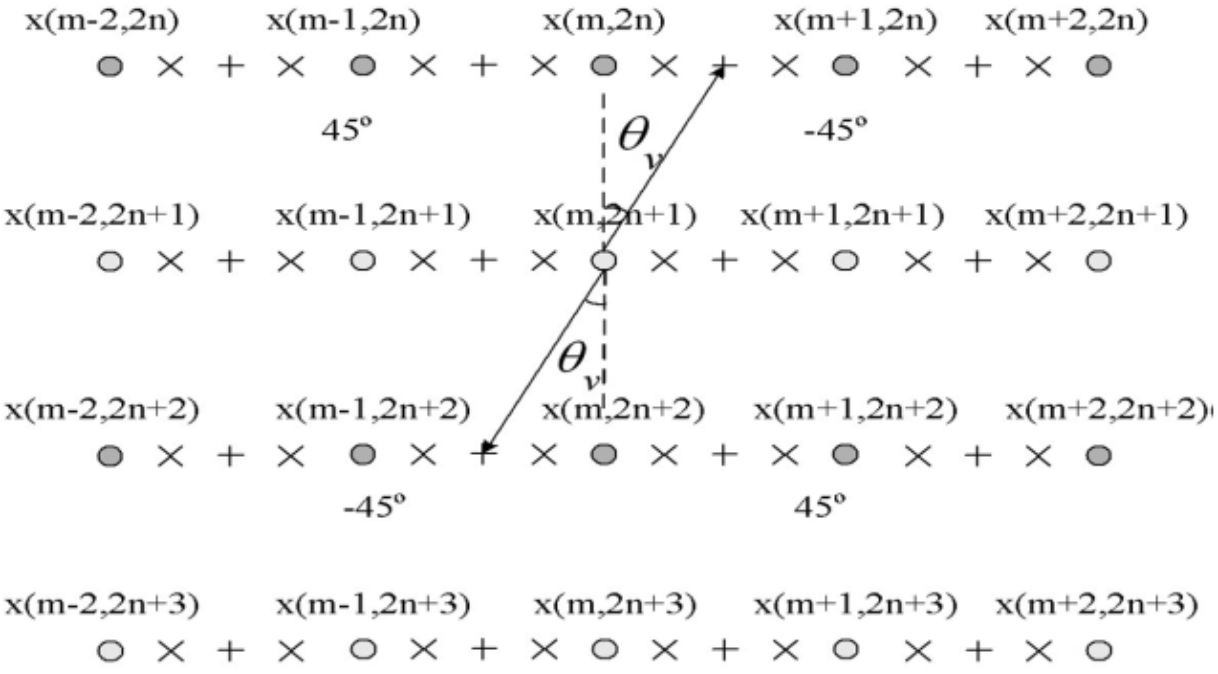

(a) The prediction process.

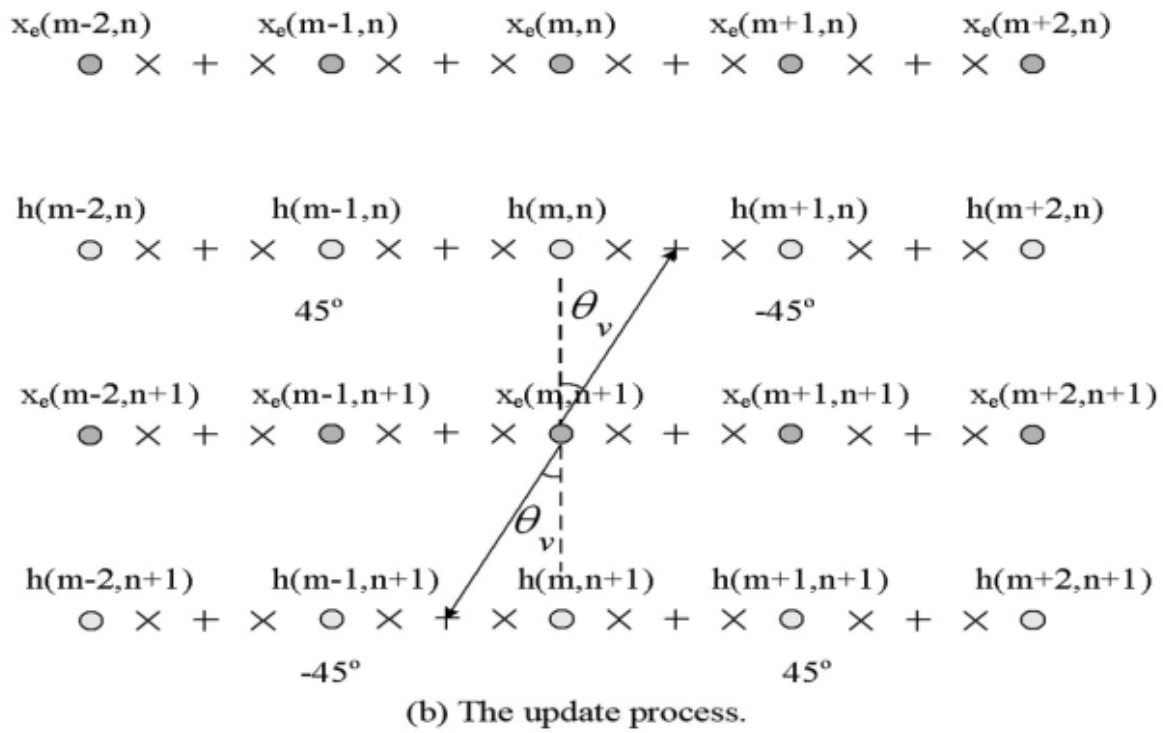

Figure 3.2: (a) Prediction process used in *ADL* (b) The update process used in *ADL*

After the prediction and updation process, the output is normalized by the weights of the particular wavelet. For more than one level wavelet transform, the process is repeated on the *LL* subband produced by the previous level lifting based wavelet transform like the convolution based wavelet transform.

Although the *ADL* scheme provides significant subjective and objective quality improvements on the texture-richl images when compared with the conventional lifting scheme, mostly due to the efficient representation of wavelet coefficients and coding of side information, this scheme still has some problems.

First of all, there exists a mismatch between predict and update steps. The odd subset are predicted from the neighboring even subsets with an optimal direction in the predict step, while in the update step the even subset are updated from the high-pass coefficients along the inverse

direction of the predict step. However, the direction inversion procedure will result in the aliasing of direction information, because the inverse procedure may be ambiguous due to the cases of many-to-one mapping and nonrefereed pixels. With sub-pixel precision, the mismatch is even more serious. When the optimal direction in the predict step is located in sub-pixel position, the high-pass coefficients cannot exactly update the pixels they have predicted, as shown in Figure 3.2(b). Therefore, the mismatch problem potentially prevents this scheme from improving further the coding efficiency for the images with more complex direction information.

Second, since always performed in either horizontal direction for vertical transform or vertical direction for horizontal transform, the sub-pixel interpolation favours horizontal and vertical direction. This process may blur the orientation property existing in original images. This type of sub-pixel interpolation may increase the directional prediction errors and, thus decrease the coding efficiency of the images with rich textures. This problem has also been recognized by Ding *et al*. (2007). A solution to this problem has been proposed by Liu and Ngan (2007; 2008) and is discussed in next section in the form of Weighted Adaptive Lifting Scheme.

3.4 Weighted Adaptive Lifting Scheme

To solve the problems mentioned in Section 3.3, Liu and Ngan (2007; 2008) proposed *WAL* scheme using Improved Weighted Lifting, which maintains a consistency between the predict and update steps as far as possible and preserves the perfect reconstruction at the same time. The mismatch problem between the predict and update steps is solved by the weighted lifting scheme using the idea that in the update step, the obtained high-pass coefficients are uniformly distributed to those even pixels that are used to calculate the high-pass coefficient in the predict step. It means that the high-pass coefficient will be added only to the pixels they have predicted. Now, the prediction and update stages are consistent.

3.5 Proposed Edge Adaptive Lifting Scheme

After going through the literature, we have found that there is still as scope of improvement in the lifting scheme on the basis of edges present in the input image which is to be decomposed using wavelet transform. In the conventional lifting scheme, the prediction is done in the horizontal/ vertical direction as shown in Figure 3.3. The edges, however might be present in subpixels directions in an image, as illustrated by Liu and Ngan (2008). So there is the need to consider these directions in implementing the steps of lifting scheme.

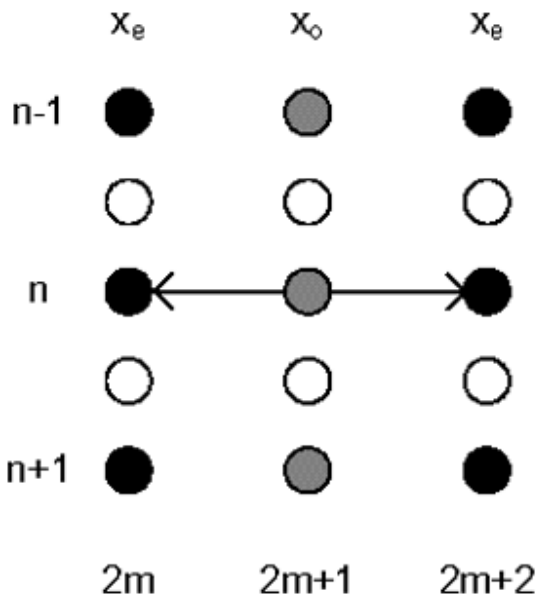

Figure 3.3: Conventional Lifting Scheme

In proposed scheme, we have used the prediction in the directions of angles of 0˚, 45˚ and 135˚. After fixing a direction out of these three directions, the proposed prediction includes the direction of half and quarter pixels. *Sinc* interpolation scheme has been used to interpolate the values of half and quarter subpixels as shown in Figure 3.4. As such the predictor is not required to be limited to use pixels from the same row (or column in columnwise processing) and also from the integer pixels positions.

Algorithm 3.1: Edge Direction Prediction Algorithm

(i) Consider six neighbours of $x(m, 2n)$ in the pairs of $x(m, 2n-1)$ and $x(m, 2n+1)$; $x(m+1, 2n-1)$ and $x(m-1, 2n+1)$; $x(m-1, 2n-1)$ and $x(m+1, 2n+1)$. Now, define three gradient approximations around $x(m, 2n)$ along angles of 0°, 45° and 135° with the horizontal axis:

$$\Delta_0 = |x(m, 2n-1) - x(m, 2n+1)|$$

$$\Delta_{45} = |x(m+1, 2n-1) - x(m-1, 2n+1)|$$

$$\Delta_{135} = |x(m-1, 2n-1) - x(m+1, 2n+1)|$$

(ii) Use Δ_0, Δ_{45} and Δ_{135} as the direction of prediction and select the direction having the minimum value (say, Δ) among these three.

(iii) If Δ_0 is minimum then select $x(m, 2n-1)$ and $x(m, 2n+1)$ for prediction purpose and interpolate the half and quarter pixels between the pixels of selected direction using *Sinc* interpolation, as shown in Figure 3.4 (a).

(iv) If Δ_{45} is minimum then select $x(m+1, 2n-1)$ and $x(m-1, 2n+1)$ for prediction purpose and interpolate the half and quarter pixels between the pixels of selected direction using *Sinc* interpolation, as shown in Figure 3.4 (b).

(v) If Δ_{135} is minimum then select $x(m-1, 2n-1)$ and $x(m+1, 2n+1)$ for prediction purpose and interpolate the half and quarter pixels between the pixels of selected direction using *Sinc* interpolation, as shown in Figure 3.4 (c).

(vi) Now, find the difference between interpolated subpixels value obtained from Sinc interpolation that are diagonally placed. These six differences and the value of Δ obtained in step (ii) are further considered for finding their minimum. This minimum value defines the direction in which even indexed pixels are predicted.

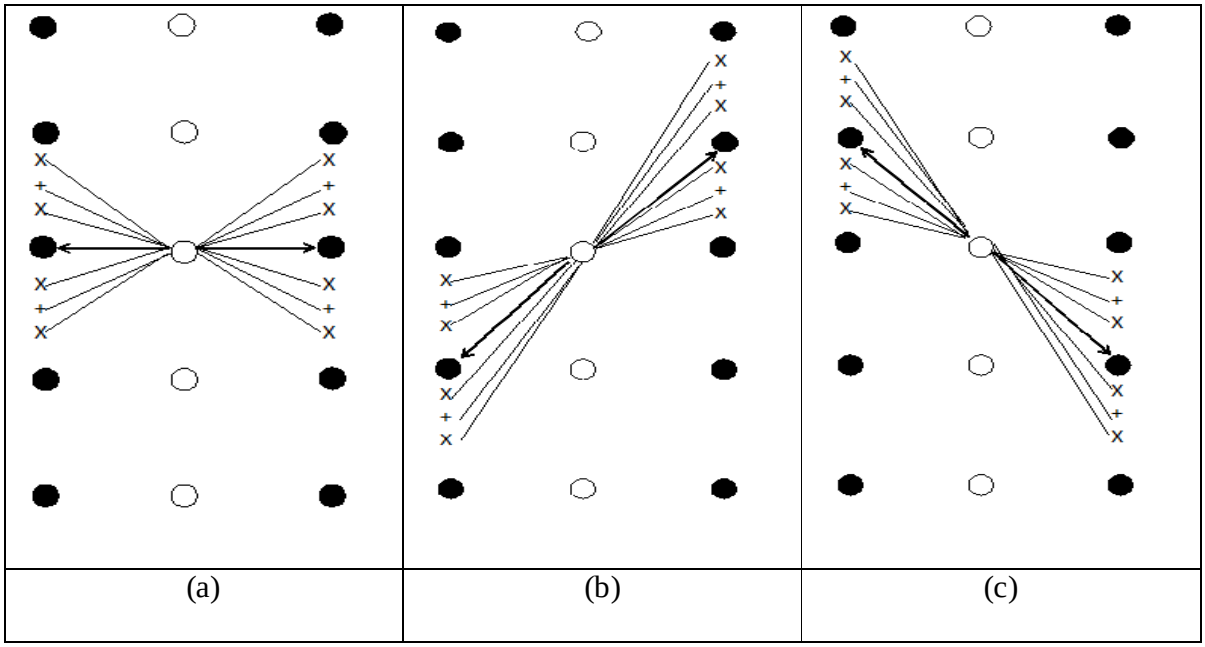

Figure 3.4: Interpolation of non integer pixels in the directions of (a) 0˚ (b) 45˚ (c) 135˚

The output of the prediction step is high pass wavelet coefficients and in the update step, these coefficients are added exactly to the pixels they are predicted. Hence the prediction and update steps in the proposed scheme are consistent. The proposed lifting scheme is implemented in two stages consisting of row-wise processing followed by a column-wise processing as in ordinary lifting scheme.

Proposed algorithm is implemented for first level wavelet transform using lifting scheme. Since the edges present in the images are aligned in the horizontal/vertical direction using this algorithm, there is not any requirement of using the proposed algorithm in the next level of wavelet decomposition. In the next level of wavelet decomposition, the conventional lifting scheme is used.

The effect of using the proposed edge adaptive lifting scheme is reflected in the reduction of the energy in the *LH*, *HL* and *HH* subbands as shown in the Table 3.1.

Table 3.1: Average magnitude of wavelet coefficient in *LH*, *HL* and *HH* subbands

Subbands	Image → / Scheme ↓	Barbara	Bike	Café	Foreman
LH	*JPEG*2000	5.31	3.01	5.01	1.30
	ADL	2.35	2.25	4.04	0.92
	WAL	2.10	1.87	3.72	0.87
	Proposed Scheme	2.05	1.53	3.52	0.80
HL	*JPEG*2000	2.26	3.19	5.51	2.07
	ADL	1.44	2.39	4.40	1.43
	WAL	1.25	2.01	4.05	1.30
	Proposed Scheme	1.05	1.85	3.90	1.25
HH	*JPEG*2000	1.48	1.05	1.56	0.60
	ADL	0.97	0.88	1.50	0.51
	WAL	0.80	0.71	1.25	0.40
	Proposed Scheme	0.75	0.61	1.10	0.35

Table 3.1 contains average magnitude of wavelet coefficient of the *LH*, *HL*, and *HH* subbands obtained by using *JPEG*2000 conventional lifting scheme, *ADL*, *WAL* and the proposed lifting scheme. As is evident from this table, there is a significant reduction in the values of wavelet coefficients when proposed scheme is used in comparison with the existing schemes and the conventional scheme used in *JPEG*2000.

Comparison of the coding performance of the proposed method with the existing methods is presented in Table 3.2. For this, we considered six test images and these images have been

compressed at different bit rates, namely, 0.125, 0.25, 0.5, 1.0 and 2.0 bits per pixel (*bpp*) using proposed scheme and also using existing schemes. The *PSNR* values of all test images after compressing at these bit rates using proposed method and the existing methods is summarised in Table 3.2. These images are lossy compressed and 5 level decomposition wavelet levels have been used. The Sinc interpolation is used in the proposed scheme to generate subpixels at quarter and half locations. For all methods, all images are decomposed by three level wavelet decomposition.

Comparison of the coding performance of the proposed scheme with the existing schemes is shown in Table 3.2 and Table 3.3. We have considered seven test images for comparison and these images have been compressed using proposed lifting scheme and also using existing lifting schemes at different bit rates, namely, 0.125, 0.25, 0.5 and 1.0 *bpp*. After compressing these test images at these bit rates, *PSNR* values have been obtained by using proposed scheme and the existing schemes and summarised in Table 3.2 and Table 3.3. These images are lossy (Table 3.2) and losslessly (Table 3.3) compressed and 5 level decomposition wavelets have been used for compression.

Table 3.2: Comparison of *PSNR* (*d*B) of different lifting schemes with *LeGall* 5/3 Filters

Image ↓	Data Rate (*bpp*)	Lifting Scheme of *JPEG*2000 Standard	*ADL* (Ding *et al*., 2007) Scheme	*WAL* (Liu *et al*., 2008) Scheme	Proposed Scheme
Barbara	0.125	24.59	25.95	26.18	26.73
	0.250	27.38	29.22	30.44	31.43
	0.500	30.95	32.95	33.64	34.93
	1.000	36.04	37.24	37.84	38.29

Lena	0.125	30.11	30.68	30.78	30.98
	0.250	33.22	33.88	33.90	34.12
	0.500	36.45	36.94	36.97	37.27
	1.000	39.51	39.73	39.80	39.92
Baboon	0.125	21.40	21.39	21.57	21.67
	0.250	22.87	23.04	23.20	23.42
	0.500	25.17	25.34	25.80	26.12
	1.000	28.62	28.88	29.03	29.28
Bike	0.125	25.74	26.61	27.26	27.71
	0.250	29.06	29.97	30.30	30.72
	0.500	33.09	33.38	34.02	34.33
	1.000	37.73	38.28	38.37	38.61
Café	0.125	20.42	20.55	20.65	20.75
	0.250	22.74	22.99	23.12	23.32
	0.500	26.42	26.67	27.05	27.45
	1.000	31.72	31.90	32.05	32.31
Woman	0.125	26.59	27.00	27.12	27.32
	0.250	29.24	29.65	29.71	29.89
	0.500	33.00	33.24	33.43	33.59
	1.000	37.96	38.07	38.15	38.24
Foreman	0.125	28.71	29.94	30.96	31.81
	0.250	32.32	33.53	34.57	34.99
	0.500	35.89	37.25	37.37	37.68

	1.000	40.60	41.30	41.44	41.68

Table 3.3: Comparison of *PSNR* (*d*B) of different lifting schemes with *CDF* 9/7 filters

Image ↓	Data Rate (*bpp*)	Lifting Scheme of *JPEG*2000 Standard	*ADL* (Ding *et al*., 2007) Scheme	*WAL* (Liu *et al*., 2008) Scheme	Proposed Scheme
Barbara	0.125	25.02	26.45	26.67	27.28
	0.250	28.27	29.78	30.00	30.63
	0.500	32.15	33.58	33.68	34.19
	1.000	37.11	37.88	38.07	38.42
Lena	0.125	30.41	31.02	31.12	31.43
	0.250	33.78	34.25	34.33	34.61
	0.500	37.02	37.30	37.34	37.55
	1.000	40.06	40.20	40.26	40.43
Baboon	0.125	21.50	21.69	21.73	21.89
	0.250	23.10	23.23	23.28	23.43
	0.500	25.52	25.73	25.82	26.03
	1.000	29.02	29.31	29.37	29.60
Bike	0.125	25.93	26.78	26.87	27.19
	0.250	29.36	30.12	30.39	30.80
	0.500	33.38	34.00	34.26	34.55
	1.000	38.04	38.48	38.76	39.00
Café	0.125	20.70	20.84	21.04	21.16

	0.250	23.09	23.32	23.42	23.53
	0.500	26.78	27.06	27.27	27.43
	1.000	32.02	32.18	32.21	32.28
Woman	0.125	26.94	27.35	27.41	27.57
	0.250	29.67	30.06	30.28	30.49
	0.500	33.42	33.72	33.81	33.95
	1.000	38.31	38.47	38.53	38.60
Foreman	0.125	29.15	30.16	30.25	30.60
	0.250	32.81	33.77	33.91	34.26
	0.500	36.33	37.43	37.48	37.85
	1.000	40.85	41.63	41.68	41.96

From Tables 3.2 and 3.3, one can observe that in case of lossless compression, maximum *PSNR* gain is 4.05 *d*B, 2.21 *d*B and 1.29 *d*B as compared to *JPEG*2000 lifting scheme, *ADL* scheme and *WAL* scheme, respectively. Also, minimum *PSNR* gain here is 0.27 *d*B, 0.19 *d*B and 0.09 *d*B as compared to *JPEG*2000 lifting scheme, *ADL* scheme and *WAL* scheme, respectively. This has also been noted that there is not much increase in encoding time and memory usage in the proposed scheme. Maximum increase in encoding time and memory usage is 1% and 2%, respectively, when compared with *JPEG*2000 lifting scheme, *ADL* scheme and *WAL* scheme.

In case of lossy compression, maximum *PSNR* gain is 2.36 *d*B, 0.85 *d*B and 0.63 *d*B when compared with *JPEG*2000 lifting scheme, *ADL* scheme and *WAL* scheme, respectively. Also, minimum *PSNR* gain here is 0.26 *d*B, 0.10 *d*B and 0.07 *d*B when compared with *JPEG*2000 conventional lifting scheme, *ADL* scheme and *WAL* scheme, respectively. Maximum increase in

encoding time and memory usage in lossy compression is 1% and 2 % when compared with *JPEG*2000 lifting scheme, *ADL* scheme and *WAL* scheme.

Since the direction prediction is incorporated into lifting scheme, the direction information is transmitted as side information to the decoder. Therefore, one of the important issues is to reduce the overhead bits from the direction information. Ideally, one optimal direction would be assigned to each pixel. In order to decrease the number of bits required for coding the direction information, the image is divided into macroblocks. Since proposed lifting scheme also involves two separable transforms, horizontal transform and vertical transform, without loss of generality, we assume that the image is first decomposed to low subband and high subband by horizontal transform, followed by vertical transform. Thus, a typical macroblock unit in the proposed scheme is defined by the combination of a 16×16 block in the horizontal transform and a doublet of 8×16 blocks in the vertical transform. The rate-distortion optimized image segmentation process of *H*.264 encoder and *WAL* scheme is used in the proposed scheme to store and pass the side information to the decoder, as it is optimal process available in the literature. But in our scheme, we have two block size as compared to the seven block size in *WAL*, as it saves some amount of side information. The comparison of bits required for information coding for *ADL*, *WAL* and proposed scheme is given in Table 3.4 and Table 3.5.

Table 3.4: Comparison of bits for side information coding (*bpp*) at different data rate for *LeGall* 5/3 wavelet transform

Data Rate	Image → / Scheme ↓	Barbara	Lena	Baboon	Bike	Cafe	Woman	Foreman
0.125	*ADL*	0.0150	0.0090	0.0080	0.0070	0.0060	0.0040	0.0170
	WAL	0.0035	0.0018	0.0016	0.0021	0.0021	0.0018	0.0021

	Proposed	0.0030	0.0015	0.0012	0.0019	0.0019	0.0016	0.0018
0.250	*ADL*	0.0190	0.0200	0.0012	0.0130	0.0090	0.0070	0.0210
	WAL	0.0047	0.0029	0.0020	0.0028	0.0021	0.0018	0.0027
	Proposed	0.0043	0.0024	0.0015	0.0023	0.0015	0.0014	0.0020
0.500	*ADL*	0.0340	0.0400	0.0210	0.0310	0.0021	0.0210	0.0330
	WAL	0.0064	0.0029	0.0025	0.0028	0.0028	0.0031	0.0033
	Proposed	0.0060	0.0022	0.0021	0.0022	0.0023	0.0021	0.0029
1.000	*ADL*	0.0340	0.0400	0.0210	0.0310	0.0021	0.0210	0.0330
	WAL	0.0064	0.0029	0.0025	0.0028	0.0028	0.0031	0.0033
	Proposed	0.0060	0.0025	0.0021	0.0022	0.0023	0.0027	0.0024

Table 3.5: Comparison of bits for side information coding (*bpp*) at different data rate for *CDF* 9/7 wavelet transform

Data Rate	Image → / Scheme ↓	Barbara	Lena	Baboon	Bike	Cafe	Woman	Foreman
0.125	*ADL*	0.008	0.005	0.004	0.003	0.003	0.002	0.011
	WAL	0.0035	0.0019	0.0016	0.0015	0.0014	0.0015	0.0021
	Proposed	0.0030	0.0014	0.0013	0.0011	0.0011	0.0012	0.0016
0.250	*ADL*	0.013	0.009	0.007	0.006	0.003	0.003	0.013
	WAL	0.0047	0.0019	0.0017	0.0019	0.0017	0.0019	0.0025
	Proposed	0.0043	0.0012	0.0010	0.0012	0.0011	0.0014	0.0021
0.500	*ADL*	0.018	0.018	0.008	0.013	0.007	0.005	0.021
	WAL	0.039	0.0022	0.0021	0.0019	0.0024	0.0019	0.0037

	Proposed	0.035	0.0017	0.0020	0.0018	0.0021	0.0016	0.0034
1.000	*ADL*	0.018	0.018	0.008	0.013	0.007	0.005	0.021
	WAL	0.045	0.0022	0.0032	0.0019	0.0024	0.0019	0.0019
	Proposed	0.034	0.0011	0.0020	0.0011	0.0016	0.0016	0.0016

From Table 3.4 and Table 3.5, one can observe that the side information used by the proposed scheme is less than *WAL* scheme and *ADL* scheme. So, a very less amount of extra information is needed to pass to the decoder so that it can select the same prediction direction used in the encoder. Also, overhead of side information at low bit rates is less than that at high bit rates because of the rate distortion optimized segmentation and direction estimation used in the scheme.

Figure 3.5: Decompressed Lena image at 0.125 *bpp* using *JPEG*2000 lifting scheme

Figure 3.6: Decompressed Lena image at 0.125 *bpp* using *ADL* scheme

Figure 3.7: Decompressed Lena image at 0.125 *bpp* using *WAL* scheme

Figure 3.8: Decompressed Lena image at 0.125 *bpp* using proposed lifting scheme

Figures 3.5, 3.6, 3.7 and 3.8 are the magnified portions of decompressed Lena images at 0.125 *bpp* obtained using *JPEG*2000 conventional lifting scheme, *ADL* scheme, *WAL* scheme and proposed lifting scheme, respectively. After decompressing Lena image at 0.125 *bpp* using our proposed lifting scheme and existing lifting schemes, a portion of these images is magnified with cubic interpolation. It can be concluded that proposed lifting scheme provides better visual quality than existing lifting schemes.

3.6 Conclusion

In this chapter, we have proposed an edge adaptive lifting scheme. In this scheme, edge direction is predicted using the neighbouring pixels of the same subset of even/odd image pixels and is also checked for the quarter and half subpixels which are interpolated using Sinc interpolation. It has been observed that there is an improvement of up to 1.29 *d*B in *PSNR* when the results of this scheme are compared with *WAL* scheme and an improvement of up to 4.05 *d*B in *PSNR* when the results of this scheme are compared with *JPEG*2000 conventional lifting scheme.

Chapter 4

Tile Artifacts Reduction in *JPEG*2000 Compressed Images

4.1 Introduction

In *JPEG*2000 standard, when memory required by an image is larger than the available memory for elaboration, the image is divided into tiles. Tiles are rectangular regions of the image that are transformed and encoded independently. Tiles can be of any size, and it is also feasible to consider the whole image as a single tile. Once the size of the tile is chosen, all the tiles will have to have the same size except, optionally, the tiles on the right and bottom borders. Tile dimensions are taken as powers of two, except for the tiles on the right and bottom boundaries of the image. The primary advantage of dividing the image into tiles is that the decoder will need less memory to decompress the image and it can opt to decode selected tiles only in order to achieve a partial decoding of the image. The compressed data in the decoders must be decoded with the same tile size as used by the encoder. As such, tiling can give better memory utilization and better access under certain circumstances. It can significantly reduce the complexity on the encoder side. It is also useful in handling high resolution images. A difficulty that tiling introduces is the blocking artifacts that are significant when the images are compressed at low bit rate using *JPEG*2000 coding system. There are two major factors contributing in tiling artifacts in *JPEG*2000 images. One factor is the symmetric extension of the original image samples which

is performed prior to applying the wavelet transform. Other factor is the difference in quantization accuracy which is due to difference in quantization errors in each tile.

4.2 Tile Boundary Artifacts Analysis

4.2.1 Wavelet Transform

Wavelet transform is a subband transform which transforms images from spatial domain to frequency domain. To achieve efficient lossy and lossless compression within a single standard, two wavelet transform filters are used in *JPEG*2000 standard. One is *CDF* 9/7 floating point filter which is used for lossy compression and the other is *LeGall* 5/3 which is simple to implement and has lossless capability. Two dimensional *DWT* is the combination of a one dimensional (1-*D*) horizontal and 1-*D* vertical *DWT*. The original image is decomposed in order to produce low pass and high pass filtered outputs of the image. These filtered outputs are then down-sampled by a factor of two in order to produce a set of subbands of the original image. Because of the down-sampling process, the total number of wavelet coefficients is same as the number of original image samples. Output of this process is the set of four subbands, namely, *LL*, *LH*, *HL* and *HH* subbands. This wavelet decomposition process can further be applied iteratively on the *LL* subband to get a multiresolution decomposition of the original image. *DWT* decorrelates the input image and also provides a good energy compaction.

To produce the reconstructed image from the compressed image, different filter pairs are needed. The subband samples of the image are first upsampled by a factor of two and then filtered to produce reconstructed low pass and high pass versions of the original image. The outputs of the reconstructed filters are then summed to produce the final reconstructed image. In order to keep the number of subband samples same as the number of original image samples, the original

image is symmetrically extended about the boundaries before performing the wavelet transformation. Here, length of extension depends upon the number of wavelet filter coefficients used in the wavelet transform. If the number of wavelet filter coefficients is *m*, then the length of extension is $\left\lfloor \frac{m}{2} \right\rfloor$ in both directions, where $\left\lfloor \frac{m}{2} \right\rfloor$ is the largest integer not exceeding $\frac{m}{2}$. In *JPEG*2000 image compression standard, a whole sample symmetric extension is used to extend the boundaries of the image/tile. For example, if the input image data is $x[0], x[1], \dots, x[n-2], x[n-1]$, then a whole sample symmetric extension would give:

$$x[2], x[1], x[0], x[1], \dots, x[n-2], x[n-1], x[n-2], x[n-3]$$

This extension depends upon the number of wavelet filter coefficients used in wavelet transform. If the number of wavelet filter coefficients is *m*, then the length of extension is $\left\lfloor \frac{m}{2} \right\rfloor$ in both directions.

In this chapter, we have analyzed and have also worked on reducing the boundary artifacts that occur at the tile boundaries of *JPEG*2000 compressed images when wavelet transforms are used to perform lossy image compression. The boundary artifacts are attributed to the error between the reconstructed and original image samples close to the boundary of a tile. To determine the cause of this error, we have investigated the error introduced by the lossy compression process at the boundary of the tile that has been transformed using *CDF* 9/7 wavelet transform.

Let us consider the following set of *n* samples of an image.

$$x[0], x[1], \dots, x[n-2], x[n-1]$$

When single level wavelet transform is applied on this image, following set of low pass and high pass subband samples are produced.

$y_0'[0], y_0'[2], \ldots, y_0'[n-4], y_0'[n-2]$ and

$y_1'[1], y_1'[3], \ldots, y_1'[n-3], y_1'[n-1]$

These low pass and high pass subband samples are interleaved to get the following sequence.

$y_0'[0], y_1'[1], y_0'[2], y_1'[3], \ldots, y_0'[n-2], y_1'[n-1]$

From this, one can observe that for an even number of input samples, one end of the sample sequence is a low pass sample and other end is a high pass sample. In case of lossy compression, these subband samples are quantized in order to reduce the precision of the subband samples to aid in achieving higher compression. Quantization of subband samples is one of the main sources of information loss in the encoder. Quantization is performed by uniform scalar quantization with dead zone about the origin and is defined as:

$$q_b[n] = sign\left(y_b'[n]\right) \left\lfloor \frac{|y_b'[n]|}{\Delta_b} \right\rfloor \quad \ldots (4.1)$$

where $y_b'[n]$ is the sample of subband b; $q_b[n]$ is the quantized sample; Δ_b is the quantization step size for subband b. The *JPEG*2000 standard supports separate quantization step size for each subband due to multiresolution feature supported by *DWT*. The quantization step size for a subband is calculated based on the dynamic range of the samples of the subband. The *sign* function in (4.1) is defined as:

$$sign(x) = \begin{cases} -1, & if\ x < 0 \\ 0, & if\ x = 0 \\ 1, & if\ x > 0 \end{cases}$$

After the quantization process, the subbands of a tile are divided into code blocks, which are compressed independently using *EBCOT* algorithm (Taubman, 2000; Lian *et al.,* 2003). *EBCOT* defines the methodology for arranging the compressed output in the form of bit stream allowing

the rate control with optimum quality. *EBCOT* consists of a process that is accomplished in two tiers. *Tier*-1 generates the collection of encoded bits for each code block. *Tier*-2 reorganizes the output of *Tier*-1 by discarding some of the encoded bits in order to obtain the best possible quality for a given compression ratio. On the decoder side, the steps of the encoder are executed in reverse order to decompress the images.

After the inverse quantization process on the decoder side, the reconstructed subband samples in subband b are given by

$$y_b''[n] = sign(q_b[n])\ (\ |\Delta_b . q_b[n]| + \delta) \quad \ldots (4.2)$$

where δ is usually taken as $\Delta_b/2$.

The reconstructed subband samples can then be expressed as

$$y_b''[n] = y_b'[n] + \varepsilon_b[n] \quad \ldots (4.3)$$

where $\varepsilon_b[n]$ is the error between the original subband sample and the reconstructed sample caused by scalar quantization. It can be noted from (4.3) that errors are present in each of the reconstructed samples of decompressed images as the quantization process is irreversible.

4.2.2 Proposed Post-Processing Method for Reducing Tile Boundary Artifacts

Let use assume that the size of each tile of the input image is $m' \times n'$. Then the last row of reconstructed vertical tile boundary samples of i^{th} tile is given by

$$y_i''[m', j] = y_i'[m', j] + \varepsilon_i[m', j], \quad j = 1, \ldots, n' \quad \ldots (4.4)$$

Also, the first row of reconstructed vertical tile boundary samples of $(i+1)^{th}$ tile is given by

$$y_{i+1}''[1, j] = y_{i+1}'[1, j] + \varepsilon_{i+1}[1, j], \quad j = 1, \ldots, n' \quad \ldots (4.5)$$

Samples of the last row are the high pass reconstructed samples, as described in section 4.2.1. The error in reconstructed high pass samples is more than the error in reconstructed low pass sample (Wei *et al.*, 2005). As such, we replace the m'^{th} row samples of i^{th} tile by the average of the $(m'\text{-}1)^{th}$ row samples of i^{th} tile and 1^{st} row samples of $(i+1)^{th}$ tile. Thus

$$y_i''[m', j] = (y_i''[m' - 1, j] + y_{i+1}''[1, j])/2 \quad \ldots (4.6)$$

Using (4.4), (4.6) can be written as

$$y_i''[m', j] = (y_i'[m' - 1, j] + \varepsilon_i[m' - 1, j] + y_{i+1}'[1, j] + \varepsilon_{i+1}[1, j])/2 \quad \ldots (4.7)$$

Or,

$$y_i''[m', j] = (y_i'[m' - 1, j] + y_{i+1}'[1, j])/2 + (\varepsilon_i[m' - 1, j] + \varepsilon_{i+1}[1, j])/2 \quad \ldots (4.8)$$

Also,

$$\varepsilon_i[m' - 1, j] < \varepsilon_i[m', j] \text{ and } \varepsilon_{i+1}[1, j]) < \varepsilon_i[m', j]$$

As such,

$$(\varepsilon_i[m' - 1, j] + \varepsilon_{i+1}[1, j])/2 < \varepsilon_i[m', j] \quad \ldots (4.9)$$

Equation (4.9) suggests that the error in updated high pass reconstructed boundary samples is less than the original high pass reconstructed boundary samples. The horizontal tile boundary samples are also post-processed on similar lines, using the left neighboring low pass samples of the same tile and right low pass reconstructed samples of the neighboring tile.

By doing this, *MSE* of the processed tile boundary samples is reduced and hence *PSNR* and visual quality of the reconstructed images are improved.

4.2.3 Error Analysis of Boundary Samples of Tiles of an Image

Wei *et al.* (2000) have shown that the error in high pass reconstructed boundary sample is higher than the low pass reconstructed boundary sample. On the lines of the work done by them, we have also computed the errors in the boundary samples of the tiles of the image. In order to analyze the errors in boundary samples of a tile, we have collected 10,000 boundary samples of the tiles of different original images, reconstructed images using *JPEG*2000 standard and reconstructed images with post-processing by proposed method. Figure 4.1 contains the results of this analysis. In this figure, sample 1 corresponds to the last but one reconstructed pixel of the i^{th} tile, sample 2 corresponds to the last reconstructed pixel of the i^{th} tile and sample 3 corresponds to first reconstructed pixel of $(i+1)^{th}$ tile. Here, it can be noted that sample 2 has a large error in comparison with sample 1 and sample 3, when the image is compressed using *JPEG*2000 standard. This error is significantly reduced when the proposed method is applied after *JPEG*2000 decompression and this leads to reduction in boundary artifacts in *JPEG*2000 reconstructed images. The reconstructed boundary samples that have been considered in this analysis are captured from different standard images used by the researchers working in this field.

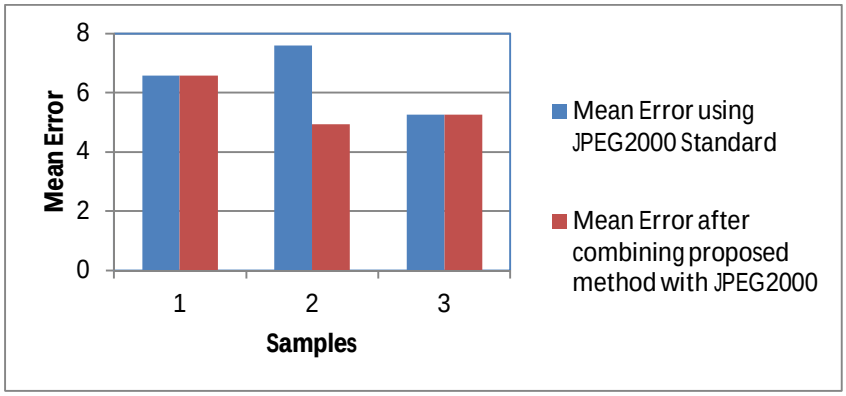

Figure 4.1: Mean Error of the pixel value differences of the boundary samples of image tiles.

Next, the *MSE* of the reconstructed samples at the tile boundaries of the decompressed images have been analyzed The reconstructed high pass boundary samples have higher *MSE* than reconstructed low pass boundary samples as shown below in Figures 4.2. When these high pass boundary samples are post-processed using the proposed method, the *MSE* of these samples decreases, as shown in Figure 4.3.

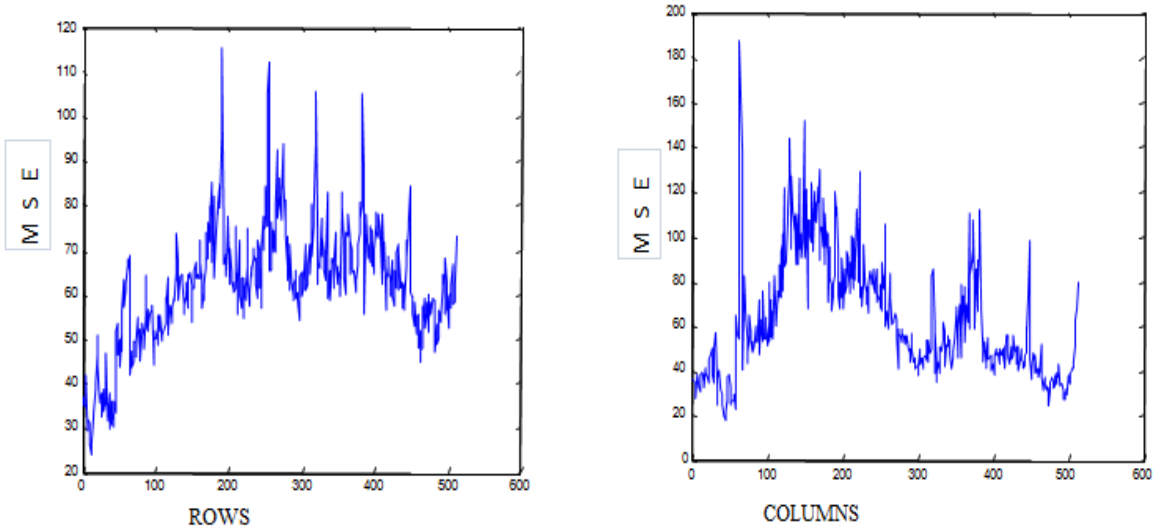

Figure 4.2: Average *MSE* for each row and column of 512×512 Lena image after compression at a bit rate of 0.1 *bpp* using *JPEG*2000 with tile size of 64×64.

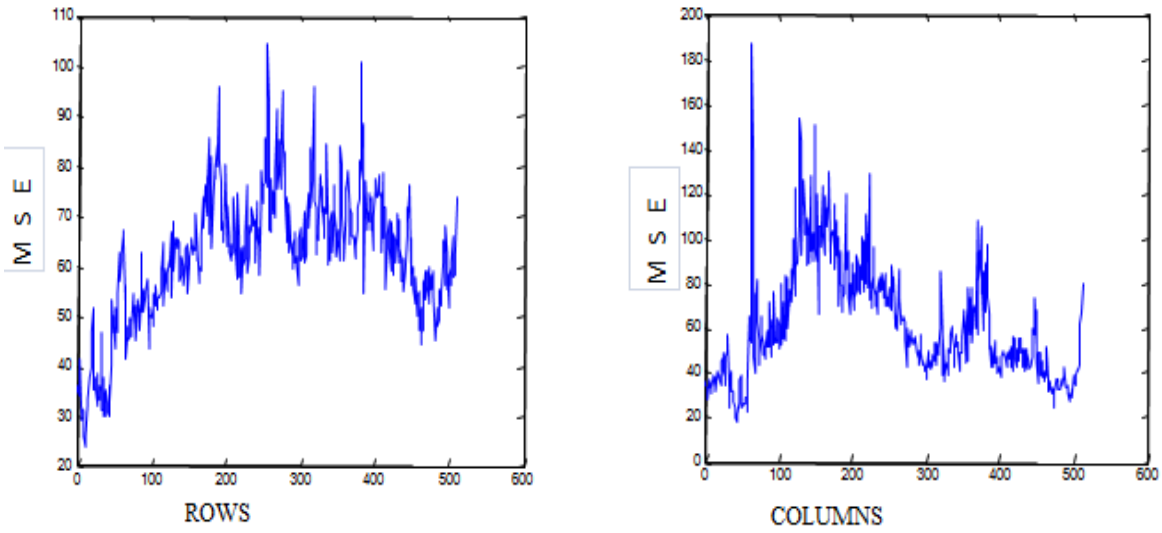

Figure 4.3: Average *MSE* for each row and column of 512×512 Lena image after post-processing the high pass boundary samples and compression at a bit rate of 0.1 *bpp* using *JPEG*2000 with tile size of 64×64.

4.3 Experimentation Results

Proposed post-processing method has been implemented using JASPER software tool (Adams, 2000). For this implementation, we have taken 10 test images, Lena, Barbara, Airplane, Baboon, Boat, Bridge, Couple, Pepper, Sailboat and Zelda images. These images are compressed at different bit rates (0.125, 0.25, 0.5 and 1.0) with five level wavelet decomposition using proposed method and other existing methods. *PSNR* values, encoding time and memory usage for these images are obtained when compressed with existing methods and also when compressed with proposed approach. Results of these comparisons are tabulated in Table 4.1.

Table 4.1: Comparison of *PSNR* (*d*B)/encoding time (sec)/memory usage (*KB*) of the proposed approach and existing approaches

Images	Data Rate (*bpp*)	*JPEG*2000 Approach	Kharitonenko *et al.* (2002) Approach	Proposed Approach
Lena	0.125	30.11/1.185/4516	30.20/1.188/4520	30.27/1.198/4525
	0.250	33.22/1.185/4516	33.23/1.188/4520	33.43/1.198/4525
	0.500	36.45/1.185/4516	36.65/1.188/4520	36.95/1.198/4525
	1.000	39.51/1.185/4516	39.81/1.188/4520	40.50/1.198/4525
Barbara	0.125	25.41/1.045/4460	25.57/1.055/4478	25.89/1.069/4515
	0.250	30.41/1.045/4460	30.51/1.055/4478	30.64/1.069/4515
	0.500	34.08/1.045/4460	34.39/1.055/4478	34.98/1.069/4515
	1.000	38.71/1.045/4460	38.83/1.055/4478	39.09/1.069/4515
Airplane	0.125	31.82/1.145/4485	31.95/1.147/4487	32.24/1.150/4490
	0.250	35.18/1.145/4485	35.38/1.147/4487	35.79/1.150/4490
	0.500	38.64/1.145/4485	38.78/1.147/4487	39.17/1.150/4490
	1.000	42.15/1.145/4485	42.45/1.147/4487	43.09/1.150/4490
Baboon	0.125	22.15/1.760/4272	22.28/1.765/4282	22.51/1.774/4298
	0.250	24.11/1.760/4272	24.371.765/4282	24.41/1.774/4298
	0.500	27.33/1.760/4272	27.53/1.765/4282	27.87/1.774/4298

	1.000	31.06/1.760/4272	31.24/1.765/4282	31.71/1.774/4298
Boat	0.125	31.78/1.045/4460	31.89/1.047/4463	32.04/1.048/4463
	0.250	35.21/1.045/4460	35.29/1.047/4463	35.84/1.048/4463
	0.500	39.10/1.045/4460	39.34/1.047/4463	39.95/1.048/4463
	1.000	45.95/1.045/4460	45.99/1.047/4463	46.65/1.048/4463
Bridge	0.125	23.31/0.933/3265	23.45/0.933/3265	23.60/0.934/3267
	0.250	24.81/0.933/3265	24.93/0.933/3265	25.30/0.934/3267
	0.500	27.18/0.933/3265	27.30/0.933/3265	28.09/0.934/3267
	1.000	30.58/0.933/3265	30.78/0.933/3265	31.47/0.934/3267
Couple	0.125	26.84/0985/3565	26.95/0985/3565	27.19/0986/3568
	0.250	29.32/0985/3565	29.41/0985/3565	29.68/0986/3568
	0.500	32.66/0985/3565	32.79/0985/3565	33.15/0986/3568
	1.000	36.80/0985/3565	36.92/0985/3565	37.74/0986/3568
Pepper	0.125	30.18/1.895/4855	30.28/1.895/4860	30.43/1.898/4870
	0.250	32.26/1.895/4855	32.38/1.895/4860	32.74/1.898/4870
	0.500	33.94/1.895/4855	33.99/1.895/4860	34.45/1.898/4870
	1.000	36.32/1.895/4855	36.53/1.895/4860	37.34/1.898/4870
Sailboat	0.125	26.45/1.895/4855	26.56/1.895/4856	26.73/1.898/4859

	0.250	28.60/1.895/4855	28.74/1.895/4856	28.97/1.898/4859
	0.500	30.67/1.895/4855	30.79/1.895/4856	31.04/1.898/4859
	1.000	33.56/1.895/4855	33.69/1.895/4856	34.53/1.898/4859
Zelda	0.125	34.55/0.750/2744	34.68/0.750/2746	34.76/0.755/2750
	0.250	37.34/0.750/2744	37.51/0.750/2746	37.84/0.755/2750
	0.500	39.60/0.750/2744	39.83/0.750/2746	40.05/0.755/2750
	1.000	43.10/0.750/2744	43.40/0.750/2746	44.07/0.755/2750

From Table 4.1, one can observe that there is an improvement of more than 1 *d*B in the *PSNR* of the compressed images when the proposed approach is used while difference in encoding time and memory usage is negligible. These comparisons are also demonstrated graphically in Figure 4.4. A reconstructed Lena image compressed at 0.125 *bpp*, using *JPEG*2000 standard with a tile size of 64×64 is shown in Figure 4.5 and a reconstructed Lena image compressed at 0.125 *bpp*, using *JPEG*2000 with proposed post-processing with a tile size of 64×64 is shown in Figure 4.6. Also, a reconstructed Barbara image compressed at 0.25 *bpp*, using *JPEG*2000 standard with a tile size of 64×64 is shown in Figure 4.7 and a reconstructed Barbara image compressed at 0.25 *bpp*, using *JPEG*2000 with proposed post-processing with a tile size of 64×64 is shown in Figure 4.8. Figures 4.6 and 4.8 clearly indicate an improvement in the visual quality of an image when one uses *JPEG*2000 with the proposed post-processing approach.

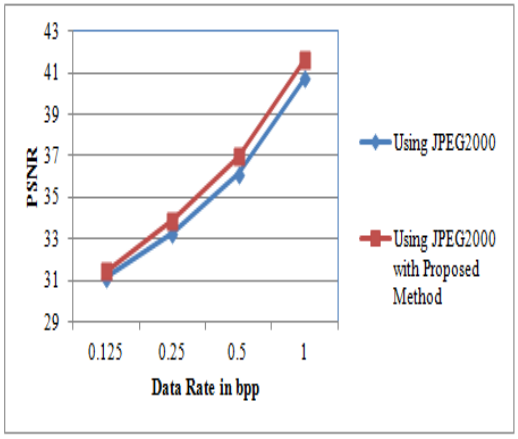
PSNR
43
41
39
37
35
33
31
29
0.125
0.25
0.5
1
Data Rate in bpp
Using JPEG2000
Using JPEG2000 with Proposed Method

(a)

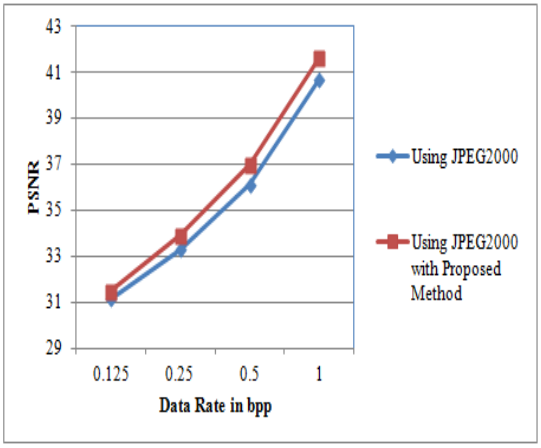
PSNR
43
41
39
37
35
33
31
29
0.125
0.25
0.5
1
Data Rate in bpp
Using JPEG2000
Using JPEG2000 with Proposed Method

(b)

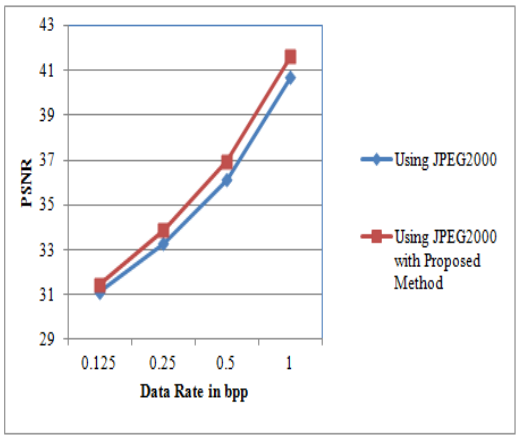
PSNR
43
41
39
37
35
33
31
29
0.125
0.25
0.5
1
Data Rate in bpp
Using JPEG2000
Using JPEG2000 with Proposed Method

®

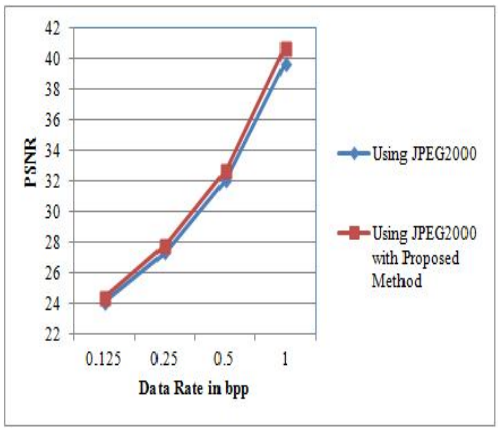
PSNR
42
40
38
36
34
32
30
28
26
24
22
0.125
0.25
0.5
1
Data Rate in bpp
Using JPEG2000
Using JPEG2000 with Proposed Method

(d)

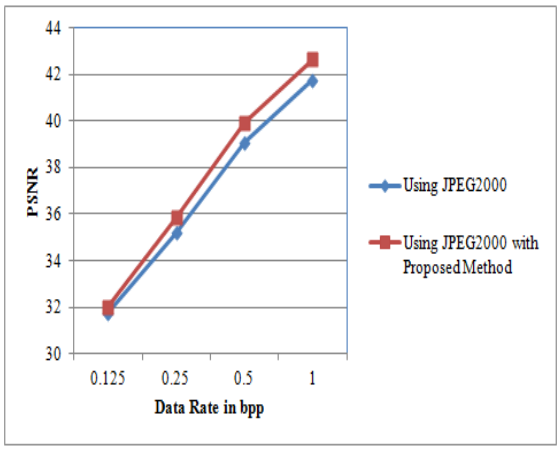
PSNR
44
42
40
38
36
34
32
30
0.125
0.25
0.5
1
Data Rate in bpp
Using JPEG2000
Using JPEG2000 with ProposedMethod

(e)

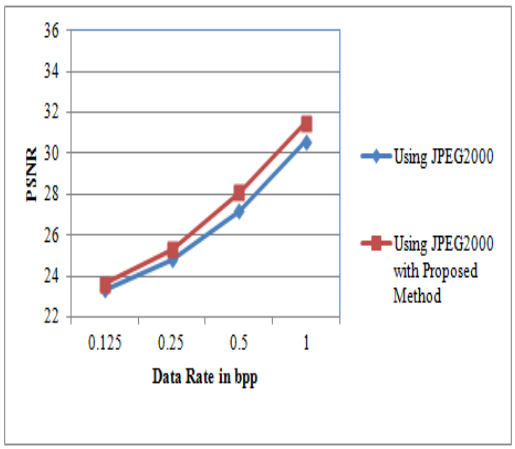
PSNR
36
34
32
30
28
26
24
22
0.125
0.25
0.5
1
Data Rate in bpp
Using JPEG2000
Using JPEG2000 with Proposed Method

(f)

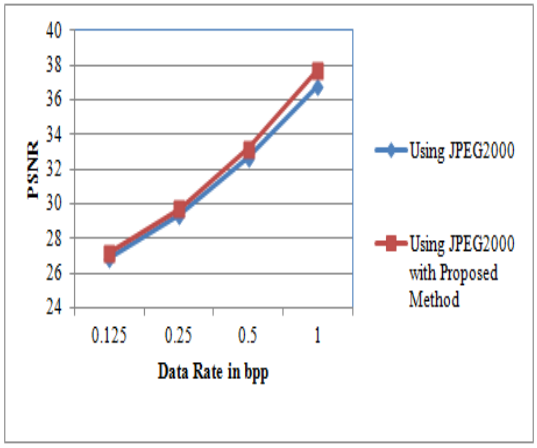

(g)

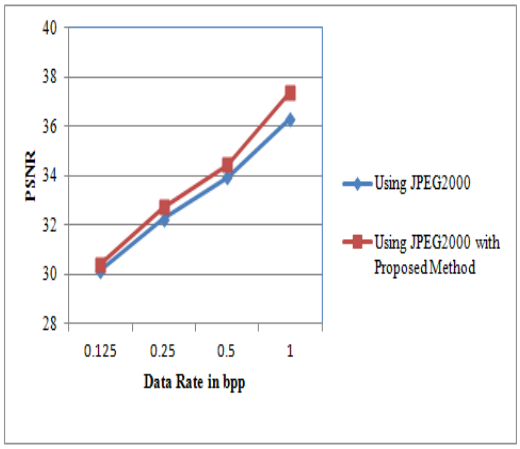

(h)

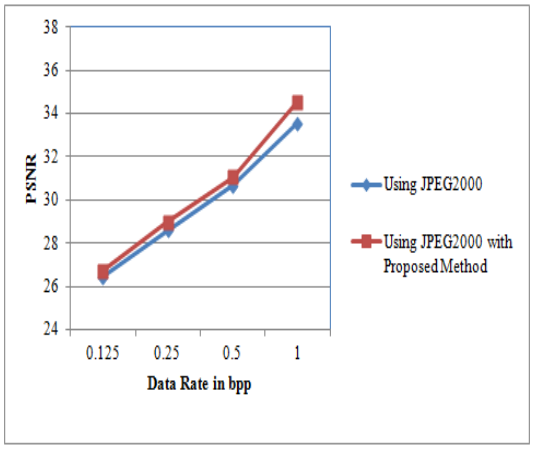

(i)

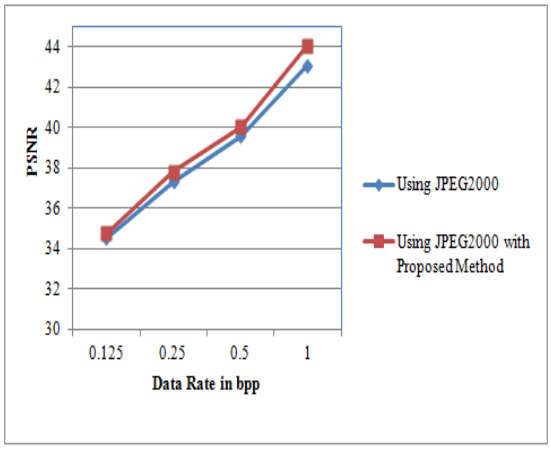

(j)

Figure 4.4: *PSNR* comparison of (a) Lena (b) Barbara (c) Airplane (d) Baboon (e) Boat (f) Bridge (g) Couple (h) Pepper (i) Sailboat and (j) Zelda images compressed at different bit rates using *JPEG*2000 standard and *JPEG*2000 standard with proposed post-processing approach.

Figure 4.5: Decompressed 512×512 Lena image after compression at a bit rate of 0.125 *bpp* using *JPEG*2000 with a tile size of 64×64.

Figure 4.6: Decompressed 512×512 Lena image after compression at a bit rate of 0.125 *bpp* using *JPEG*2000 with proposed post-processing method and a tile size of 64×64.

Figure 4.7: Decompressed 512×512 Barbara image after compression at a bit rate of 0.25 *bpp* using *JPEG*2000 with a tile size of 64×64.

Figure 4.8: Decompressed 512×512 Barbara image after compression at a bit rate of 0.25 *bpp* using *JPEG*2000 with proposed post-processing method and a tile size of 64×64.

4.4 Conclusion

In this chapter, a post-processing methodology has been implemented that can be applied along with *JPEG*2000 standard for reducing tile boundary artifacts of *JPEG*2000 compressed images. The methodology is motivated by the higher error in high pass reconstructed boundary samples than low pass boundary samples. It has been shown that when one uses proposed method, tile boundary artifacts are reduced in terms of increase in *PSNR* value. This increase in *PSNR* value varies from 0.1 *d*B to 1 *d*B for different images considered in this work. The reductions in boundary artifacts have also been observed in visual quality of decompressed images.

Chapter 5

Weighted Bit Rate Allocation for *JPEG*2000 Tile Encoding

5.1 Introduction

*JPEG*2000 standard allows an image to be divided into rectangular nonoverlapping blocks if the image size is larger than the available memory for the elaboration. These rectangular nonoverlapping blocks are called as tiles and this process of division is known as tiling. The *JPEG* standard decomposes an image into 8×8 size blocks. However, in *JPEG*2000 standard the tile size is not fixed and this is chosen by the user. This can even be the complete size of an image. All the tiles have same dimension, however, if dimension of image is not an integer multiplication of tile dimension, then dimensions of the tiles at boundary of the image may be different. For an image with multiple components, each tile also consists of these components. These tiles are then compressed independently.

After tiling, *DWT* is applied on each tile, which is a subband transform that transfers image/tile from spatial domain to frequency domain. In order to achieve efficient lossy and lossless compression within a single encoder, two wavelet transforms: *LeGall* 5/3 for lossless and *CDF* 9/7 for lossy compression are employed.

After this transformation, the wavelet coefficients are quantized to reduce precision if the lossy compression is employed. Then wavelet coefficients are encoded by *EBCOT* which is a two tier coding algorithm. In *EBCOT*, each wavelet subband is divided into code blocks and these code blocks are encoded independently. If precision of wavelet coefficients in a code block is *p*, then the code block is decomposed into *p* bit planes. Wavelet coefficients of a code block are represented by their sign-magnitude and encoded from most significant bit plane to least significant bit plane by *Tier*-1. Each bit plane is encoded with three coding passes. These passes are significant propagation pass, magnitude refinement pass and cleanup pass and each pass generates independent bit streams.

After generating bit stream for each code block, *Tier*-2 coding engine efficiently creates the layers from bit stream and code block summary information. A layer consists of consecutive bit plane coding passes from each code block, including all subbands of all the components in a tile. The code block summary information consists of length of compressed code words of the code block, the most significant magnitude bit plane at which any sample in the code block is non-zero, as well as truncation point between the bit stream layers, rate distortion slope optimized property and the features specified by the user.

Equal bit rate is assigned to all the tiles of an image when compressed with *JPEG*2000 standard. This assignment is suitable for the images with information contents that are equally distributed throughout the image. This bit rate is selected without taking information contents of the tiles into account. The tiles of an image may have different complexities; some of the tiles may have larger texture area while others may have larger smooth area. This results into poor performance of *JPEG*2000 standard for the tiles that have higher complexity. The quality of a reconstructed

image varies a lot if all tiles in the image don't have similar complexity. As such, the complexity of a tile while assigning a bit rate to it should be included.

Keeping in view the fact that entropy of a complex tile is more than the entropy of a smooth tile, a method is proposed to assign bit rate to a tile based on the weights computer from the entropy of a tile. Using this method, tiles of an image are assigned different compression bit rates. Visual quality of reconstructed image is improved by assigning these bit rates to the tiles of an image.

5.2 Effect of Tiling on Compression Performance of *JPEG*2000 Standard

As stated earlier, if the input image is of large size, it is divided into non overlapping blocks, called tiles and the size of a tile is not fixed. When an image is compressed using tiling approach at low bit rate, then the boundary artifacts arise on the boundaries of the tiles.

In this section, we have analyzed the effect of tiling on the compression performance of *JPEG2000* standard. For this purpose, different images available in the literature have been considered. These images are compressed without tiling and also with tiles of different sizes, at different bit rate using lossless as well lossy compression mode. In tiling approach, we have taken different sizes of tiles and these tiles are compressed at different bit rates at five level wavelet decomposition. Table 5.1 and Table 5.2 contain the results of this analysis.

Table 5.1: *PSNR* of the test images at different data rate and different tile sizes with *CDF* 9/7 wavelet filters

Image	Tile Size ⟶	64×64	128×128	No Tiles
	Data Rate (*bpp*)	*PSNR* (in *d*B)		
City	2.000	41.34	43.54	47.08

	1.000	32.96	36.06	40.64
	0.500	27.25	30.19	33.99
	0.250	23.49	26.49	29.31
	0.125	20.61	23.46	26.42
House	2.000	40.82	42.07	43.91
	1.000	34.74	36.58	39.09
	0.500	29.97	31.96	34.59
	0.250	26.50	28.63	30.89
	0.125	23.12	25.84	28.04
Boat	2.000	39.11	40.74	41.99
	1.000	33.23	35.25	36.67
	0.500	28.37	31.27	33.29
	0.250	24.47	27.59	30.04
	0.125	21.50	24.40	27.26
Scenery	2.000	46.86	48.70	48.59
	1.000	41.74	44.84	48.15
	0.500	36.65	40.68	45.09
	0.250	33.66	36.77	41.67
	0.125	30.65	33.95	38.79
Lena	2.000	44.12	44.97	45.66
	1.000	41.08	41.94	42.66
	0.500	36.67	37.80	38.92
	0.250	33.37	35.15	36.33

	0.125	29.94	32.48	34.37
Cameraman	2.000	48.02	48.76	49.06
	1.000	38.97	43.87	48.10
	0.500	31.27	37.11	42.11
	0.250	25.73	31.14	36.34
	0.125	21.46	26.12	31.84

Table 5.2: *PSNR* of the test images at different data rate and different tile size with *LeGall* 5/3 wavelet filters

Image	Tile Size →	64×64	128×128	No Tiles
	Data Rate (*bpp*)	*PSNR* (in *d*B)		
City	2.000	41.38	43.29	45.62
	1.000	33.22	36.18	40.18
	0.500	27.39	30.14	33.91
	0.250	23.67	26.29	29.08
	0.125	20.74	23.43	25.94
House	2.000	40.48	41.50	43.56
	1.000	34.50	36.22	38.22
	0.500	29.87	31.81	34.16
	0.250	26.56	28.53	30.62
	0.125	23.47	25.86	27.75

Boat	2.000	38.29	39.48	40.42
	1.000	32.80	34.63	35.82
	0.500	28.28	30.90	32.66
	0.250	24.32	27.32	29.49
	0.125	21.46	24.38	26.83
Scenery	2.000	47.04	49.02	50.41
	1.000	41.29	44.16	46.52
	0.500	36.76	40.34	43.53
	0.250	33.34	36.36	40.60
	0.125	30.46	33.77	38.05
Lena	2.000	44.24	44.96	45.43
	1.000	40.13	40.92	41.36
	0.500	36.06	37.13	37.87
	0.250	32.98	34.50	35.63
	0.125	29.74	32.04	33.63
Cameraman	2.000	47.24	49.30	51.04
	1.000	38.05	41.90	45.07
	0.500	31.18	36.19	39.81
	0.250	25.76	31.06	35.05
	0.125	21.45	26.36	31.02

From Tables 5.1 and 5.2, one can observe that tiling reduces the performance of *JPEG*2000 standard. This reduction can also be noted from the Figure 5.1 in which images at different bit rates and different tile sizes are shown.

(a)

(b)

(c)

Figure 5.1: (a) City image after decompression with 64×64 tile size and 0.125 *bpp* data rate (b) City image after decompression with 128×128 tile size and 0.125 *bpp* data rate (c) City image after decompression without tiling and 0.125 *bpp* data rate.

One can observe that when tile size is small, this reduction in performance is higher when compared with larger tile size. This phenomenon is due to the fact that equal bit rate is allocated to all of the tiles independent of their contents. This has motivated us to have an adaptive rate

allocation scheme for *JPEG*2000 standard which can allocate the bit rate to a tile using its contents.

5.3 Weighted Bit Rates and Proposed Approach

5.3.1 Zero-order Entropy of an Image

The zero-order entropy *e* of an image is defined as,

$$e = -\sum_{i=1}^{N} Pr(a_i) \log \left(Pr(a_i)\right) \quad \ldots (5.1)$$

where a_i, *i*= 1, 2, …, *N*, is the value of i^{th} gray level of image, *N* is the total number of different gray levels in the image and $Pr(a_i)$ is the probability of gray level a_i of the image.

5.3.2 Proposed Approach

Weighted bit rate allocation method proposed in this work is illustrated in Figure 5.2. Ardizzone *et al*. (2003) also gave a method for bit rate allocation. Their method is given in Figure 5.3. In the proposed method of bit rate allocation, the weights are derived from the zero-order entropy of tiles of an image. This bit rate allocation is passed to *Tier*-2 process of *EBCOT*, which assigns different bit rates to bit streams of each tile of the source image. After this, final bit stream is generated by *Tier*-2 process in order to output the compressed image.

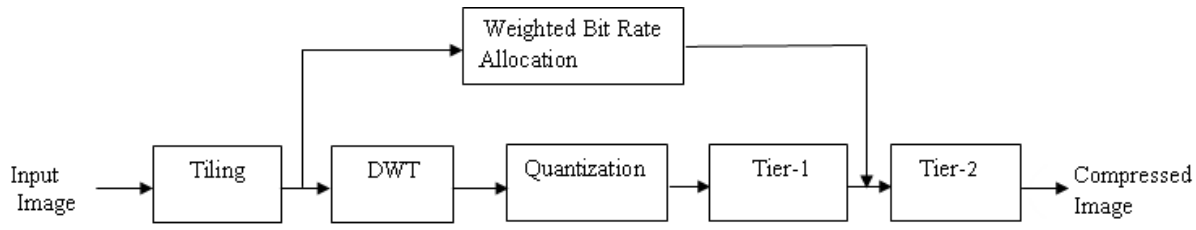

Figure 5.2: Weighted bit rate allocation in *JPEG*2000 standard

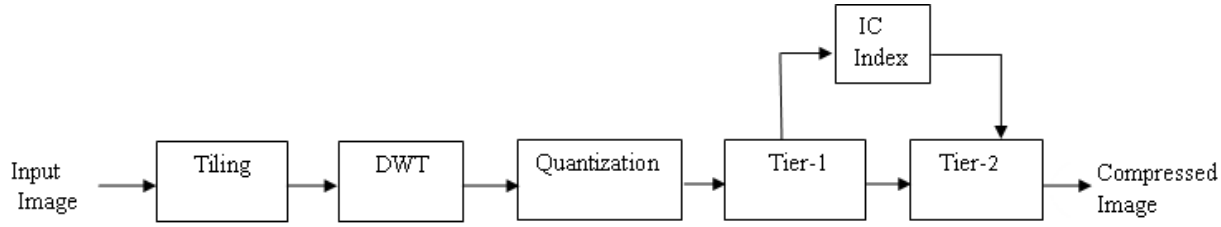

Figure 5.3: Bit rate allocation in Ardizzone *et al.* (2003) method

Zero-order entropy of each tile is calculated using (5.1). The weight $w(t)$ assigned to the tile *t* is given by,

$$w(t) = \frac{e(t)}{\sum_{t=1}^{N_T} e(t)} \times N_T \quad \ldots(5.2)$$

where $e(t)$ is zero-order entropy of t^{th} tile and N_T is total number of tiles in the image. This can also be noted that,

$$\frac{\sum_{t=1}^{N_T} w(t)}{N_T} = 1 \quad \ldots(5.3)$$

It is woth mentioning here that number of bits N_b, assigned to a *JPEG*2000 compressed image is calculated as,

$$N_b = R_0 \times image\_size$$

where R_0 is global compression bit rate given by the user and *image_size* is size of the original image.

Weighted bit rate R_i, based on zero-order entropy of a tile, is assigned to each tile, using the following formula.

$$R_t = R_0 \times w(t) \quad \ldots(5.4)$$

Thus total number of bits $N_b^{'}$ assigned to the compressed image is given by,

$$N_b^{'} = \sum_{t=1}^{N_T} R_t \times tile\_size$$

$$= \sum_{t=1}^{N_T} R_0 \times w(t) \times tile\_size$$

$$= R_0 \times N_t \times tile\_size$$

$$= R_0 \times image\_size$$

$$= N_b \quad \ldots (5.5)$$

where *tile_size* is the size of a tile. It can be noted from (5.5) that total number of compressed bits of an image remains unchanged when proposed algorithm is combined in *JPEG*2000 encoder to compress an image. The above steps can be summarized in following algorithm.

Algorithm 5.1: Weighted bit rate allocation algorithm

Step 1: Calculate zero-order entropy and weight of each tile of original image using (5.1) and (5.2), respectively.

Step 2: Assign weighted bit rate to each tile using (5.4). Now, compress each tile using *JPEG*2000 coder.

5.4 Results and Discussion

For implementing proposed algorithm, we have modified KAKADU software (Taubman, 2007). In this implementation, we have considered six standard images taken from literature. These images are compressed using 5 level wavelet decomposition with *CDF* 9/7 wavelet transform and a tile size of 64×64. In order to demonstrate effectiveness of the proposed algorithm, five bit

rates, namely, 1.000, 0.500, 0.250, 0.125 and 0.050 have been considered for each of these six images. The results are presented in Table 5.3.

Analysis of these results is presented in Figure 5.4. This contains RPI in $PSNR$ values for images considered in this work for different bit rates. Figure 5.4(a) depicts RPI in $PSNR$ values as a function of data rate when the percentage improvement is calculated on the basis of standard algorithm used in *JPEG*2000 and algorithm proposed by Ardizzone *et al.* (2003). $PSNR$ values vary from 1.687% to 3.25% when bit rate is 1.000; vary from 1.246% to 2.560% when bit rate is 0.500; vary from 0.821% to 1.804% when bit rate is 0.250; vary from 0.696% to1.351 when bit rate is 0.125 and vary from 0.424% to 0.835% when bit rate is 0.050, as indicated in Figure 5.4(a).

Also, Figure 5.4(b) depicts this RPI in $PSNR$ values when the percentage improvement is calculated on the basis of standard algorithm used in *JPEG*2000 and proposed algorithm. This figure indicates that RPI in $PSNR$ values vary from 2.403% to 5.352% when bit rate is 1.000; vary from 1.815% to 3.4495% when bit rate is 0.500; vary from 1.5693% to 2.3369% when bit rate is 0.250; vary from 1.4234% to 2.1920 when bit rate is 0.125 and vary from 0.5875% to 1.3359% when bit rate is 0.050 for the six images considered in this work.

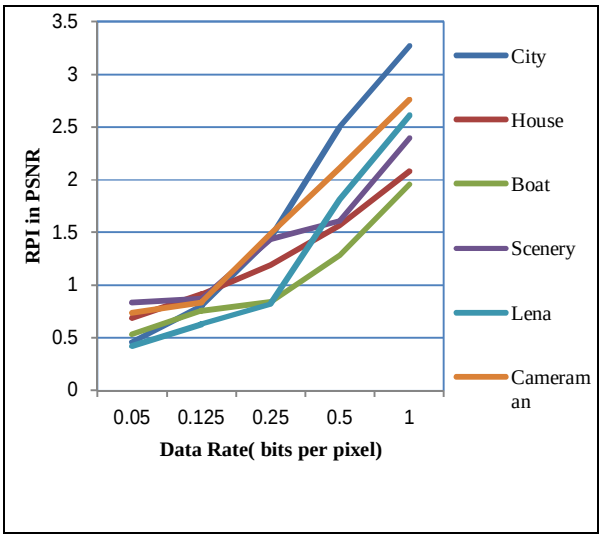

(a)

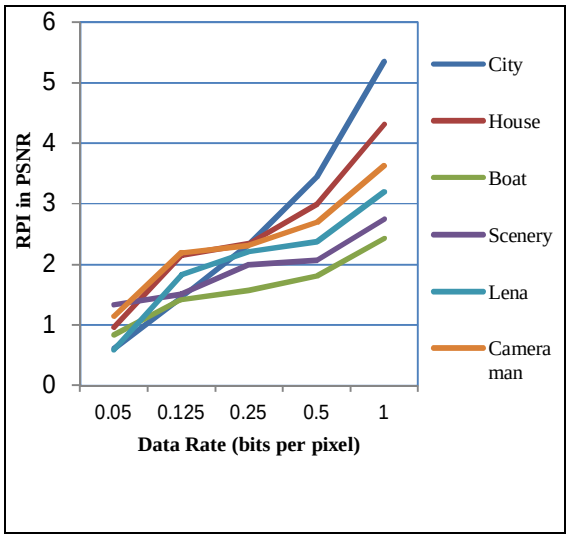

(b)

Figure 5.4: *RPI* in *PSNR* values

Table 5.3: *PSNR* (*d*B)/encoding time (sec)/memory usage (*KB*) comparison of the proposed approach with existing approaches

Image	Data Rate (*bpp*)	*JPEG*2000	Ardizzone Approach	Proposed Approach
City	2.000	41.34/1.38/4520	42.30/1.41/4525	43.25/1.49/4535
	1.000	32.96/1.38/4520	33.72/1.41/4525	34.57/1.49/4535
	0.500	27.25/1.38/4520	27.85/1.41/4525	28.48/1.49/4535
	0.250	23.49/1.38/4520	23.80/1.41/4525	24.10/1.49/4535
	0.125	20.61/1.38/4520	20.83/1.41/4525	21.10/1.49/4535
House	2.000	40.82/0.92/3365	41.69/0.99/3369	42.57/1.02/3375
	1.000	34.74/0.92/3365	35.13/0.99/3369	36.32/1.02/3375

	0.500	29.97/0.92/3365	30.51/0.99/3369	31.08/1.02/3375
	0.250	26.50/0.92/3365	26.96/0.99/3369	27.43/1.02/3375
	0.125	23.12/0.92/3365	23.44/0.99/3369	23.64/1.02/3375
Boat	2.000	39.11/1.045/4460	40.61/1.049/4474	41.00/1.061/4485
	1.000	33.23/1.045/4460	33.59/1.049/4474	34.09/1.061/4485
	0.500	28.37/1.045/4460	28.74/1.049/4474	29.06/1.061/4485
	0.250	24.47/1.045/4460	25.08/1.049/4474	25.37/1.061/4485
	0.125	21.50/1.045/4460	21.96/1.049/4474	22.17/1.062/4485
Scenery	2.000	46.86/0.75/2825	48.07/0.77/2827	48.83/0.86/2841
	1.000	41.74/0.75/2825	42.70/0.77/2827	43.34/0.86/2841
	0.500	36.65/0.75/2825	37.19/0.77/2827	38.15/0.86/2841
	0.250	33.66/0.75/2825	34.37/0.77/2827	34.84/0.85/2841
	0.125	30.65/0.75/2825	31.22/0.77/2827	31.51/0.86/2841
Lena	2.000	44.12/1.185/4516	44.24/1.190/4527	44.54/1.199/4558
	1.000	41.08/1.185/4516	41.20/1.190/4527	41.68/1.199/4558
	0.500	36.67/1.185/4516	37.58/1.190/4527	37.97/1.199/4558
	0.250	33.37/1.185/4516	34.09/1.190/4527	34.45/1.199/4558
	0.125	29.94/1.185/4516	30.45/1.190/4527	30.92/1.199/4558
Camera Man	2.000	48.02/0.84/3127	49.63/0.88/3145	50.03/0.88/3152
	1.000	38.97/0.84/3127	40.32/0.88/3145	40.67/0.88/3152
	0.500	31.27/0.84/3127	32.14/0.88/3145	32.77/0.88/3152
	0.250	25.73/0.84/3127	26.28/0.88/3145	26.83/0.88/3152
	0.125	21.46/0.84/3127	21.93/0.88/3145	22.37/0.88/3152

This can also be inferred from Table 5.3 that $PSNR$ values for all images and for all bit rates is improved when proposed algorithm is used *vis-a-vis* the algorithm implemented in *JPEG*2000 standard and algorithm proposed by Ardizzone *et al.* (2003). Maximum *PSNR* improvement by the proposed method is 2 *d*B. The increase in encoding time and memory taken by the proposed algorithm is very small when compared with the encoding time and memory taken by existing algorithms.

5.5 Conclusion

In this chapter, a weighted bit rate allocation algorithm for *JPEG*2000 image tiles has been proposed. The proposed methodology improves $PSNR$ values for all images and for all bit rates considered in this work. It has been observed that proposed methodology provides better visual quality in *JPEG*2000 reconstructed images than the conventional approach of *JPEG*2000 standard. This improvement has been shown taking place when compared with *JPEG*2000 encoder and also with the algorithm proposed by Ardizzone *et al.* (2003).

Chapter 6

Efficient Rate Control Approach for *JPEG*2000 Image Coding

6.1 Introduction

*JPEG*2000, the new image coding standard is more efficient when compared with old *JPEG* standard. However, most of the computations and memory usage in *PCRD* optimization scheme in *JPEG*2000 is redundant. In this chapter, an efficient rate control approach for *JPEG*2000 encoder is proposed. In this approach, optimal *RD* slope threshold is selected using minimum *RD* slope of lower level horizontal and vertical low pass (LL_0) subband of the wavelet decomposed image. Also, the passes of the code blocks of other subbands, whose *RD* slopes are less than the optimal *RD* slope, are skipped. The proposed approach reduces memory requirements and encoding time when compared with existing rate control approaches for *JPEG*2000 standard and also provides the same image quality as that of *PCRD* approach used in the *JPEG*2000 standard.

6.2 *PCRD* Optimization in *JPEG*2000

The block diagram of *JPEG*2000 encoder is shown in Figure 6.1. *JPEG*2000 has adopted *DWT* for its compression process. *DWT* is used to represent an image as a sum of wavelet functions,

known as wavelets, with different scale and location. It represents image data into a set of low pass and high pass coefficients. For this, input data is

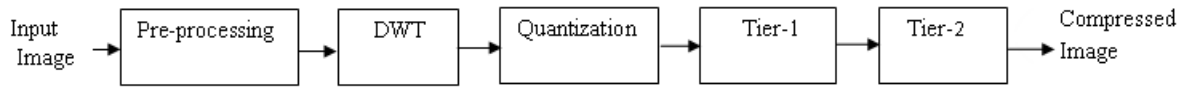

Figure 6.1: Block diagram of *JPEG*2000 encoder.

filtered using set of low pass and high pass filters. The output of this filtering step is down sampled by 2. This procedure is followed in 1-*D DWT*. In case of 2-*D DWT*, the data of the image is filtered through a set of low pass and high pass filters in two directions: along rows and columns of the image. The output is then down sampled by 2, as in case of 1-*D DWT*, to obtain a set of four subbands: horizontally low pass and vertically low pass (*LL)*, horizontally low pass and vertically high pass (*LH*), horizontally high pass and vertically low pass (*HL*) and horizontally high pass and vertically high pass (*HH*). If we number the resolution levels as 0, 1, . . ., *R*-1, then wavelet decomposition of $(R\text{-}1)^{th}$ level is associated with previous resolutions at lower levels. At each resolution level, except the lowest, *LL* subband alone is considered for further decomposition. For example, LL_{R-1} is decomposed to yield LL_{R-2}, LH_{R-2}, HL_{R-2}, and HH_{R-2}. This process is repeated until LL_0 is obtained, as shown in Figure 6.2.

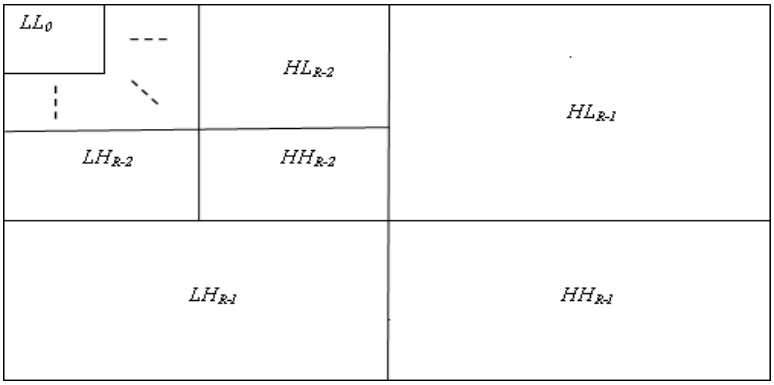

Figure 6.2: Wavelet decomposition structure.

Three level wavelet decomposed Lena image is shown in Figure 6.3.

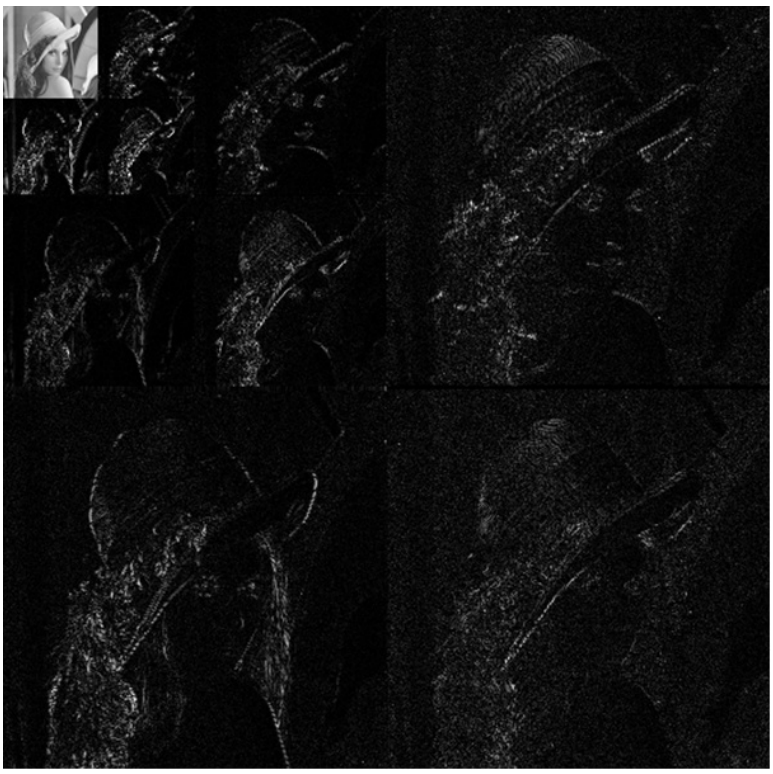

Figure 6.3: Three level wavelet decomposed Lena image.

DWT correlates the energy of an image with small number of wavelet coefficients in lower level *LL* subband, as can be observed from Figure 6.3. Around 98% of the image energy is stored into LL_0 subband of the wavelet decomposed image (Fang *et al*., 2011).

After the *DWT*, a scalar quantization is applied to wavelet coefficients. This entropy coding, *EBCOT* in *JPEG*2000 employs a two tiered process. *Tier*-1 of *EBCOT* uses context based arithmetic coding to compress each code block into separately embedded bit streams independently. Each code block is encoded bitplane by bitplane from the most significant bit to the least significant bit using three coding passes. These coding passes are: significance propagation pass, refinement pass and cleanup pass. *Tier*-2 of *EBCOT* is called the *PCRD* optimization, which truncates the embedded bit streams at a target bit rate to provide optimal image quality. *Tier*-1 process is the most complex part of *JPEG*2000, which consumes more than 50% of the total computations. *Tier*-2 process of *EBCOT* finds the set of truncation points for each code block which obtains the best image quality.

In *PCRD* optimization, each coding pass is a candidate of truncation point of a code block. The candidate corresponding to pass m of the bit plane k in the code block B_i is represented by,

$$n_i(k, m) = 3k - m + 3 \quad \ldots (6.1)$$

where n_i is the truncation point for the code block B_i.

In further illustrations in this chapter, n_i has been used for $n_i(k, m)$.

The distortion D of the final reconstructed image is given by,

$$D = \sum_i D_i^{n_i} \quad \ldots (6.2)$$

where $D_i^{n_i}$ represents the distortion at the truncation point n_i for the code block B_i.

If we take R as the number of code bytes associated with some set of truncation points $\{n_i\}$, then

$$R = \sum_i R_i^{n_i} \quad \ldots (6.3)$$

where $R_i^{n_i}$ is the number of code bytes at the truncation point n_i for the code block B_i.

Let R_{max} be the target data rate specified by the user. In order to find the set of truncation points $\{n_i\}$ that minimizes total distortion D with constraint $R = R_{max}$, one will have to use Lagrange optimization. Here, Lagrange function L becomes,

$$L = D + \lambda R \quad \ldots (6.4)$$

PCRD algorithm is used to find optimal λ_{opt} that minimizes D subject to the constraint $R \leq R_{max}$.

After encoding, for each code block of the input image, rate distortion slope $S_i^{n_i}$ is calculated at each truncation point n_i. The rate distortion slope $S_i^{n_i}$ is given by,

$$S_i^{n_i} = \frac{\Delta D_i^{n_i}}{\Delta R_i^{n_i}} = \frac{D_i^{n_i-1} - D_i^{n_i}}{R_i^{n_i} - R_i^{n_i-1}} \quad \ldots (6.5)$$

Following Langrage multiplier method, one can iterate to find λ_{opt} and the set of truncation points $\{n_i\}$ satisfying $S_i^{n_i} > \lambda_{opt}$ for all code blocks with R very close to R_{max}.

6.3 Proposed Rate Control Approach

The *EBCOT Tier*-1 encodes all the passes of every code block of the input image and thus takes considerable amount of computation and encoding time. The optimal value of the slope threshold

is found after calculating actual *RD* slopes of all the truncation points n_i. Also, the whole compressed bit stream must be stored in the memory while a large portion of compressed data will be discarded from the final code stream after *EBCOT Tier*-2 processing. Thus, a lot of *Tier*-1 encoding efforts and memory are wasted.

One can observe the following typical properties of *RD* slopes of the encoded passes of the code blocks of an input image. Firstly, the values of *RD* slopes in a code block are non-increasing. The second property is that the values of *RD* slopes of the finally included passes in code stream are higher than λ_{opt}, when the set of optimized truncation point is achieved. Third property is that the higher numbers of bytes are included in the final compressed code stream from the code blocks of LL_0 subband of the input image, as most of the image energy is stored into LL_0 subband (Fang *et al.*, 2011). Fourth property is that in each code block, there are *RD* slopes that are discarded by *Tier*-2 process after deciding the optimized truncation points. Fifth property is that λ_{opt} is very small at high bit rate than λ_{opt} at low bit rate. Taking a motivation from these properties, following Algorithm is proposed for rate control approach. In this approach, code blocks are processed in the scan order shown in Figure 6.4.

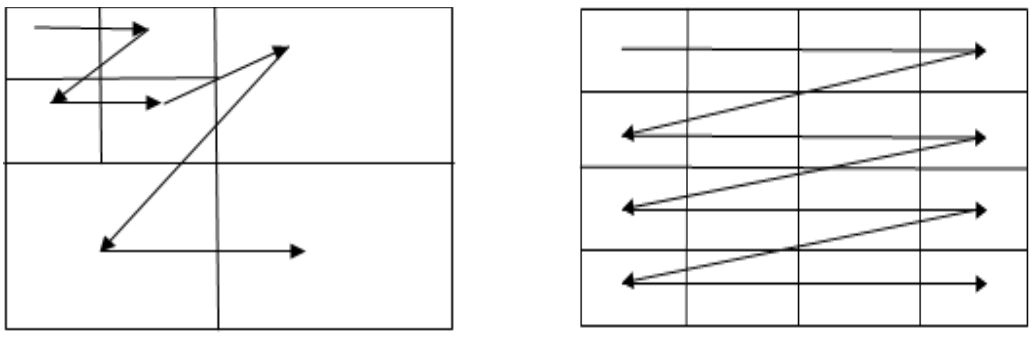

(a) (b)

Figure 6.4: Scan order of (a) subbands (b) code blocks of a subband.

Algorithm 6.1: Algorithm for efficient rate control approach

Step 1: Encode code blocks of LL_0 subband of the image using *Tier*-1 process of *JPEG*2000. Find the minimal *RD* slope of this subband using *Tier*-2 and designate it as λ_{min}. Take optimal *RD* slope threshold λ_{opt} as

$$\lambda_{opt} = \frac{\lambda_{min}}{user\ rate} \quad \ldots (6.6)$$

where *user rate* is bit rate in *bpp* defined by the user**.**

Step 2(i): If encoded bit rate is larger than the target bit rate, then discard the encoded pass(es) which has minimum *RD* slope(s) such that the accumulated bit rate is less than or equal to the target bit rate, and then stop *Tier*-1 process; else go to Step 2(ii).

Step 2(ii): Encode the passes of the code blocks of the next level subands block-wise, if their *RD* slopes are greater than λ_{opt}, otherwise skip the remaining passes of the code block, as the values of *RD* slopes in a code block is monotonically decreasing. Repeat Step 2 for the next code block of the current subband of the image.

Using the proposed approach, all passes of every code block of LL_0 subband are processed by *Tier*-1 and *Tier*-2 processes. The minimum *RD* slope, λ_{min} of the LL_0 subband is used to find the optimal *RD* slope threshold λ_{opt}. The passes of code blocks of the remaining subbands are processed by the *Tier*-1 if their *RD* slopes are greater than or equal to λ_{opt}. This process decreases the number of passes significantly. The passes of the code blocks that are left are those passes which have higher probability of rejection by the baseline *JPEG*2000 standard. Thus, the proposed approach is skipping those passes which were stored by *Tier*-1 till the completion of the *Tier*-2 process. This decreases the memory requirement and encoding time of *JPEG*2000. Also, as the optimal *RD* slope threshold is selected using the minimum *RD* slope of LL_0 subband

of the wavelet decomposed image, the quality of the decompressed image is very close to the quality produced by the *PCRD* optimization of *JPEG*2000.

6.4 Experimental Results

The proposed rate control algorithm has been tested on ten images using JASPER software (Adams, 2000) tool. For all these images, we used *CDF* 9/7 wavelet filters with five level wavelet decomposition and the code block size was taken as 64×64. These images were compressed using (i) *JPEG*2000 standard's *PCRD* algorithm for rate control, (ii) the rate control approach proposed in this work and (iii) approaches given by Masuzaki *et al*. (2002), Chang *et al.* (2002), Du *et al.* (2004), Yeung and Au (2005) and Chang *et al.* (2006), along with other steps of *JPEG*2000 standard. The comparison of *PSNR*, encoding time and memory usage of the proposed approach with existing approaches (as given above) and also with *JPEG*2000 standard's *PCRD* algorithm is given in Table 6.1.

Table 6.1: Comparison of *PSNR* (*d*B)/encoding time (sec)/memory usage (KB) of the proposed approach with the existing approaches and *PCRD*.

Bit Rate (*bpp*)	***PCRD***	**Masuzaki *et al*., (2002)**	**Chang *et al*., (2002)**	**Du *et al.* (2004)**	**Yeung and Au, (2005)**	**Chang *et al*., (2006)**	**Proposed Approach**
Lena Image							
0.125	31.15/ 1.185/ 4516	30.56/ 0.450/ 2240	30.82/ 0.450/ 2240	30.82/ 0.425/ 2240	30.92/ 0.398/ 2235	30.98/ 0.398/ 2235	31.15/ 0.390/ 2210

0.250	33.97/ 1.185/ 4516	33.04/ 0.525/ 2478	33.18/ 0.525/ 2482	33.35/ 0.479/ 2465	33.40/ 0.479/ 2446	33.61/ 0.479/ 2448	33.96/ 0.468/ 2425
0.500	37.15/ 1.185/ 4516	36.65/ 0.639/ 2664	36.62/ 0.639/ 2664	36.69/ 0.639/ 2664	36.72/ 0.645/ 2664	36.98/ 0.645/ 2664	37.13/ 0.639/ 2634
1.000	40.70/ 1.185/ 4516	40.30/ 0.915/ 3080	40.31/ 0.915/ 3080	40.31/ 0.905/ 2970	40.33/ 0.856/ 2898	40.34/ 0.856/ 2898	40.58/ 0.845/ 2860
2.000	44.64/ 1.185/ 4516	43.53/ 0.955/ 2965	43.64/ 0.955/ 2965	43.64/ 0.950/ 2965	44.02/ 0.924/ 2928	44.10/ 0.924/ 2928	44.41/ 0.904/ 2904
Barbara Image							
0.125	25.41/ 1.045/ 4460	24.82/ 0.429/ 2180	24.93/ 0.425/ 2180	24.95/ 0.425/ 2145	24.99/ 0.368/ 2130	25.16/ 0.361/ 2125	25.39/ 0.358/ 2120
0.250	30.41/ 1.045/ 4460	29.20/ 0.429/ 2180	29.23/ 0.425/ 2180	29.34/ 0.425/ 2145	29.95/ 0.368/ 2130	29.95/ 0.361/ 2125	30.41/ 0.358/ 2120
0.500	34.08/ 1.045/ 4460	33.57/ 0.445/ 2345	33.62/ 0.435/ 2345	33.62/ 0.435/ 2345	33.85/ 0.415/ 2345	33.87/ 0.415/ 2345	34.08/ 0.405/ 2345
1.000	38.71/	37.62/	37.83/	37.65/	37.72/	37.95/	38.71/

	1.045/ 4460	0.580/ 2456	0.576/ 2454	0.575/ 2454	0.565/ 2450	0.565/ 2450	0.561/ 2450
2.000	44.86/ 1.045/ 4460	43.75/ 0.825/ 2685	43.95/ 0.825/ 2685	43.98/ 0.825/ 2675	44.52/ 0.830/ 2680	44.52/ 0.811/ 2672	44.76/ 0.811/ 2670
Airplane Image							
0.125	31.82/ 1.145/ 4485	30.45/ 0.405/ 2256	30.45/ 0.405/ 2256	31.06/ 0.399/ 2246	31.46/ 0.399/ 2246	31.52/ 0.392/ 2239	31.81/ 0.390/ 2232
0.250	35.18/ 1.145/ 4485	34.21/ 0.472/ 2285	34.26/ 0.472/ 2285	34.64/ 0.470/ 2260	34.82/ 0.470/ 2250	34.83/ 0.452/ 2245	35.17/ 0.452/ 2245
0.500	38.64/ 1.145/ 4485	37.73/ 0.644/ 2455	37.82/ 0.624/ 2455	37.82/ 0.642/ 2445	38.15/ 0.634/ 2448	38.15/ 0.624/ 2435	38.64/ 0.624/ 2435
1.000	42.15/ 1.145/ 4485	41.04/ 0.905/ 2705	41.09/ 0.905/ 2705	41.29/ 0.896/ 2690	41.82/ 0.895/ 2690	41.86/ 0.889/ 2675	42.01/ 0.889/ 2675
2.000	44.34/ 1.145/ 4485	43.75/ 0.953/ 2965	43.79/ 0.953/ 2965	43.95/ 0.953/ 2965	43.96/ 0.943/ 2864	43.97/ 0.933/ 2864	44.15/ 0.933 2864
Baboon Image							
0.125	22.15/	21.70/	21.72/	21.80/	21.92/	22.02/	22.15/

	1.760/ 4272	0.408/ 2178	0.408/ 2178	0.408/ 2175	0.407/ 2176	0.407/ 2176	0.405/ 2170
0.250	24.11/ 1.760/ 4272	23.20/ 0.408/ 2178	23.20/ 0.408/ 2178	23.21/ 0.408/ 2175	23.62/ 0.407/ 2176	23.68/ 0.407/ 2176	24.10/ 0.405/ 2170
0.500	27.33/ 1.760/ 4272	26.75/ 0.456/ 2316	26.75/ 0.457/ 2316	26.87/ 0.457/ 2316	26.84/ 0.452/ 2290	26.85/ 0.452/ 2285	27.33/ 0.452/ 2285
1.000	31.06/ 1.760/ 4272	30.38/ 0.645/ 2460	30.39/ 0.645/ 2460	30.38/ 0.645/ 2460	30.80/ 0.639/ 2456	30.85/ 0.639/ 2455	31.01/ 0.639/ 2450
2.000	35.70/ 1.760/ 4272	34.17/ 0.889/ 2675	34.17/ 0.889/ 2675	34.17/ 0.889/ 2675	34.21/ 0.889/ 2675	34.30/ 0.889/ 2675	35.63/ 0.889 2675
Boat Image							
0.125	31.78/ 1.045/ 4460	30.79/ 0.425/ 2315	30.81/ 0.428/ 2315	30.94/ 0.415/ 2308	31.34/ 0.410/ 2295	31.30/ 0.405/ 2285	31.78/ 0.405/ 2285
0.250	35.21/ 1.045/ 4460	34.27/ 0.421/ 2455	34.27/ 0.421/ 2455	34.65/ 0.421/ 2455	34.90/ 0.421/ 2455	34.93/ 0.421/ 2455	35.21/ 0.421/ 2455
0.500	39.10/ 1.045/	38.14/ 0.625/	38.16/ 0.625/	38.19/ 0.610/	38.35/ 0.589/	38.39/ 0.577/	39.10/ 0.577

	4460	2685	2685	2665	2665	2645	2645
1.000	45.95/ 1.045/ 4460	44.91/ 0.876/ 2736	44.92/ 0.876/ 2736	44.99/ 0.870/ 2730	45.35/ 0.845/ 2724	45.35/ 0.826/ 2705	45.95/ 0.826/ 2705
2.000	46.90/ 1.045/ 4460	45.99/ 0.931/ 2890	45.99/ 0.931/ 2890	46.01/ 0.930/ 2885	46.13/ 0.931/ 2890	46.15/ 0.911/ 2876	46.90/ 0.911/ 2876
Bridge Image							
0.125	23.31/ 0.933/ 3265	22.42/ 0.165/ 2210	22.43/ 0.165/ 2210	22.56/ 0.166/ 2210	22.72/ 0.159/ 2210	22.73/ 0.156/ 2175	23.31/ 0.156/ 2175
0.250	24.81/ 0.933/ 3265	23.86/ 0.185/ 2260	23.84/ 0.185/ 2260	23.95/ 0.182/ 2255	24.35/ 0.182/ 2250	24.37/ 0.181/ 2248	24.81/ 0.181/ 2248
0.500	27.18/ 0.933/ 3265	26.21/ 0.259/ 2370	26.23/ 0.259/ 2370	26.41/ 0.255/ 2365	26.72/ 0.252/ 2360	26.72/ 0.249/ 2355	27.17/ 0.249/ 2355
1.000	30.58/ 0.933/ 3265	29.62/ 0.352/ 2469	29.65/ 0.352/ 2469	29.80/ 0.348/ 2461	30.04/ 0.345/ 2459	30.07/ 0.345/ 2459	30.56/ 0.343/ 2456
2.000	36.68/ 0.933/ 3265	35.81/ 0.510/ 2528	35.83/ 0.510/ 2525	35.92/ 0.510/ 2528	36.15/ 0.510/ 2525	36.17/ 0.499/ 2512	36.66/ 0.499/ 2512

Couple Image							
0.125	26.84/ 0.985/ 3565	25.92/ 0.158/ 2170	25.95/ 0.158/ 2170	25.98/ 0.150/ 2165	26.31/ 0.145/ 2150	26.32/ 0.140/ 2140	26.84/ 0.140/ 2140
0.250	29.32/ 0.985/ 3565	28.43/ 0.171/ 2245	28.45/ 0.171/ 2245	28.53/ 0.171/ 2245	28.94/ 0.171/ 2245	28.96/ 0.171/ 2245	29.32/ 0.171/ 2245
0.500	32.66/ 0.985/ 3565	31.74/ 0.260/ 2380	31.76/ 0.260/ 2380	31.83/ 0.260/ 2380	31.12/ 0.255/ 2365	31.16/ 0.249/ 2350	32.66/ 0.249/ 2350
1.000	36.80/ 0.985/ 3565	35.92/ 0.345/ 2450	35.95/ 0.345/ 2450	36.15/ 0.340/ 2445	36.31/ 0.335/ 2430	36.35/ 0.327/ 2416	36.80/ 0.327/ 2416
2.000	42.03/ 0.985/ 3565	41.15/ 0.490/ 2558	41.16/ 0.490/ 2558	41.25/ 0.491/ 2560	41.54/ 0.490/ 2554	41.58/ 0.483/ 2524	42.03/ 0.483/ 2524
Pepper Image							
0.125	30.18/ 1.895/ 4855	29.34/ 0.456/ 2250	29.37/ 0.456/ 2250	29.55/ 0.454/ 2245	29.75/ 0.440/ 2238	29.79/ 0.436/ 2232	30.17/ 0.436/ 2232
0.250	32.26/ 1.895/ 4855	31.35/ 0.499/ 2495	31.38/ 0.499/ 2495	31.46/ 0.499/ 2495	31.76/ 0.499/ 2485	31.78/ 0.499/ 2476	32.25/ 0.499/ 2476

0.500	33.94/ 1.895/ 4855	32.96/ 0.705/ 2690	32.98/ 0.705/ 2690	33.04/ 0.705/ 2690	33.46/ 0.696/ 2678	33.49/ 0.686/ 2670	33.94/ 0.686/ 2670
1.000	36.32/ 1.895/ 4855	35.45/ 0.975/ 2895	35.49/ 0.975/ 2895	35.68/ 0.975/ 2895	35.71/ 0.970/ 2880	35.71/ 0.967/ 2875	36.32/ 0.967/ 2875
2.000	40.66/ 1.895/ 4855	39.75/ 1.490/ 3208	39.78/ 1.492/ 3208	39.87/ 1.492/ 3208	40.14/ 1.482/ 3178	40.18/ 1.482/ 3175	40.66/ 1.482/ 3175
Sailboat Image							
0.125	26.45/ 1.895/ 4855	25.54/ 0.460/ 2165	25.56/ 0.460/ 2165	25.64/ 0.455/ 2160	25.95/ 0.452/ 2152	25.97/ 0.452/ 2150	26.45/ 0.452/ 2150
0.250	28.60/ 1.895/ 4855	27.72/ 0.585/ 2470	27.74/ 0.585/ 2470	27.92/ 0.580/ 2465	28.04/ 0.565/ 2450	28.06/ 0.546/ 2448	28.60/ 0.546/ 2445
0.500	30.67/ 1.895/ 4855	29.74/ 0.705/ 2725	29.76/ 0.705/ 2725	29.89/ 0.685/ 2705	30.19/ 0.685/ 2720	30.21/ 0.655/ 2650	30.66/ 0.655 2650
1.000	33.56/ 1.895/ 4855	32.64/ 0.825/ 2945	32.64/ 0.825/ 2950	32.82/ 0.820/ 2925	33.04/ 0.810/ 2910	33.02/ 0.798/ 2872	33.56/ 0.798/ 2872
2.000	39.17/	38.23/	38.23/	38.45/	38.64/	38.65/	39.16/

	1.895/ 4855	1.513/ 3345	1.513/ 3345	1.513/ 3375	1.513/ 3360	1.513/ 3250	1.513/ 3250
Zelda Image							
0.125	34.55/ 0.750/ 2744	33.43/ 0.145/ 1954	33.45/ 0.145/ 1954	33.49/ 0.148/ 1925	33.85/ 0.130/ 1870	33.85/ 0.125/ 1858	34.55/ 0.124/ 1850
0.250	37.34/ 0.750/ 2744	35.64/ 0.158/ 1939	35.64/ 0.158/ 1939	35.72/ 0.156/ 1929	36.67/ 0.156/ 1929	36.68/ 0.156/ 1928	37.34/ 0.156/ 1925
0.500	39.60/ 0.750/ 2744	38.68/ 0.190/ 2065	38.67/ 0.190/ 2070	38.73/ 0.190/ 2065	38.93/ 0.187/ 2065	38.93/ 0.187/ 2050	39.60/ 0.187 2050
1.000	43.10/ 0.750/ 2744	42.07/ 0.305/ 2315	42.09/ 0.305/ 2315	42.21/ 0.298/ 2315	42.35/ 0.296/ 2318	42.35/ 0.296/ 2285	43.10/ 0.296/ 2285
2.000	46.21/ 0.750/ 2744	45.36/ 0.470/ 2580	45.36/ 0.470/ 2580	45.37/ 0.472/ 2585	45.42/ 0.475/ 2575	45.43/ 0.468/ 2540	46.21/ 0.468/ 2520

From this table, one can conclude that the maximum difference between the *PSNR* of the images considered in this work is 0.23 *d*B when the proposed approach is compared with that of the *PCRD* approach available in *JPEG*2000. The value of *PSNR* with proposed approach is consistently higher than the *PSNR* values with the algorithms proposed by Masuzaki *et al.*

(2002), Chang *et al.* (2002), Du *et al.* (2004), Yeung and Au, (2005) and Chang *et al.* (2006). The encoding time and memory usage in the proposed approach is 50%-60% less than *PCRD* approach and comparable with the other approaches. Thus proposed approach is producing the same *PSNR* more efficiently.

We have also compared the number of passes processed by *Tier*-2 of *JPEG*2000 standard in case of *JPEG*2000 baseline *PCRD* approach, other existing approach and the proposed approach. The results of this comparison are given in Table 6.2.

Table 6.2: Comparison of number of passes processed by the proposed approach with the existing approaches and *PCRD* approach.

Bit Rate (*bpp*)	***PCRD***	**Masuzaki *et al.*, (2002)**	**Chang *et al.*, (2002)**	**Du *et al.* (2004)**	**Yeung and Au, (2005)**	**Chang *et al.*, (2006)**	**Proposed Approach**
Lena Image							
0.125	2646	1500	1457	1300	1200	705	511
0.250	2646	1805	1602	1602	1602	797	594
0.500	2646	2095	1803	1803	1803	998	794
1.000	2646	2187	2056	2095	1876	1459	1162
2.000	2646	2454	2405	2316	2312	1895	1846
Barbara Image							
0.125	1087	504	525	504	351	325	223
0.250	1087	621	603	520	405	375	342
0.500	1087	798	805	705	570	565	497

1.000	1087	806	840	825	662	628	520
2.000	1087	950	905	870	835	839	797
Airplane Image							
0.125	2460	1562	1520	1462	1262	862	475
0.250	2460	1605	1515	1525	1405	905	542
0.500	2460	1989	1860	1765	1663	1260	910
1.000	2460	2139	2045	2048	1939	1579	1596
2.000	2460	2250	2135	2107	2115	1950	1864
Baboon Image							
0.125	2146	1204	1124	650	506	506	430
0.250	2146	1409	1409	1007	996	837	545
0.500	2146	1605	1535	1105	925	905	620
1.000	2146	1834	1728	1494	1305	1194	753
2.000	2146	1854	1842	1595	1442	1243	988
Boat Image							
0.125	1057	495	483	474	456	342	227
0.250	1057	536	525	510	473	453	335
0.500	1057	624	615	624	664	624	527
1.000	1057	905	925	916	905	876	846
2.000	1057	1045	1015	970	976	956	950
Bridge Image							
0.125	1177	495	483	474	459	348	232

0.250	1177	536	515	506	475	453	248
0.500	1177	724	707	684	664	624	340
1.000	1177	909	905	816	786	676	506
2.000	1177	1124	1115	996	976	956	836
Couple Image							
0.125	1120	516	489	465	405	349	225
0.250	1120	539	525	510	479	484	245
0.500	1120	624	615	624	664	629	325
1.000	1120	936	912	836	804	775	540
2.000	1120	1045	1015	970	976	956	847
Pepper Image							
0.125	2910	1510	1529	1350	1106	662	563
0.250	2910	1725	1615	1521	1405	805	669
0.500	2910	1989	1860	1765	1663	1160	740
1.000	2910	2139	2055	2068	1905	1279	893
2.000	2910	2250	2135	2107	2115	1950	1296
Sailboat Image							
0.125	2982	1562	1495	1432	1262	862	575
0.250	2982	1605	1515	1487	1405	905	655
0.500	2982	1989	1860	1765	1663	1260	759
1.000	2982	2145	2035	2048	1939	1579	890
2.000	2982	2250	2205	2127	2018	1950	930
Zelda Image							

0.125	1841	525	483	495	462	405	360
0.250	1841	561	528	510	473	453	405
0.500	1841	636	615	624	564	496	427
1.000	1841	1029	934	904	892	831	565
2.000	1841	1045	1015	970	926	856	745

From this table, one can conclude that decrease in number of passes processed by proposed approach in *Tier*-2 is more than 80% when compared with that of *PCRD* approach and other existing approaches proposed by Masuzaki *et al*. (2002), Chang *et al.* (2002), Du *et al.* (2004), Yeung and Au, (2005) and Chang *et al*. (2006). This decrease in the number of passes decreases the encoding time and memory usage in the proposed approach when compared with *PCRD* approach and other existing approaches. Thus proposed approach is less complex than existing approaches.

One can judge the efficiency of the proposed approach by browsing the quality of the compressed images as well. In order to support this claim, the decompressed Lena, Baboon, Pepper and Zelda images at different bit rates are shown in Figure 6.5.

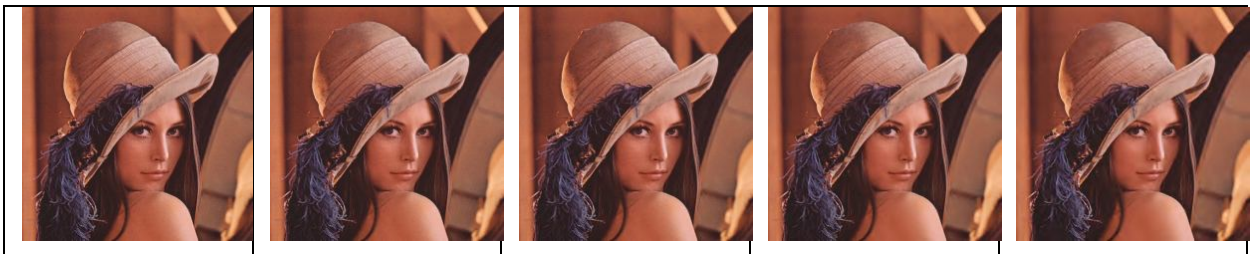

(a) Original Lena | (b) Lena at 1 *bpp* | (c) Lena at 0.5 *bpp* | (d) Lena at 0.25 *bpp* | (e) Lena at 0.125 *bpp*

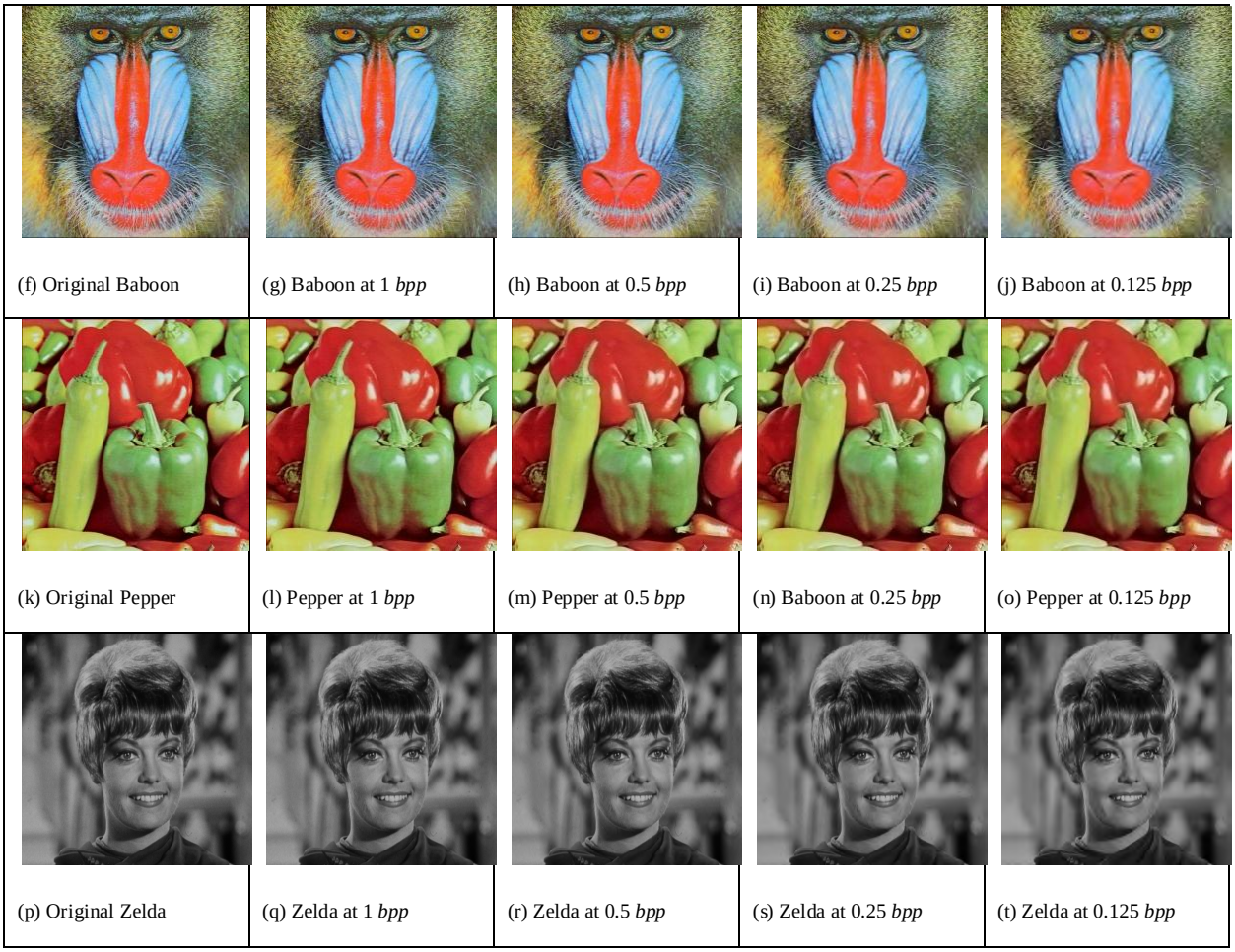

(f) Original Baboon | (g) Baboon at 1 *bpp* | (h) Baboon at 0.5 *bpp* | (i) Baboon at 0.25 *bpp* | (j) Baboon at 0.125 *bpp*

(k) Original Pepper | (l) Pepper at 1 *bpp* | (m) Pepper at 0.5 *bpp* | (n) Baboon at 0.25 *bpp* | (o) Pepper at 0.125 *bpp*

(p) Original Zelda | (q) Zelda at 1 *bpp* | (r) Zelda at 0.5 *bpp* | (s) Zelda at 0.25 *bpp* | (t) Zelda at 0.125 *bpp*

Figure 6.5: Original and decompressed Lena, Baboon, Pepper and Zelda images at different bit rates

We have also compared the percentage decrease in number of passes required to compress the images and relative percentage decrease in *PSNR* values. For all test images, relative percentage decrease in number of passes required to compress the image at a given bit rate and relative percentage decrease in *PSNR* at the same bit rate are calculated. Figures 6.6(a) to 6.6(j) contain the results of these calculations for the test images.

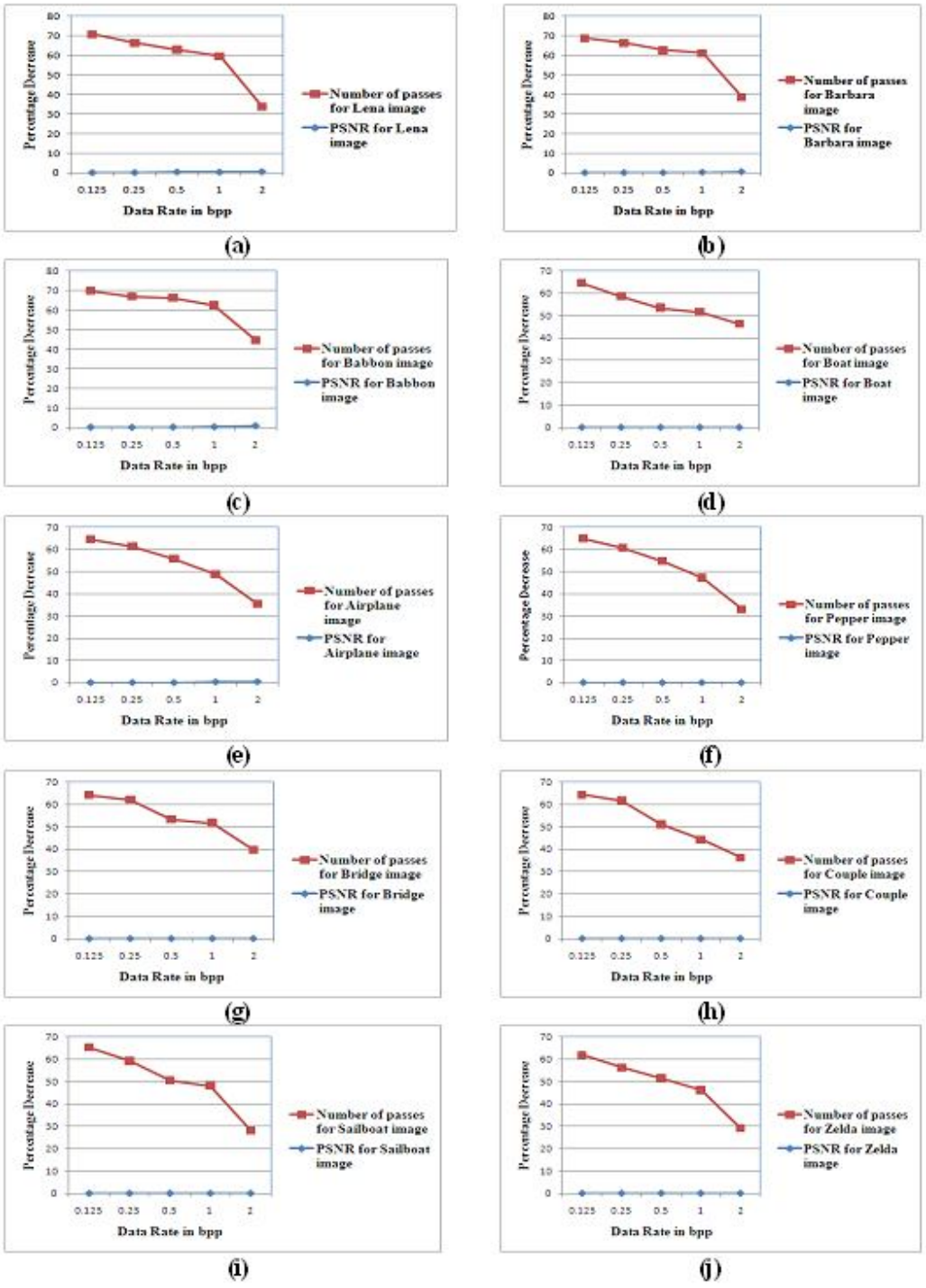

Figure 6.6: Comparison of percentage decrease in number of passes and percentage decrease in *PSNR* using proposed approach over *PCRD*.

For all the ten images considered in this study, it has been noted that the number of passes required to compress an image at a given bit rate decreases sharply when the proposed approach is combined with *JPEG*2000 compression process, in place of conventional *PCRD* approach. The value of *PSNR* also decreases when we use the proposed approach but the relative decrease in *PSNR* is negligible in comparison with the decrease in the number of passes. Maximum percentage decrease in number of passes is 80.70% in case of Lena image at 0.125 *bpp* and minimum percentage decrease in number of passes is 10.12% in case of Boat image at 2 *bpp*. Also, maximum percentage decrease of *PSNR* is 0.52% in case of Lena image at 2 *bpp*. This establishes the effectiveness of proposed rate control approach.

6.5 Conclusion

In this chapter, an efficient rate control approach based on *RD* slope of LL_0 subband is proposed. The maximum decrease in *PSNR* value is 0.23 *d*B when this approach is compared with *PCRD* approach of *JPEG*2000, while *PSNR* value is higher than the *PSNR* values produced by the approaches used by Masuzaki *et al*. (2002), Chang *et al.* (2002), Du *et al*. (2004), Yeung and Au, (2005) and Chang *et al.* (2006). The memory usage and encoding time with the proposed approach is reduced by 50% to 60% when compared with the *PCRD* approach and is almost similar with other existing approaches. The proposed approach saves up to 80.70% passes when it is used with the *JPEG*2000 standard. Maximum degradation in *PSNR* is 0.23 *d*B for Lena image at 2.0 *bpp*. The proposed approach can further be explored by implementing this in small devices having relatively less memory and less computation power.

Chapter 7

Conclusion and Future Scope

7.1 Conclusion

This thesis consists of seven chapters. Chapter 1 introduces the problem tackled in this thesis and also introduces the fundamentals related to the problem. In Chapter 2, literature survey related to *JPEG*2000 is carried out. In Chapter 3, edge adaptive lifting scheme is proposed in which the edge direction is predicted using the neighboring pixels of the same subset of even/odd image pixels. The edge direction is also checked for the quarter and half subpixels which are interpolated using *Sinc* interpolation. It has been observed that there is an improvement of 1 *d*B when compared with *WAL* scheme and an improvement of more than 4 *d*B when compared with *JPEG*2000 lifting scheme.

In Chapter 4, a post-processing methodology has been implemented that can be applied along with *JPEG*2000 standard for reducing tile boundary artifacts of *JPEG*2000 compressed images. The methodology is motivated by the higher error in high pass reconstructed boundary samples than low pass boundary samples. It has been shown that when one uses proposed method, tile boundary artifacts are reduced in terms of increase in *PSNR* value. This increase in *PSNR* value

varies from 0.1 *d*B to 1 *d*B for different images considered in this work. The reductions in boundary artifacts have also been observed in visual quality of decompressed images.

In Chapter 5, a weighted bit rate allocation algorithm for *JPEG*2000 image tiles has been proposed, which improves *PSNR* values for all images and for all bit rates considered in the presented work. The proposed methodology provides better visual quality in *JPEG*2000 reconstructed images than the conventional approach of *JPEG*2000 standard. This improvement has been shown taking place when compared with *JPEG*2000 encoder and also with the existing algorithm.

In Chapter 6, an efficient rate control approach based on *RD* slope of LL_0 subband is proposed. The maximum decrease in *PSNR* value is 0.23 *d*B when this approach is compared with *PCRD* approach of *JPEG*2000, while *PSNR* value is higher than the *PSNR* values produced by the existing approaches. The memory usage and encoding time with the proposed approach is reduced by 50% to 60% when compared with the *PCRD* approach and is almost similar with other existing approaches. The proposed approach saves up to 80.70% passes when it is used with the *JPEG*2000 standard.

7.2 Future Scope

This work has focused on the improvements in different processes of *JPEG*2000 standard of compression. Four different processes have been improved by proposing suitable modifications in the existing methodologies. However, there is still now a scope of improvement in the implementation of these processes. This section discusses a few possible improvements that can further improve *JPEG*2000 compression standard.

In edge adaptive lifting scheme, *Sinc* interpolation filter with constant coefficients is used for subpixel interpolation in the horizontal and vertical directions. Directional adaptive interpolation filters having less number of taps can be used in this scheme. This may further decrease its computational complexity and probably a better visual quality can be achieved.

In weighted bit rate allocations technique, weights can be derived using entropy and motion activity of the Motion *JPEG*2000 standard to assign variable bit rates to the frames of video files. As moving portions of video are often the interested regions for human visual systems, combining the motion activity parameter in rate assignment may improve visual quality of the Motion *JPEG*2000 images. Also, there will not be a requirement of changing the format of the code stream and hence the decoder also requires no change.

In post-processing methodology, we can consider more than two neighbors and assign weights to them in order to reduce the error present in high pass reconstructed tile boundary samples, as there is a correlation present among the neighboring samples of a natural image. We can also consider these neighbors in other directions than the horizontal and vertical.

Distortion estimation of *JPEG*2000 requires noninteger processing and the overwhelming computational burden is the distortion calculation which is calculated for every bit of the uncompressed image. In the approach proposed in this work, distortion calculation is performed using the same concept of *JPEG*2000. We can propose an integer based approach for distortion calculation and combine that approach with proposed rate control approach to further reduce the computational requirements of *PCRD* optimization. Also, proposed rate allocation approach can be explored by implementing this in small devices having relatively less memory and less computation power.

References

[1] Adams M. D. and Kossentini F., "Reversible Integer to Integer Wavelet Transforms for Image Compression: Performance Evaluation and Analysis", *IEEE* Transactions on Image Processing, Vol. 9, No. 6, pp. 1010-1024, 2000.

[2] Adams M. D., "JASPER version 1.900.1", http://www.ece.uvic.ca/~mdadams/jasper/, 2000.

[3] Antonini M., Barlaud M., Mathieu P. and Daubechies I., "Image Coding Using Wavelet Transforms," *IEEE* Transactions on Image Processing, Vol. 1, No.2, pp. 205–220, 1992.

[4] Ardizzone E., Cascia M. L. and Testa F., "A New Algorithm for Bit Rate Allocation in *JPEG*2000 Tile Encoding", Proceedings of *IEEE* 12th International Conference on Image Analysis and Processing, Italy, pp. 658-661, 2003.

[5] Battiato S., Buemi A. Impoco G. and Mancuso M., "*JPEG*2000 Coded Images Optimization Using a Content Dependent Approach", *IEEE* Transactions on Consumer Electronics, Vol. 48, No. 3, pp. 400-408, 2002.

[6] Berkner K. and Schwartz E. L. "Removal of tile artifacts using projection onto scaling functions for *JPEG*2000", Proceedings *IEEE* International Conference on Image Processing, Rochester, NY, pp. 373-376, 2002.

[7] Bhalod J., Fahmy G. F. and Panchanathan S., "Region-based Indexing in the *JPEG*2000 framework", Proceedings of *SPIE* Internet Multimedia Management Systems, Vol. 4519, pp. 91-96, 2001.

[8] Boettcher J. B. and Fowler J. E., "Video Coding using a Complex Wavelet Transform and Set Partitioning", *IEEE* Signal Processing Letters, Vol. 14, No. 9, pp.

633–636, 2007.

[9] Boulgouris N. V., Tzovaras D. and Strintzis M. G., “Lossless Image Compression Based on Optimal Prediction, Adaptive Lifting and Conditional Arithmetic Coding,” *IEEE* Transactions on Image Processing, Vol. 10, No. 1, pp. 1–14, 2001.

[10] Brislawn C. M., “Classification of Non Expansive Symmetric Extension Transforms for Multirate Filter Banks,” Applied and Computational Harmonic Analysis, Vol. 3, pp. 337–357, 1996.

[11] Calderbank R., Daubechies I., Sweldens W. and Yeo B., “Wavelet Transforms that Map Integers to Integers,” Applied and Computational Harmonic Analysis, Vol. 5, No. 3, pp. 332-369, 1998.

[12] Chang C. L., Maleki A. and Girod B., “Adaptive Wavelet Transform for Image Compression via Directional Quincunx Lifting,” Proceedings of *IEEE* Workshop on Multimedia Signal Processing, Shanghai, China, pp. 1-4, 2005.

[13] Chang C. L. and Girod B., “Direction-Adaptive Discrete Wavelet Transform via Directional Lifting and Bandeletization,” Proceedings of *IEEE* International Conference on Image Processing, Atlanta, GA, pp. 1149-1152, 2006

[14] Chang C. L. and Girod B., “Direction-Adaptive Discrete Wavelet Transform for Image Compression”, *IEEE* Transactions on Image Processing, Vol. 16, No. 5, pp. 1289-1302, May 2007.

[15] Chang C. L. and Girod B., “Direction-Adaptive Partitioned Block Transform for Image Coding,” Proceedings of *IEEE* International Conference on Image Processing, San Diego, CA, pp. 145–148, 2008.

[16] Chang T. H., Chen L. L., Lian C. J., Chen H. H. and Chen L. G., “Computation

Reduction Technique for Lossy *JPEG*2000 Encoding Through *EBCOT Tier*-2 Feedback Processing", Proceedings of *IEEE* International Conference on Image Processing, NY, pp. 85-88, 2002.

[17] Chang Y. W., Fang H. C., Cheng C. C., Chen C. C. and L. C. Chen, "Precompression Quality Control Algorithm for *JPEG*2000", *IEEE* Transactions on Image Processing, Vol. 15, No. 11, pp. 3279-3293, 2006.

[18] Chen K. F., Lian C. J., Chen H. H., and Chen L. G., "Analysis and architecture design of EBCOT for JPEG—2000," Proceedings *IEEE* International Symposium on Circuits and Systems, Vol. 2, pp. 765–768, May 2001.

[19] Christopoulos C., Skodras A., and Ebrahimi T., "The *JPEG*2000 Still Image Coding System: An Overview," *IEEE* Transactions on Consumer Electronics, Vol. 46, No. 6, pp. 1103–1127, 2000.

[20] Christophe G. P., Tillier C. and Popescu B. P., "Optimization of the Predict Operator in Lifting-based Motion Compensated Temporal Filtering," Proceedings of *SPIE* Visual Communications and Image Processing, San Jose, CA, Jan. 2004.

[21] Claypoole R. L., Davis G. M., Sweldens W. and Baraniuk R. G., "Nonlinear Wavelet Transforms for Image Coding via Lifting," *IEEE* Transactions on Image Processing, Vol. 12, No. 12, pp. 1449–1459, 2003.

[22] Cohen A. and Matei B., "Compact Representation of Images by Edge Adapted Multiscale Transforms," Proceedings of *IEEE* International Conference on Image Processing, Thessaloniki, Greece, pp. 8-11, 2001.

[23] Daly S., Zeng W., Li J. and Lei S., "Visual Masking in Wavelet Compression for *JPEG*2000", Proceedings *IS&T SPIE* Image and Video Communications and

Processing", Vol. 3, pp. 1016-1026, 2000.

[24] Daubechies I. and Sweldens W., "Factoring Wavelet Transforms into Lifting Steps", Journal of Fourier Analysis and Applications, Vol. 4, No. 3, pp. 247–269, 1998.

[25] Ding W., Wu F. and Li S., "Lifting-based Wavelet Transform with Directionally Spatial Prediction," Picture Coding Symposium, San Francisco, CA, pp. 1-6, 2004.

[26] Ding W., Wu F., Wu X., Li S. and Li H., "Adaptive Directional Lifting-based Wavelet Transform for Image Coding," *IEEE* Transactions on Image Processing, Vol. 16, No. 2, pp. 416–427, 2007.

[27] Dong W., Shi G. and Xu J., "Adaptive Nonseparable Interpolation for Image Compression with Directional Wavelet Transform", *IEEE* Signal Processing Letters, Vol. 15, No. 1, pp. 233-236, 2008.

[28] Hashimoto M., Matsuo K., & Kioke A., "*JPEG*2000 Encoding Method for Reducing Tiling Artifacts", *IEICE* Transaction on Information and Systems, Vol. E88-D, No. 12, pp. 2839 – 2848, 2005.

[29] Hyuk C. and Kim T., "Blocking Artifacts Reduction in Block coded Images Using Wavelet Based Subband Decomposition", *IEEE* Transactions on Circuits and Systems for Video Technology, Vol. 10, No. 5, pp. 801-805, 2000.

[30] Du W., Sun J. and Ni Q., "Fast and Efficient Rate Control Approach for *JPEG*2000", *IEEE* Transactions on Consumer Electronics, Vol. 50, No. 4, pp. 1218-1221, 2004.

[31] Fahmy G. F. and Panchanathan S., "A lifting Based System for Compression and Classification Trade off in *JPEG*2000 Framework", Journal of Visual Communication and Image Representation, Vol. 15, No.2, pp. 145-162, 2004.

[32] Fang Z., Xiong N., Yang L. T., Sun X. and Yang Y., "Interpolation Based Direction

Adaptive Lifting *DWT* and Modified *SPIHT* for Image Compression in Multimedia Communications", *IEEE* Systems Journal, Vol. 5, No. 4, pp. 584-593, 2011.

[33] Feng B., Xu J., Wu F. and Yang S., "Energy Distributed Update Steps in Lifting Based Motion Compensated Video Coding," Proceedings of *IEEE* International Conference on Image Processing, China, pp. 2267–2270, 2004.

[34] Florido M. A. R., Alzola J. R. and Westin C. F., "Artifact Reduction in Sinc Interpolation Using Adaptive Filtering," Proceedings of *IEEE* International Conference on Image Processing, Thessaloniki, Greece, Vol. 3, pp. 884–887, 2001.

[35] Fowler J. E., Boettcher J. B. and Popescu B. P., "Image Coding Using a Complex Dual Tree Wavelet Transform", Proceedings of European Signal Processing Conference, Poznan, Poland, pp. 994–998, 2007.

[36] Gerek O. N. and Cetin A. E., "Adaptive Polyphase Subband Decomposition Structures for Image Compression," *IEEE* Transaction on Image Processing, Vol. 9, No. 10, pp. 1649–1660, 2000.

[37] Gerek O. N. and Cetin A. E., "A 2-D Orientation-Adaptive Prediction Filter in Lifting Structures for Image Coding," *IEEE* Transactions on Image Processing, Vol. 15, No. 1, pp. 106–111, 2006.

[38] Golwelkar A. and Woods J. W., "Motion-Compensated Temporal Filtering and Motion Vector Coding Using Biorthogonal Filters", *IEEE* Transactions on Circuits and Systems for Video Technology, Vol. 17, No. 4, pp. 417–428, 2007.

[39] Gouze A., Antonini M. and Barlaud M., "Quincunx Filter Lifting Scheme for Image Coding," Proceedings of *SPIE* Visual Communication and Image Processing, Vol. 1, pp. 1-11, Jan. 1999.

[40] Gouze A., Antonini M., Barlaud M. and Macq B., "Design of Signal-Adapted Multidimensional Lifting Scheme for Lossy Coding," *IEEE* Transactions on Image Processing, Vol. 13, No. 12, pp. 1589–1603, 2004.

[41] Guangjun Z., Lizhi C. and Huowang C., ''A simple 9/7- Tap Wavelet Filter Based on Lifting Scheme,'' Proceedings of International Conference on Image Processing, Thessaloniki, Greece, Vol. 2, pp. 249–252, Oct. 2001.

[42] Han Z. Z., Liu Z. B. and Xu Y. S., "A New Adaptive Wavelet Transform Using Lifting Scheme", Proceedings of International Conference on Wavelet Analysis and Pattern Recognition, Guilin, pp. 224-229, 2011.

[43] Heijmans H., Piella G. and Popescu B. P., "Building Adaptive 2-D Wavelet Decompositions by Update Lifting," Proceedings of *IEEE* International Conference on Image Processing, Rochester, NY, pp. 397-400, 2002.

[44] Hui C. W. and Siu W. C., "Coding Directional Angles Using Context Based Adaptive Arithmetic Code", Proceedings of International Conference on Signal Processing, pp. 1190-1193, 2008.

[45] Hung C. H. and Hang H. M., "Decision Directed Adaptive Wavelet Image Coding with Directional Decomposition", Proceedings of *IEEE* International Symposium on Circuits and Systems, Taipei, pp. 3186-3189, 2009.

[46] Jansen M. and Oonincx P., "Second Generation Wavelets and Applications", Springer-Verlag, London, 2005.

[47] Jianfen Z. and Zhengming M., "Lifting Scheme and Image Coding: Average Interpolating Image Coding", Proceedings of *IEEE* International Symposium on Signal Processing and its Applications, pp. 561-564, 2001.

[48] Kaaniche M., Benyahia A. B., Popescu B. P. and Pesquet J. C., "Non Separable Lifting Scheme with Adaptive Update Step for Still and Stereo Image Coding," Elsevier Signal Processing: Special issue on Advances in Multirate Filter Bank Structures and Multiscale Representations, Vol. 91, No. 12, pp. 2767–2782, 2011.

[49] Kaaniche M., Popescu B. P., Benyahia A. B. and Pesquet J. C., "Adaptive Lifting Scheme with Sparse Criteria for Image Coding", *EURASIP* Journal on Advances in Signal Processing, No. 10, pp. 1-22, 2012.

[50] Kasner J. H., Marcellin M. W. and Hunt B. R., "Universal Trellis Coded Quantization", *IEEE* Transactions on Image Processing, Vol. 8, No. 12, pp. 1677-1687, 1999.

[51] Kharitonenko I., Zhang X. and Twelves S., "A Wavelet Transform With Point-Symmetric Extension at Tile Boundaries", *IEEE* Transaction on Image Processing, Vol. 11, No. 2, pp. 1357-1364, December 2002.

[52] Li H., Liu G. and Zhang Z., "Optimization of Integer Wavelet Transforms Based on Difference Correlation Structures", *IEEE* Transactions on Image Processing, Vol. 14, pp. 1831-1847, 2005.

[53] Li M. and Nguyen T. Q., "Markov random field model-based edge-directed image interpolation", *IEEE* Transactions on Image Processing, Vol. 17, No. 7, pp.1121-1128, 2008.

[54] Liang D., Cheng L. and Zang Z., "General Construction of Wavelet Filters via a Lifting Scheme and Its Application in Image Coding", Optical Engineering, Vol. 42, pp. 1949–1955, 2003.

[55] Lian C. J., Chen K. F., Chen H. H. and Chen L. G., "Analysis and Architecture

Design of Block Coding Engine for *EBCOT* in *JPEG*2000," *IEEE* Transactions on Circuits Systems and Video Technology, Vol. 13, No. 3, pp. 219-230, 2003.

[56] Liu J. and Zhang D., "A Novel Bit Rate Allocation Algorithm for Motion *JPEG*2000", Proceedings of *IEEE* 6th World Congress on Intelligent Control and Automation, China, pp. 9907-9910, 2006.

[57] Liu Y. and Ngan K. N., "Weighted Adaptive Lifting Based Wavelet Transform," Proceedings of *IEEE* International Conference on Image Processing, San Antonio, TX, pp. 189-192, 2007.

[58] Liu Y. and Ngan K. N., "Weighted Adaptive lifting Based Wavelet Transform for Image Coding," IEEE Transactions on Image Processing, Vol. 17, No. pp. 500–511, 2008.

[59] Mandal M. K. and Panchanathan S., "Integrated Compression and Indexing of Video in the Wavelet Domain", Journal of Electronic Imaging, Vol. 9, No. 2, pp. 85-100, 2000.

[60] Masuzaki T., Tsutsui H., Uzumi T., Onoye T. and Nakamura Y., "*JPEG*2000 Adaptive Rate Control for Embedded Systems", Proceedings of *IEEE* International Symposium Circuits. Systems, Scottsdale, pp.333-336, 2002.

[61] Mittal R. C., "Orthogonal Wavelets", Journal of Discrete Mathematical Sciences and Cryptography, Vol. 3, pp. 253-262, 2000.

[62] Mittal R. C., "Data Compression Through Wavelets", Proceedings of Conference on Mathematics and its Applications in Engineering and Industry, Roorkee, pp.187-205, 2000.

[63] Mittal R. C., Ghosh J. K. and Somvanshi A., "Fractal Compression of Satellite

Images," Photonirvachak, Journal of the Indian Society of Remote Sensing, Vol. 36, No. 4, pp. 299-311, 2008.

[64] Mehrseresht N. and Taubman D., "Adaptively Weighted Update Steps in Motion Compensated Lifting Based on Scalable Video Compression," Proceedings of *IEEE* International Conference on Image Processing, Vol. 3, pp. 771–774, 2003.

[65] Murakami T., Takahashi K. and Naemura T., "Direction Adaptive Hierarchical Decomposition for Image Coding", Proceedings of 28th Picture Coding Symposium, Nagoya, Japan, pp.570-573, 2010.

[66] Pannebaker W. and Mitchell J. L., "*JPEG*: Still Image Data Compression Standard", Kluwer Academic Publishers, 1992.

[67] Parrilli S., Cagnazzo M., Popescu B. P., "Distortion Evaluation in Transform Domain for Adaptive Lifting Schemes", Proceedings of International Workshop on Multimedia Signal Processing, Cairns, Queensland, Australia, pp. 200–205, 2008.

[68] Peng X., Wu F. and Xu J., "Directional Filtering Transform," Proceedings of *IEEE* International Conference on Multimedia Expo, pp. 1–4, 2009.

[69] Peng X., Xu J. and Wu F., "Directional Filtering Transform for Image/ Intra-Frame Compression", *IEEE* Transactions on Image Processing, Vol. 19, No. 11, pp. 2935-2946, 2010.

[70] Pennec E. L. and Mallat S., "Image Compression with Geometric Wavelets," Proceedings of *IEEE* International Conference on Image Processing, Vancouver, BC, Canada, pp. 661–664, 2000.

[71] Piella G., Popescu B. P. and Heijmans H., "Adaptive Update Lifting with a Decision Rule Based on Derivative Filters," *IEEE* Signal Processing Letters, Vol. 9, No. 10,

pp. 329–332, 2002.

[72] Piella G. and Heijmans H., “Adaptive Lifting Schemes with Perfect Reconstruction,” *IEEE* Transactions on Signal Processing, Vol. 50, No. 7, pp. 1620–1630, 2002.

[73] Qin X., Yan X., Yang C., and Ye Y.,“Tiling Artifact Reduction for *JPEG*2000 Image at Low Bit Rate”, Proceedings *IEEE* International Conference on Multimedia and Expo, Taipei, Taiwan, pp. 1419-1422, 2004.

[74] Quan D. and Ho Y. S., “Efficient wavelet Lifting Scheme based on Filter Optimization and Median Operator”, Proceedings of International Conference on Computing and Communication Technologies, Gwangju, South Korea, pp. 1-6, 2009.

[75] Quan D. and Ho Y. S., “Optimized Median Lifting Scheme for Lossy Image Compression”, *IEICE* Transaction on Information and Systems, Vol. E94-D, No. 3, pp. 721- 724, 2011.

[76] Ramkumar M. and Anand G. V., “An FFT-based Technique for Fast Fractal Image Compression”, Signal Processing, Vol. 63, No. 3, pp. 263-268, 1997.

[77] Rolon J. C. and Salembier P., “Generalized Lifting for Sparse Image Representation and Coding”, Picture Coding Symposium, Lisbon, Portugal, pp. 1-4, 2007.

[78] Saha S., “Image Compression - from *DCT* to Wavelets: A Review”, ACM Crossroads Magazine, Vol. 6, No. 3, pp. 12-21, 2000.

[79] Saha S. and Vemuri R., “Adaptive Wavelet Coding of Multimedia Images”, Proceedings of ACM Multimedia, Orlando, Florida, pp. 71-74, 1999.

[80] Saha S. and Vemuri R., “Adaptive Wavelet Filters in Image Coders - How Important are They?” Proceedings of *IEEE* Annual Conference on Industrial Electronic, San Jose, California, pp. 559-564,1999.

[81] Saha S. and Vemuri R., “Analysis based Adaptive Wavelet Filter Selection in Lossy Image Coding Schemes”, *IEEE* International Symposium on Circuits and Systems, Geneva, pp. 29-32, 2000.

[82] Said A. and Pearlman W. A., “An Image Multiresolution Representation for Lossless and Lossy Image Compression,” *IEEE* Transactions on Image Processing, Vol. 5, No. 8, pp. 1303–1310, 1996.

[83] Said A. and Pearlman W. A., “A New Fast and Efficient Image Codec Based on Set Partitioning in Hierarchical Trees,” *IEEE* Transactions on Circuits and Systems for Video Technology, Vol. 6, No. 3, pp. 243–250, 1996.

[84] Satyabama R. and Annadurai S., “Adaptive Spatial Prediction for Lifting Scheme in Image Compression”, International Journal of Computer Science and Network Security, Vol. 10, No. 2, pp. 292-299, 2010.

[85] Sayood K., “Introduction to Data Compression”, Academic Press, 2000.

[86] Shapiro J. M., “Embedded Image Coding using Zerotrees of Wavelet Coefficients,” *IEEE* Transactions on Signal Processing, Vol. 41, No. 12, pp. 3445–3462, 1993.

[87] Seo Y. G. and Kang K. J., “A Slope Information Based Fast Mask Generation Technique for *ROI* Coding in *JPEG*2000”, International Journal of Innovative Computing, Information and Control, Vol. 6, No. 6, pp. 2817-2826, 2010.

[88] Skodras A., Christopoulos C., and Ebrahimi T., “The *JPEG*2000 Still Image Compression Standard,” *IEEE* Signal Processing Magazine, Vol. 18, No. 5, pp. 36-58, 2001.

[89] Sole J. and Salembier P., “Adaptive Discrete Generalized Lifting for Lossless Compression,” Proceedings of *IEEE* International Conference on Acoustics, Speech,

and Signal Processing, Montreal, Quebec, Canada, Vol. 3, pp. 57–60, 2004.

[90] Sweldens W., "The Lifting Scheme: A Custom Design Construction of Biorthogonal Wavelets", Applied and Computational Harmonic Analysis, Vol. 3, No. 2, pp. 186-200, 1996.

[91] Taubman D. and Zakhor A., "Orientation Adaptive Subband Coding of Images," *IEEE* Transactions on Image Processing, Vol. 3, No. 4, pp. 421–437, 1994.

[92] Taubman D., "Adaptive, Non-Separable Lifting Transforms for Image Compression," Proceedings of *IEEE* International Conference on Image Processing, Kobe, Japan, Vol. 3, pp. 772–776, 1999.

[93] Taubman D. S., "High Performance Scalable Image Compression with *EBCOT*", IEEE Transactions on Image Processing, Vol. 9, No. 7, pp.1158-1170, 2000.

[94] Taubman D. S., "KAKADU Software version 6.0", http://kakadusoftware.com/, 2007.

[95] Taubman D. S. and Marcellin M. W. "*JPEG*2000: Image Compression Fundamentals, Standards and Practice", Kluwer Academic Publishers, 2002.

[96] Taubman D. S., Ordentlich E., Weinberger M. and Seroussi G., "Embedded Clock Coding in *JPEG*2000", Signal Processing: Image Communication, Vol. 17, pp. 49-72, 2002.

[97] Tillier C., Popescu B. P. and Schaar M. V. D., "Improved Update Operators for Lifting-based Motion Compensated Temporal Filtering," *IEEE* Signal Processing Letters, Vol. 12, No. 2, pp.146-149, 2005

[98] Tran T. D., Liang J. and Tu C., "Lapped Transform via Time-Domain Pre- and Post-Filtering", *IEEE* Transactions on Signal Processing, Vol. 51, No. 6, pp. 1557-1571,

2003.

[99] Vargic R., “An Approach to Directional Wavelet Construction and Their Use for Image Compression”, Proceedings of *IEEE* International Symposium on Video/Image Processing and Multimedia Communications, pp. 201-204, 2002.

[100] Velisavljevic V., Dragotti P. L. and Vetterli M., “Directional Wavelet Transforms and Frames,” Proceedings of *IEEE* International Conference on Image Processing, Rochester, NY, pp. 589–592, 2002.

[101] Velisavljevic V., Lozano B. B., Vetterli M. and Dragotti P. L., “Directionlets: Anisotropic Multi-directional Representation with Separable Filtering,” *IEEE* Transactions on Image Processing, Vol. 15, No. 7, pp. 1916–1933, 2006.

[102] Vetterli M. and Kovacevic J., “Wavelets and Subband Coding”, Englewood Cliffs, NJ, Prentice Hall, 1995.

[103] Wang D., Zhang L. and Vincent A., “Improvement of *JPEG*2000 using Curved Wavelet Transform,” Proceedings of *IEEE* International Conference on Acoustics, Speech, Signal Processing, Philadelphia, PA, Vol. 2, pp. 365–368, 2005.

[104] Wang D., Zhang L. and Vincent A., “Curved Wavelet Transform for Image Coding,” *IEEE* Transactions on Image Processing, Vol. 15, No. 8, pp. 2413–2421, 2006.

[105] Wei J., Pickering M., Frater M., Arnold J., Boman J., and Zeng W.: ‘Tile Boundary Artifacts Reduction Using Odd Tile Size and the Low Pass First Convention’. IEEE Transactions on Image Processing, Vol. 14, No. 8, pp. 1033- 1042, 2005.

[106] Wu F. and Li S., “System and Method for Image Coding Employing a Hybrid Directional Prediction and Wavelet Lifting”, US Patent US 2006/0008164, January 2006.

[107] Xu H., Xu J. and Wu F., "Lifting Based Directional *DCT* Like Transform for Image Coding", *IEEE* Transactions for Circuits and Systems for Video Technology, Vol. 17, No. 10, pp. 1325-1335, 2007.

[108] Yaroslavsky L., "Fast Signal Sinc-Interpolation and its Applications in Signal and Image Processing," Proceedings of *SPIE* Conference Image Processing: Algorithms and Systems, 2002.

[109] Yeung Y. M. and Au O. C., "Efficient Rate Control for *JPEG*2000 Image Coding", *IEEE* Transactions on Circuits Systems and Video Technology, Vol. 15, No. 3, pp. 335-344, 2005.

[110] Zhang N., Wu F., Wu X. and Yin B., "Efficient Multiple-Description Image Coding Using Directional Lifting-Based Transform", *IEEE* Transactions on Circuits and Systems for Video Technology, Vol. 18, No. 5, pp. 646-656, 2008.

List of Publications by the Author

I Singara Singh, R. K. Sharma, and M. K. Sharma, "Efficient Rate Control Approach for *JPEG2000* Image Coding", Journal of Electronic Imaging, Vol. 21, No. 3, pp. 033004(1-8), 2012. SCI Indexed (Impact Factor = 0.694)

Ii Singara Singh, R. K. Sharma, and M. K. Sharma, "Weighted Bit Rate Allocation in *JPEG2000* Tile Encoding", International Journal of Computer Science Issues, Vol. 8, No. 5, pp. 458-462, 2011. Elsevier Indexed (Impact Factor = 0.242)

iii. Singara Singh, R. K. Sharma, and M. K. Sharma, "Post-Processing Technique to Reduce Tile Boundary Artifacts in *JPEG2000* Compressed Images", International Journal of Multimedia and its Applications, Vol. 4, No. 1, pp. 127-136, 2012.

iv. Singara Singh, R. K. Sharma, and M. K. Sharma, "Use of Wavelet Transform Extension for Graphics Images", International Journal of Image Processing, Vol. 3, No. 1, pp. 55-60, 2009.

v. Singara Singh, R. K. Sharma, and M. K. Sharma, "Tile Boundary Artifacts Reduction of *JPEG2000* Compressed Images", Proceedings of International Workshop on Signal and Image Processing, Bangalore, India, pp. 281-290, 2012.